12-2009

Reconciling Holocene Alluvial Records in Buckskin Wash, Southern Utah

Jonathan E. Harvey
Utah State University

RECONCILING HOLOCENE ALLUVIAL RECORDS IN BUCKSKIN WASH, SOUTHERN UTAH

by

Jonathan E. Harvey

A thesis submitted in partial fulfillment
of the requirements for the degree

of

MASTER OF SCIENCE

in

Geology

Approved:

_____	_____
Joel L. Pederson, Ph.D.	Tammy M. Rittenour, Ph.D.
Major Professor	Committee Member
_____	_____
John C. Schmidt, Ph.D.	Byron R. Burnham, Ed.D.
Committee Member	Dean of Graduate Studies

UTAH STATE UNIVERSITY
Logan, Utah

2009

ABSTRACT

Reconciling Holocene Alluvial Records in Buckskin Wash, Southern Utah

by

Jonathan E. Harvey, Master of Science

Utah State University, 2009

Major Professor: Dr. Joel L. Pederson
Department: Geology

Most approaches to interpreting alluvial records in drylands fall into one of two categories: (1) The "arroyo problem," wherein workers study cycles of streambed aggradation and degradation in broad, unconstricted alluvial valleys; and (2) paleoflood hydrology, where alluvial sequences in constricted bedrock canyons are interpreted as paleoflood deposits from streams with stable channel grade and geometry. Both approaches can be valid in their end-member settings, but there is confusion about how the two record types relate in a single drainage. We address this disconnect in Buckskin Wash, an ephemeral stream that consists of a broad alluvial reach draining into a tightly constricted slot canyon. By employing detailed sedimentology, stratigraphy, and geochronology in both the alluvial and constricted reaches of the watershed, we test the hypothesis that the slot canyon deposits are anticorrelated to valley-fill deposits upstream, implying that arroyo cutting is driven by episodic flooding.

Alluvial reach deposits are characterized by stratal packages representing incremental, long-term aggradation bound by erosion surfaces representing channel

entrenchment. At least four packages younger than ~3 ka are present, the youngest spanning ~0.7 – 0.15 ka. Each is composed of interfingering imbricated gravels, laminated sands, and massive silty clays. Constricted reach deposits consist of five discrete packages, each composed of tabular beds of silty sand that were deposited relatively rapidly. The oldest package dates to ~1.9 – 1.1 ka whereas the rest of the deposits are younger than ~0.15 ka.

Traditional paleoflood techniques would suggest that the constricted reach deposits record a ~1000-year absence of paleofloods followed by ~100 years of frequent, high-magnitude flooding that indeed correlate to arroyo cutting upstream. We argue instead that the constricted reach deposits record an episode of higher preservation potential. Transport of sediment from the alluvial reaches during historic arroyo cutting likely led to a pulse of sediment storage and changed stage-discharge relations in the slot canyon downstream, allowing even moderate floods to overtop existing deposits and be preserved. This new interpretation suggests that, because preservation may be a function of episodic sediment loading from upstream, constricted-reach deposits may not accurately record the paleoflood history of a stream.

(135 pages)

ACKNOWLEDGMENTS

First I would like to thank my advisor, Dr. Joel Pederson, for helping me identify such an interesting problem to tackle with my Masters thesis. His presence in the field was a critical component of my education and has helped me more than he knows. I would also like to thank my committee members: Dr. Tammy Rittenour, for going out of her way to teach me the fundamentals of OSL dating and for generously donating machine time to expedite my results; and Dr. Jack Schmidt, for giving me a rigorous introduction to fluvial geomorphology and its societal applications.

I am indebted to the Utah State University Geology Department for all of its support during my graduate work, and for awarding me the J.S. Williams Graduate Scholarship. Thank you to colleagues Erin Tainer and Michelle Summa for tolerating my presence for the past two years, and to my field helpers Todd Parr and Chris Tressler. This thesis was also financially supported in part by a graduate student research grant from the Geological Society of America. I would especially like to thank the Quaternary Geology and Geomorphology division for awarding this project the Arthur D. Howard award.

Lastly, I would like to thank my family. Their unwavering support and encouragement over the years as I bounced from subject to subject was critical to my eventual discovery of the Earth sciences. This work is dedicated to them.

Jonathan E. Harvey

CONTENTS

LIST OF TABLES

LIST OF FIGURES

CHAPTER 1

INTRODUCTION

The southwestern United States has been the epicenter of geologic research aimed at exploring the relation of Holocene landscape dynamics to cultural development in the region. A large portion of the archeological record is concentrated along fluvial networks, as water has always been a critical component of survival in this semiarid landscape. Accordingly, much research has been devoted to understanding the paleohydrology of these drainages via alluvial records. This thesis attempts to bridge a major conceptual divide between the two dominant paradigms in studying these alluvial records – arroyo cut and fill reconstructions and paleoflood hydrology.

In Chapter 2, I lay out the background and motivation for this study. In it, I review the development and evolution of arroyo cut-and-fill studies and paleoflood hydrology. I describe the nature of the disconnect between these two paradigms, as well as the few existing attempts at bridging the disconnect. Finally, I describe and advocate the type of study that can link these two approaches, which I then demonstrate with the remainder of the thesis. This chapter is a review paper coauthored by Dr. Joel Pederson, with a target submittal to the journal *Quaternary Science Reviews*.

In Chapter 3, I present the results of a new chronostratigraphic study in southern Utah's Buckskin Wash – a large tributary in the Paria River basin. Its headwaters feature a network of broad, alluvial valleys that drain into a world-famous slot canyon. These two vastly different valley geometries contain classic examples of both types of alluvial records that have been the subject of previous research efforts demonstrating both

approaches. I describe and compare the late Holocene alluvial records of the two reaches of the drainage using a combination of detailed sedimentology and stratigraphy; surveying of stream geometry; and a diverse geochronology including optically stimulated luminescence, radiocarbon, ^{137}Cs, and tree-ring dating. This paper is primarily written by me, and with coauthors Joel Pederson and Tammy Rittenour, its target journal is *GSA Bulletin*.

Finally, Chapter 4 summarizes the work and its implications.

CHAPTER 2

RECONCILING APPROACHES TO ALLUVIAL RECORDS IN DRYLANDS

INTRODUCTION

Holocene alluvial deposits stored along dryland streams in the southwestern U.S. provide a record of environmental change in their watersheds. These alluvial archives are used as primary sources of information about changes in hydrology, climate, and cultural activity over the Holocene (Bryan, 1925), changes similar in scale to that predicted for the upcoming century (Hughes and Diaz, 2008). With the advent of paleoflood hydrology in recent decades, a newer approach to the interpretation of these records has emerged (e.g. Patton et al. 1979); leading to some confusion. Now, two distinct paradigms exist in the literature: reconstruction of arroyo cut and fill histories from deposits in broad alluvial valleys, and paleoflood reconstructions from deposits stored in constricted bedrock canyons. These contrasting approaches have quite different implications for how we interpret long-term stream behavior, yet we suggest they can be complementary rather than contradictory. Reconciliation of these approaches will be essential for a complete and systematic understanding of the responses and trajectories of these sensitive systems.

In the southwestern U.S., stream valleys range from broad, unconstricted reaches a kilometer or more wide to bedrock slot canyons only meters wide, often within the same watershed. Large volumes of sediment ("valley-fill alluvium") can be stored along the broader reaches, where bedrock exerts little to no control on channel form. Early workers in the southwestern U.S. recognized that the inset terraces and filled

paleochannels revealed in exposures of valley fills record episodes of aggradation and degradation on the scale of centuries or millennia, and that these have key relations to archeology (e.g. Bryan, 1925; Hack, 1942; Antevs, 1952; Haynes, 1968; Hall, 1977). Much debate has been centered on the cause of these cutting and filling cycles, but it is clear that climate plays a primary role in modulating catchment processes at this scale (Cooke and Reeves, 1976; Knox, 1983; Graf, 1987; Hereford, 2002).

In stark contrast to broad, alluvial reaches, very little sediment can be stored in narrow bedrock canyons. The few places where sediment can be accommodated (alcoves, confluences, expansions, etc.) have been utilized by paleoflood hydrologists to reconstruct individual flood events and Holocene-scale flood chronologies (e.g. Kochel and Baker, 1982; Ely, 1992; O'Connor et al., 1994; Harden, 2007**)**. Accurate interpretation of such deposits is dependent on correct understanding of the history of channel change over the time period of interest. For many studies, channel grade and geometry are simply assumed to be stable over centennial to millennial timescales. This implies that the centennial-scale cycles of sediment storage and channel change recorded in the alluvial reaches are not manifested in the constricted reaches of the same drainages. This is a hypothesis that has not been rigorously tested.

Despite the number of contributions demonstrating both paradigms in the study of dryland alluvial records, the two approaches and resulting interpretations remain poorly reconciled. Many drainages feature both end-member valley geometries, but the landscape also contains transitional reaches with a more ambiguous affinity. Workers in these reaches may have difficulty determining whether deposits represent only large floods in a stable channel or a more complex suite of valley-filling depositional events.

Additionally, it is unclear how the two end-member records relate laterally along a drainage (Webb, 1985; Tooth, 2000; Hereford, 2002).

Here we review the body of work representing both end-member approaches to dryland alluvial records with a focus on the much-studied U.S. Southwest. We explore the nature of the disconnect between these two paradigms and efforts at linking them into a greater model of dryland fluvial response to climate forcing. Finally, we advocate studies based on focused chronostratigraphy and modeling to highlight the distinction and stratigraphic relationship between record types within individual drainages.

The Arroyo Problem

Geologists and archeologists have been studying the alluvial records of semiarid streams for over a century. Much of this work was motivated by a widespread episode of channel incision in the American Southwest from ~1880 – 1915 AD (Bryan, 1925). Over these few decades, drainages entrenched up to 30 meters into their alluvium, leaving former floodplains behind as terraces. Because many farms and settlements were built on these former floodplains in the preceding decades, erosion accompanying the arroyo-cutting event resulted in substantial property damage, agricultural losses, and abandonment of entire communities (Cooke and Reeves, 1976).

The cause of this historic arroyo cutting event has been the subject of longstanding debate in the literature. A number of reviews discuss the variety of hypothesized mechanisms (e.g. Cooke and Reeves, 1976; Graf, 1983; Hereford, 2002). Early workers suspected that the introduction of grazing accompanying settlement had disturbed vegetation and surface hydrology, leading to increased runoff and arroyo

entrenchment (Bailey, 1935; Antevs, 1952). However, infilled paleoarroyos exposed in the walls of modern cutbanks indicate that there have been several cycles of alluviation and erosion over the Holocene prior to the influence of Anglo settlers. Thus it is recognized that human activity alone is unlikely to have driven the most recent entrenchment episode (Cooke and Reeves, 1976).

Other workers have emphasized the role of autogenic adjustments in driving cycles of aggradation and erosion. They document field examples and experimental studies wherein pulses of incision followed by widening and alluviation migrate up-network in response to the formation of local slope anomalies (Schumm and Hadley, 1957; Schumm and Parker, 1973; Patton and Schumm, 1981; Tucker et al., 2006). These anomalies represent local baselevel changes that do not necessarily occur simultaneously across regional catchments. For example, local oversteepening may result from deposition of a tributary debris fan or deposition resulting from downstream losses in sediment transport capacity due to bed infiltration. The resulting oversteepened reaches are subject to higher shear stresses and bed incision during floods, potentially generating a knickpoint that migrates up the stream network. This, in turn, sets up a complex response wherein widening and deposition downstream of an actively migrating knickpoint generates another local slope alnomaly and migrating knickpoint. The signature of such internal complex response is a sequence of relatively small-scale, time-transgressive (younging upstream) terraces (Schumm and Parker, 1973; Daniels, 2008).

Waters (1985) concluded that such "intrabasin geomorphic parameters" were stronger influences than external climatic drivers on the timing of alluviation and erosion for a network of streams in northeastern New Mexico. In a different example of internal

response, Patton and Boison (1986) showed that recent landslide-generated debris overwhelms the fluvial system of Harris Wash, a tributary of the Escalante River in southern Utah, causing the spatial and temporal patterns of alluviation and incision to differ from that seen in other regional streams.

Despite anthropogenic influences and scattered examples of asynchronous complex response, broad regional correlations in stream behavior mark most late Holocene alluvial records (Hack, 1942; Graf, 1987; Hereford, 2002). The product of decades of research into the arroyo problem is a rich dataset of alluvial records throughout the Southwest, which has inspired comparison of the timing of aggradation and incision across drainages. In the Colorado Plateau, at least four episodes over the past millennium have been readily correlated across several catchments: 1) a period of aggradation before ~1200 AD coincident with the rise of Puebloan cultures (Tsegi alluvium, Chaco alluvium); 2) a prehistoric arroyo cutting around ~1200 AD that coincides roughly with the Puebloan abandonment; 3) a period of aggradation from ~1350-1880 AD (Naha alluvium, Settlement alluvium), and 4) the historic arroyo cutting from ~1880-1920 AD (Hall, 1977; Graf, 1987; Hereford, 2002; Figure 2-1). Incipient re-filling of the historic arroyos began around 1940 AD, a date that is consistent across many southern Plateau streams (Leopold, 1976; Hereford, 1986; Graf et al., 1991) and coincides with a regional mid-century drought. Though many episodes of arroyo cutting and filling have been recognized prior to 1200 AD (e.g. Waters and Haynes, 2001; Mann and Meltzer, 2007), records of these older dynamics lack the detail or resolution necessary to determine how well these previous cycles correlate across drainages.

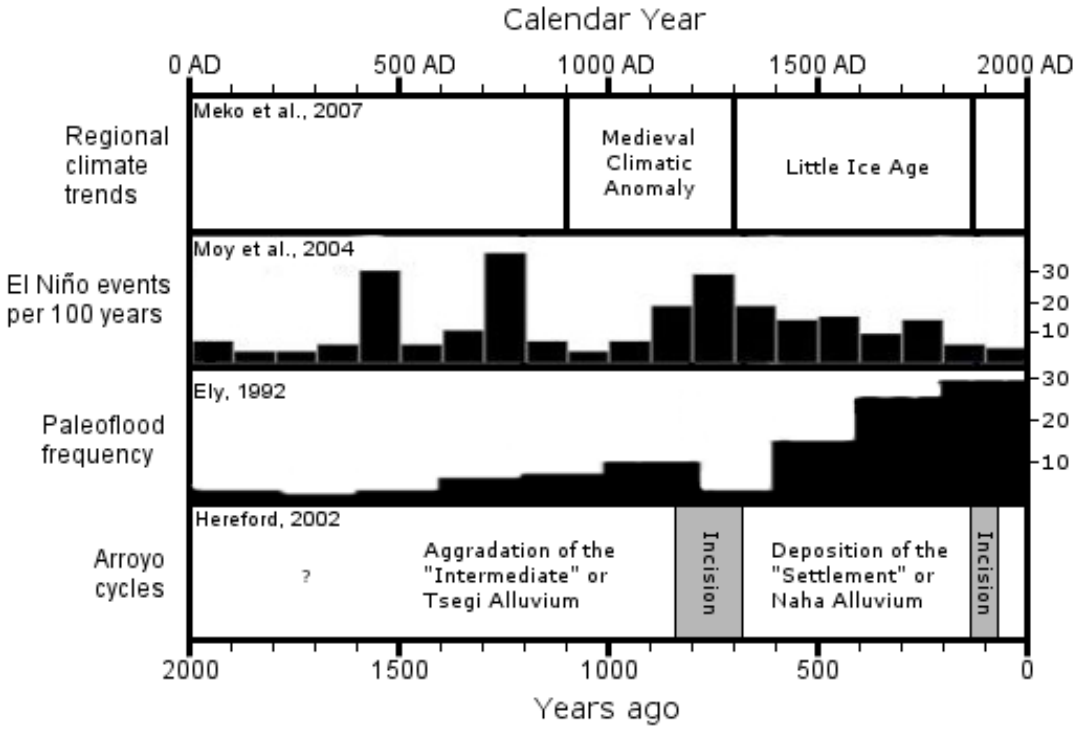

Figure 2-1 – Records for the interior West: A) Regional climate trends; B) Number of strong El Niño events per 100 years; C) Paleoflood frequency in the southwestern U.S.; D) Regional arroyo cycles.

Mechanisms linking decadal- to centennial-scale climate cycles to arroyo cut and fill cycles are debated. Hereford (2002) suggested that during cooler, wetter periods, increased freeze-thaw action on hillslopes may increase sediment yield sufficiently to result in regional channel aggradation. Each of Graf (1987), Graf et al. (1991), and Pederson (2000) concluded that sediment storage and mobilization within upper fluvial systems, rather than from hillslopes, is a key process in the changes in sediment load and transport associated with valley filling and arroyo cutting. Alternatively, many have pointed to changing hydrology, rather than sediment supply, as the primary driver of channel change. Relating to changes in runoff hydrology, Mann and Meltzer (2007) speculatively tie their reconstructed history of aggradation and incision in northeastern

New Mexico to an undefined millennial-scale cycle in the intensity of the summer monsoon. Others have cited a centennial- to millennial-scale cycle in the frequency of El Niño-Southern Oscillation (ENSO) events as the driver of changes in the frequency and intensity of larger fall and winter cyclonic storm systems (Hereford and Webb, 1992; Ely, 1997; Waters and Haynes, 2001; Hereford, 2002). Regardless of the specific storm types, peaks in the frequency and magnitude of large floods are commonly-cited triggers for the transition from alluviation to incision in semiarid drainages. Naturally, one would look toward historic and prehistoric flood records to test this hypothesis.

Paleoflood Hydrology of Bedrock Canyons

The field of paleoflood hydrology is based on using depositional and erosional evidence to reconstruct floods that occurred before the instrumented record (Patton et al., 1979; Kochel and Baker, 1982). Like for arroyo cycles, there are existing reviews of paleoflood hydrology (Costa, 1987; Baker et al., 2002; Benito and Thorndycraft, 2005; Baker, 2008). Early paleoflood studies were focused on characterizing catastrophic flood events such as glacial outburst floods (Dana, 1882; Bretz, 1923). More common applications of these methods include extending the flood record to refine flood recurrence intervals (e.g. Kochel and Baker, 1982) and paleoflood reconstructions related to climatic trends (e.g. Ely, 1997). Depositional evidence for paleofloods includes slackwater sediments, perched debris, and silt lines plastered on bedrock walls (Patton et al., 1979). Erosional evidence includes scarring on trees within the flood zone, abrasion of bedrock walls, and truncation of landforms such as debris fans.

In the Southwest, paleoflood studies on Holocene timescales rely heavily on slackwater sediments in bedrock canyons. These sand and silt deposits rapidly fall out of suspension in alcoves, interior channel bends, and backwaters upstream of flow constrictions. Repeated deposition in these zones by progressively larger floods produces series of distinct flood deposits, constituting a paleoflood package (Baker et al., 1983; Kochel and Baker, 1988; Benito and Thorndycraft, 2005). The stratigraphy of these packages can then be described and dated, resulting in a paleoflood chronology (e.g. Webb et al., 2002). Workers interested in determining the discharge of specific paleofloods rely on careful identification and surveying of paleostage indicators such as silt lines and slackwater deposit surfaces. Water-surface profiles reconstructed from these PSIs are then input into a hydraulic modeling package such as HEC-RAS to estimate paleoflood discharge (Webb and Jarrett, 2002).

A critical factor in specific discharge reconstructions is knowledge of channel geometry at the time of deposition (Patton et al., 1979). Some researchers have attempted to correct for changes in stream grade and/or channel geometry occurring since deposition from geological evidence (e.g. Webb et al, 2002), although most make the assumption that the modern channel geometry was the same at the time of deposition (Benito and Thorndycraft , 2005). Clearly, this assumption would be invalid in the alluvial reaches described above, where grade typically has changed on the order of 10s of meters on the timescale of decades. Indeed, minimizing this uncertainty is certainly one reason paleoflood hydrologists have focused on constricted bedrock reaches with relatively stable channel boundaries. Still, the validity of this assumption in wider bedrock canyons and transitional reaches is questionable, and some have noted

significant channel aggradation and temporary storage of sediment in these reaches (e.g. Tinkler and Wohl, 1998; Webb et al., 2002).

The southwestern U.S. benefits from an abundance of intact slackwater deposits in bedrock canyons, and there is a large body of work on paleoflood frequency and magnitude across the region as a result. Analyses of this work suggest large floods tend to cluster into particular episodes during the Holocene (Ely, 1997; Harden, 2007), though it is important to note that these analyses include streams ranging from the large trunk drainage of the Colorado River that heads in the Rocky Mountains to lower-order streams on the Colorado Plateau. Ely (1997) noted that these episodes of increased frequency of large floods generally occurred during cooler, wetter periods, such as the Little Ice Age (~1500-1900 AD). Alternatively, overall drier and warmer episodes like the preceding Medieval Warm Period (~1100-1400 AD) are poorly represented in the flood record. She suggested that these centennial-scale climatic variations are related to variations in the frequency of El Niño events, which have been statistically linked to cooler, wetter conditions in the U.S. Southwest (Cayan et al., 1999). Yet, this climate relation is not simple or clear. For example, based on the interpretation that high-magnitude flooding initiated older epicycles of arroyo incision and an independent paleo-lacustrine record of effective moisture, Pederson (2000) concluded that not all peak-erosive flooding corresponded to overall wetter episodes.

Recognizing the Disconnect Between Paradigms

Both geologists studying valley cut-and-fill histories and paleoflood hydrologists reconstructing flood chronologies rely upon alluvial records. In some cases, both

approaches have been demonstrated on the same or nearby streams. For example, Kanab Creek, a tributary of the Colorado River in Grand Canyon, has seen work reconstructing arroyo cut-and-fill cycles (Smith, 1990) as well as studies of paleoflood deposits in its downstream constricted bedrock canyon (Smith, 1990; Y. Enzel, unpublished data). Less than a hundred miles to the east, the Paria River has also seen both cut-and-fill (Hereford, 1986, 2002) and paleoflood (Webb et al., 2002) approaches. In a much larger-scale example, workers have studied the Colorado River through Grand Canyon from both perspectives (O'Connor et al., 1994; Hereford et al., 1996). Yet little work has been done to reconcile these records and their distinct interpretations regarding channel processes and controls.

Another problematic aspect of this disconnect is the fact that a gray zone or transition exists between end-member reaches of slackwater flood deposits and more complex aggradational valley fills. The landscape is full of only somewhat constricted reaches with alluvial records that have an unclear affinity. For instance, a single drainage featuring an alluvial reach that grades into a constricted reach must at some point transition from one record type to the other. This transition should be quantifiable; perhaps via thresholds relating to the hydraulic environments that favor transport versus storage of sediment.

Few workers have addressed the first issue of the chronostratigraphic relation between the record types. Graf (1987) studied the patterns of sediment storage and evacuation for streams of different order. He concluded that storage and transport of sediment was most sensitive to climatic and land-use changes in local streams (drainage areas of 10^1 - 10^3 $km^{2)}$, while regional streams (10^3 – 10^4 km^2) stored and evacuated

sediment in response to the supply from local streams upstream. This suggests that sediment storage propagates from local streams toward regional streams over time; a pattern that should be visible in the stratigraphy.

For his doctoral dissertation, Webb (1985) attempted to directly address and reconcile alluvial records from both valley geometries in a single drainage in the Escalante River drainage of south-central Utah. The Escalante River has a pattern common to the Colorado Plateau, consisting of an upstream reach with an arroyo cut into a broad valley fill and a downstream reach that is significantly constricted by bedrock walls. Webb studied deposits in the upper alluvial reach to reconstruct its arroyo cut-and-fill history, as well as deposits in the constricted reach to develop a paleoflood chronology for the river. Constraining the age of deposits with radiocarbon, the instrumented record, and historic photographs, he identified several downstream flood deposits that can be correlated to times when an incised arroyo was present upstream. Especially convincing were those flood deposits associated with historic arroyo-cutting. Despite this recent anti-correlation, many large floods in the Escalante record also apparently occurred while there was no arroyo upstream. Overall, Webb's work suggests that flood deposits in constricted reaches are not correlated in a simple way to periods of arroyo entrenchment upstream.

Working on Harris Wash, a tributary in the greater Escalante River basin, Patton and Boison (1986) identified sandy flood deposits that they speculate are temporally correlated with incision of valley-fills upstream. They noted that the flood deposits linked to upstream incision were generally best-preserved in areas of flow separation near bedrock walls, yet, the sedimentological characteristics that distinguish these deposits

from the alluvial-valley fills are not clearly described. Despite linking the flood deposits to incision episodes, they argue that landslides along the nearby Straight Cliffs have been the primary control on the timing of aggradation and incision in the stream. However, they do suggest that further identification and dating of these incision-related flood packages can greatly refine the complex alluvial history of the region.

Harden (2007) approached the relation of alluvial and paleoflood deposits from a different perspective. For her M.S. thesis, she compiled a database of radiocarbon dates from published paleoflood and arroyo cut-and-fill archives from the low deserts of southern Arizona to the high deserts of the Colorado Plateau. From this database, she constructed cumulative probability distribution functions (CPDFs) for "flood deposits" found in both bedrock reaches and alluvial reaches. The temporal pattern of these data illustrates a complex relationship between deposition in alluvial and bedrock reaches (Figure 2-2). The reaches appear to be broadly anticorrelated, especially toward the latter part of the record. It is somewhat problematic that this study covered such a large region. Climate changes can be manifested differently across the study area, and individual signals could be obscured when summing data across disparate localities. Additionally, drainages of many different sizes were included in the study, running into some of the issues highlighted by Graf (1987). For instance, localized monsoonal thunderstorms may produce geomorphically-significant floods on lower-order streams and have no effect on regional trunk drainages. Finally, no distinction was made between those flood deposits that could be attributed to rare, high magnitude floods and those that occur more frequently. While the exercise is a good first-order approach, it leaves many questions about the complex relations between bedrock and alluvial reach deposits.

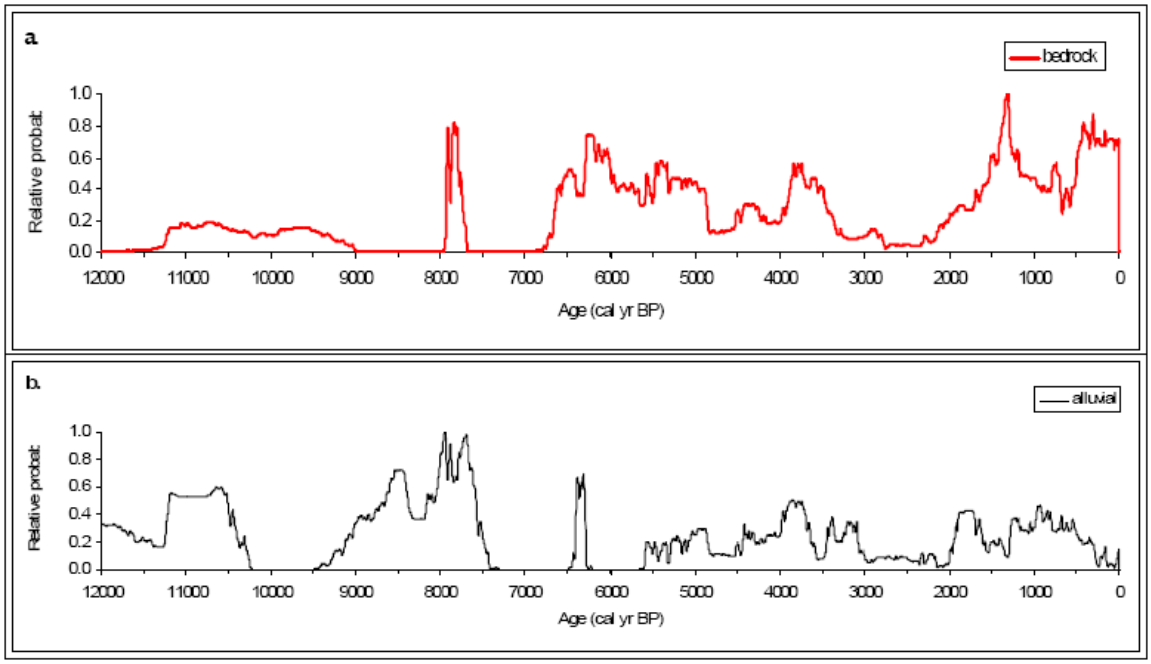

Figure 2-2 – Cumulative probability distribution functions (CPDFs) for radiocarbon dated deposits in (a) bedrock and (b) alluvial reaches. Reproduced from Harden (2007).

The same approach is taken by Benito et al. (2008). They compile 79 radiocarbon dates from 17 studies spanning 11 kyr into CPDFs of alluvial overbank deposits from reaches characterized by cutting-and-filling cycles and slackwater deposits for a series of 13 rivers throughout Spain. Again, in the early-mid Holocene portion of the record, there appears to be no correlation or anticorrelation between the two alluvial record types. Toward the late Holocene, however, an anti-correlation is more apparent. This supports the tentative results of Webb (1985) and Harden (2007) that incision of alluvial fills can be related to the same floods that emplace slackwater deposits along the streams of the study area for recent geological history.

Direct comparison of the published paleoflood record with the record of arroyo cutting and filling is difficult, in part due to the contrasting temporal resolution between

them. Arroyo cut-and-fill records are more numerous and supported by a close association with archaeological studies, radiocarbon ages, and dendrochronology. The paleoflood record, on the other hand, is limited to a far smaller dataset. Additionally, the regional flood chronology constructed by Ely (1997) bins large flood events into 200-year intervals. We know, however, that arroyo headcuts can pass through a drainage in a matter of a few years to decades. Similarly, climatic shifts like those Hereford (2002) invokes can take place over decadal timescales. For example, the transition from the Medieval Warm Period to the Little Ice Age (~1200-1400 AD) was characterized by a local minimum in flood frequency in Ely's reconstruction (Figure 2-1), while the Prehistoric (post-Tsegi) arroyo cutting took place in many regional drainages during that same period (Hereford, 2002) (Figure 2-1). Regional summaries of radiocarbon dates on slackwater deposits in constricted reaches and floodplain deposits in alluvial reaches such as those published by Benito et al. (2008) and Harden (2007) improve upon the problem of low temporal resolution. However, these studies rely solely on radiocarbon dates, which carry a range of uncertainties associated with residence times, post-depositional alteration of organic material, and calibration from radiocarbon to calendar years.

Reconciliation

The studies summarized above are examples of how varying alluvial records have been used to reconstruct the behavior of streams in the southwestern U.S.. They also illustrate the questions that remain regarding the reconciliation of the resulting records. Are constricted-reach channels truly stable over Holocene time, while neighboring alluvial reaches of the same streams see grade changes on the order of 10s of meters?

How do alluvial records geometrically transition from one record type to the other along a single drainage? Are large floods only recorded as slackwater deposits in constricted reaches, or do they leave erosional or depositional evidence in valley fills? In a single drainage, do the largest floods drive arroyo-cutting whereas most floods result in valley-filling? Can we define the hydraulic and geometric transition or threshold beween end members and clarify their utility?

We suggest that resolving these issues will require a series of focused chronostratigraphic studies following the lead of Webb (1985); wherein records from both end-member reach types of a single drainage are studied and compared in detail. A suite of geochronologic methods must be used, including new tools like optically-stimulated luminescence, short-lived isotopes, and more traditional radiocarbon, dendrochronologic, and archeological methods. Such a multi-pronged approach can provide the high-resolution temporal constraints required to conduct inter-drainage correlations. Also needed are more detailed sedimentological studies in order to achieve a process-based understanding of deposition across the two major reach types.

Thanks to advances in hydraulic modeling techniques, exploration of the role that valley geometry plays in controlling long-term stream behavior in constricted vs. alluvial reaches is becoming increasingly possible. Two-dimensional models such as MD-SWMS may be better able to capture the complex boundary conditions and across-channel variations in velocity or shear stress than existing one-dimensional models (Miller and Cluer, 1998). It will be newer tools like these that can be used to help identify thresholds in valley geometry that lead to the preservation of different records.

What follows is an example of a focused chronostratigraphic study in Buckskin Wash, a tributary to the Paria River that features both a broad alluvial reach and a narrow constricted reach. The approach builds on Graf's (1987) concepts of stream response as a function of drainage area, and is similar to the along-stream approach taken by Webb (1985) and Webb et al. (1991). We also build upon previous paleohydrologic efforts in the drainage by Hereford (2002) and Ely (1992) with new study sites, more detailed sedimentology and stratigraphy, and new geochronological techniques.

REFERENCES

Antevs, Ernst, 1952, Arroyo-cutting and filling: Journal of Geology, v. 60, p. 375–385.

Bailey, R. W., 1935, Epicycles of erosion in the valleys of the Colorado Plateau province: Journal of Geology, v. 60, p. 375-385.

Baker, V. R., 2008, Paleoflood hydrology: Origin, progress, prospects: Geomorphology, v. 101, p. 1-13.

Baker, V. R., Kochel, R. C., Patton, P. C., Pickup, G., 1983, Palaeohydrologic analysis of Holocene flood slack-water sediments: Special Publications in Ass. Sediment, v. 6, pp. 229-239.

Baker, V. R., Webb, R. H., House, P. K., 2002, The Scientific and Societal Value of Paleoflood Hydrology, *in* House, P. K., Webb, R. H., Baker, V. R., Levish, D. R., eds., Ancient Floods Modern Hazards – Principles and Applications of Paleoflood Hydrology: Washington DC, American Geophysical Union, p. 1-19.

Benito, G., and Thorndycraft, V. R., 2005, Paleoflood hydrology and its role in applied hydrological sciences: Journal of Hydrology, v. 313, p. 3-15.

Benito, G., Thorndycraft, V.R., Rico, M., Sanchez-Moya, Y., and Sopena, A., 2008, Palaeoflood and floodplain records from Spain: Evidence for long-term climate variability and environmental changes: Geomorphology, v. 101, p. 68-77.

Bretz, J.H., 1923, The Channeled Scabland of the Columbia Plateau: Journal of Geology, v. 31, 617–649.

Bryan, K., 1925, Date of channel trenching (arroyo-cutting) in the arid Southwest: Science, v. 62, p. 338-344.

Cayan, D. R., Redmond, K. T., and Riddle, L. G., 1999, ENSO and hydrologic extremes in the western United States: Journal of Climate, v. 12, p. 2881-1893.

Cooke, R.U., and Reeves, R.W., 1976, Arroyos and environmental change: Oxford, Clarendon Press, 213 p.

Costa, J. E., 1987, A History of Paleoflood Hydrology in the United States, 1800-1970, *in* Landa, E. R., Ince, S., eds., History of Hydrology. History of Geophysics Number 3: Washington, DC, American Geophysical Union, p. 49-53.

Dana, J.D., 1882. The flood of the Connecticut River valley from the melting of the Quaternary glacier: American Journal of Science, v. 123, 179–202.

Daniels, J. M., 2008, Distinguishing allogenic from autogenic causes of bed elevation change in late Quaternary alluvial stratigraphic records: Geomorphology, v. 101, p. 159-171.

Ely, L. L., 1992, Large Floods in the Southwestern United States in Relation to Late-Holocene Climatic Variations [Ph.D. dissertation]: Tucson, University of Arizona, 326 p.

Ely, L. L., 1997, Response of extreme floods in the south-western United States to climatic variations in the late Holocene: Geomorphology, v. 19, p. 175-201.

Graf, J. B., Webb, R. H., and Hereford, R., 1991, Relation of sediment load and flood-plain formation to climatic variability, Paria River drainage basin, Utah and Arizona: Geological Society of America Bulletin, v. 103, p. 1405-1415.

Graf, W. L., 1983, The arroyo problem—Paleohydrology and paleohydraulics in the short term, *in* Gregory, K.G., ed., Background to Paleohydrology: New York, John Wiley and Sons, p. 279-302.

Graf, W.L., 1987, Late Holocene sediment storage in canyons of the Colorado Plateau: Geological Society of America Bulletin, v. 99, p. 261–271.

Hack, J. T., 1942, The changing physical environment of the Hope Indians of Arizona: Peabody Museum Papers, v. 25, no. 1., 85 p., 12 plates.

Hall, S.A., 1977, Late Quaternary sedimentation and paleoecologic history of Chaco Canyon, New Mexico: Geological Society of America Bulletin, v. 88, 1593–1618.

Harden, T. M., 2007, A 12,000-year Probability-Based Flood Record in the Southwestern United States [M.S. thesis]: Tucson, University of Arizona, 34 p.

Haynes, C. V. Jr., 1968, Geochronology of late-Quaternary alluvium, *in* Morrison, R. B., and Wrigh, H. E., Jr., eds., Means of Correlation of Quaternary Successions: Salt Lake City, University of Utah Press, p. 591-631.

Hereford, R., 1986, Modern alluvial history of the Paria River drainage basin: Quaternary Research, v. 25, p. 293-311.

Hereford, R., 2002. Valley-fill alluviation during the Little Ice Age (ca. A.D. 1400-1880), Paria River basin and southern Colorado Plateau, United States: Geological Society of America Bulletin, v. 114, p. 1550-1563.

Hereford, R., Thompson, K. S., Burke, K. J., and Fairley, H. C., 1996, Tributary debris fans and the late Holocene alluvial chronology of the Colorado River, eastern Grand Canyon, Arizona: Geological Society of America Bulletin, v. 108, p. 3-19.

Hereford, R, and Webb, R. H., 1992, Historic variation of warm-season rainfall, southern Colorado Plateau, southwest United States: Climatic Change, v. 22, p. 239-256.

Hughes, M. K., and Diaz, H. F., 2008, Climate variability and change in the drylands of western North America: Global and Planetary Change, v. 64, p. 111-118.

Knox, J. C., 1983, Response of river systems to Holocene climates, *in* Wright, H.E., Jr., ed., Late Quaternary environments of the United States, Volume 2, The Holocene: Minneapolis, University of Minnesota Press, p. 26–41.

Kochel, R. C., and Baker, V. R., 1982, Paleoflood Hydrology: Science, v. 215, p. 353-362

Kochel, R.C., Baker, V.R., 1988. Palaeoflood analysis using slackwater deposits. *in* Baker, V.R., Kochel, R.C., Patton, P.C., eds., Flood Geomorphology: New York, Wiley, p. 357-376.

Leopold, L.B., 1976, Reversal of erosion cycle and climatic change: Quaternary Research, v. 6, p. 557-562.

Mann, D. H., and Meltzer, D. J., 2007, Millennial-scale dynamics of valley fills over the past 12,000 14C yr in northeastern New Mexico, USA: Geological Society of America Bulletin, v. 119, p. 1433-1448.

Meko, D. M., Woodhouse, C. A., Baisan, C. A., Knight, T. K., Lukas, J. J., Hughes, M. K., and Salzer, M. W., 2007, Medieval drought in the upper Colorado River Basin: Geophysical Research Letters, v. 34, p.

Miller, A. J., and Cluer, B. L., 1998, Modeling considerations for simulation of flow in bedrock channels, *in* Tinkler, K. J., and Wohl, E. E., eds*.,* Rivers over Rock – Fluvial Processes in Bedrock Channels: Washington, D. C., American Geophysical Union, 323 p.

Moy, C. M., Seltzer, G. O., Rodbell, D. T., and Anderson, D. M., 2004, Variability of El Niño/Southern Oscillation activity at millennial timescales during the Holocene epoch: Nature, v. 420, p. 162-165.

O'Connor, J. E., Ely, L. L., Wohl, E. E.,Stevens, L. E., Melis, T. S., Kale, V. S., and Baker, V. R., 1994, A 4500-year record of large floods on the Colorado River in the Grand Canyon, Arizona: Journal of Geology, v. 102, p. 1-9.

Patton, P. C., Baker, V. R., and Kochel, R. C., 1979, Slackwater deposits: A geomorphic technique for the interpretation of fluvial paleohydrology, *in* Rhodes, D. D., and Williams, G. P., Adjustments of the Fluvial System: Dubuque, IA, Kendall-Hunt, 1979, p. 225-252.

Patton, P. C., and Schumm, S. A., 1981, Ephemeral-stream processes: Implications for studies of Quaternary valley fills: Quaternary Research, v. 15, p. 24-43.

Patton, P. C., and Boison, P. J., 1986, Processes and rates of formation of Holocene alluvial terraces in Harris Wash, Escalante River basin, south-central Utah: Geological Society of America Bulletin, v. 97, p. 369-378.

Pederson, J. L., 2000, Holocene paleoloakes of Lake Canyon, Colorado Plateau: Paleoclimate and landscape response from sedimentology and allostratigraphy: Geological Society of America Bulletin, v. 112, p. 147-158.

Schumm, S. A., and Hadley, R. F., 1957, Arroyos and the semiarid cycle of erosion: American Journal of Science, v. 255, p. 161-172.

Schumm, S. A., and Parker, R. S., 1973, Implications of complex response of drainage systems for Quaternary alluvial stratigraphy: Nature (Physical Science), v. 243, p. 99-100.

Smith, S. S., 1990, Relationship of large floods and rapid entrenchment of Kanab Creek, southern Utah [M.S. thesis]: Tucson, University of Arizona, 82 p.

Tinkler, K. J., and Wohl, E. E., 1998, A primer on bedrock channels, *in* Tinkler, K. J., and Wohl, E. E., eds*.,* Rivers over Rock – Fluvial Processes in Bedrock Channels: Washington, DC, American Geophysical Union, 323 p.

Tooth, S., 2000, Process, form, and change in dryland rivers; a review of recent research: Earth-Science Reviews, v. 51, p. 61-107.

Tucker, G. E., Arnold, L., Bras, R. L., Flores, H., Istanbulluoglu, E., and Solyon, P., 2006, Headwater channel dynamics in semiarid rangelands, Colorado high plains, USA: Geological Society of America Bulletin, v. 118, p. 959-974.

Waters, M. R., 1985, Late Quaternary alluvial stratigraphy of Whitewater Draw, Arizona: Implications for regional correlation of fluvial deposits in the American Southwest: Geology, v. 13, p. 705-708.

Waters, M. R., and Haynes, C. V. Jr., 2001, Late Quaternary arroyo formation and climate change in the American Southwest. Geology, v. 29, p. 399-402.

Webb, R.H., 1985, Late Holocene flooding on the Escalante River, south-central Utah [Ph.D. thesis]: Tucson, University of Arizona, 204 p.

Webb, R. H., Blainey, J.B., and Hyndman, D.W., 2002, Paleoflood hydrology of the Paria River, southern Utah and northern Arizona, USA, *in* House, P.K., Webb, R.H., Baker, V.R., and Levish, D.R., eds., Ancient Floods and Modern Hazards: Principles and Applications of Paleoflood Hydrology: American Geophysical Union Water Science and Application Series, v. 5, p. 295–310.

Webb, R. H., and Jarrett, R. D., 2002, One-Dimensional estimation techniques for discharges of paleofloods and historical floods, *in* House, P.K., Webb, R.H., Baker, V.R., and Levish, D.R., eds., Ancient Floods and Modern Hazards: Principles and Applications of Paleoflood Hydrology: American Geophysical Union Water Science and Application Series, v. 5, p. 111-125.

CHAPTER 3

THE ALLUVIAL RECORDS OF BUCKSKIN WASH, COLORADO PLATEAU

INTRODUCTION

Alluvial deposits stored along dryland streams preserve a record of environmental change in their watersheds. Approaches to the interpretation of these records have diverged in recent decades, leading to some confusion (see Chapter 2). While workers reconstructing arroyo cut-and-fill histories have focused on broad alluvial valleys characterized by high channel variability and sediment storage, the bulk of the work done by paleoflood hydrologists has focused on constricted bedrock canyons where sediment storage and changes in channel geometry are often assumed to be negligible over millennial timescales.

While both arroyo cut-and-fill and paleoflood approaches are suited to their respective end-member valley geometries, the landscape is full of stream reaches that have an ambiguous, potentially transitional geometry. In these enigmatic places, it is unclear which paradigm is applicable to the alluvial deposits therein. Are there specific sedimentologic characteristics that can be used to determine whether deposits in a particular reach record only large paleofloods or a more complex suite of valley-filling events? In a single stream featuring both end-member geometries along its length, at what point does it transition from one record type/assumed stream behavior to the other?

A second component of the problem is that the stratigraphic and temporal relations between the two types of records are poorly understood, despite often occurring in different reaches of the same drainage. Many workers have shown that late Holocene

cut-and-fill cycles occur over century-to-millennial timescales and can be correlated regionally (e.g. Hack, 1942; Graf, 1983; Hereford, 2002). Such agreement across adjacent drainages is strongly indicative of an allogenic forcing such as climate change. One popular conceptual model suggests that alluvial valleys aggrade during periods with relatively few large, erosive floods and are incised during episodes of increased flood frequency (Graf, 1988; Webb et al., 1991; Hereford, 2002). These episodes of flood-induced erosion of valley-fills, then, should be recorded by paleoflood deposition in bedrock canyons of the same drainages. A testable hypothesis of this model is that in a single stream, deposition is temporally anti-correlated between alluvial valleys and bedrock canyons downstream.

Here I address this hypothesis via focused chronostratigraphic study in an ephemeral stream of the Colorado Plateau. The greater Buckskin drainage features a classic alluvial reach with a broad valley fill draining into a constricted slot canyon with locally preserved paleoflood deposits. Previous efforts in the study area include both contrasting approaches of arroyo cut-and-fill reconstructions (Hereford, 2002) and paleoflood hydrology (Ely, 1992). Detailed sedimentology and stratigraphy was performed to compare the style of deposition across the reaches, and new geochronological data was collected to improve upon and expand existing records. Finally, I gathered survey data to document the geometry of key reaches for input into a future hydraulic modeling effort aimed at exploring the geometric transition between the two end-member valley geometries.

STUDY AREA

Buckskin Wash is a major tributary of the Paria River in the southern Colorado Plateau, with a drainage area of 987 km^2 (Figure 3-1). It includes two main forks: Kitchen Corral Wash and Coyote Wash. Kitchen Corral Wash heads in the Mesozoic - Tertiary sandstones and mudstones of the Grand Staircase before cutting across the Permian limestones and sandstones of the Kaibab Plateau (Doelling and Davis, 1989) (Table 3-1, Figures 3-1, 3-2). Coyote Wash drains the Kaibab and Paria plateaux and flows north along a strike valley of the East Kaibab monocline. The two forks meet in the upstream end of Buckskin Gulch, a narrow slot canyon incised into the relatively resistant Navajo Sandstone. The slot canyon continues eastward for over 12 km to its confluence with the Paria River in Paria Canyon. Buckskin Gulch is thought to be the longest slot canyon in North America and is very popular with hikers.

The watershed ranges in elevation from ~2800 m at the top of the Grand Staircase to ~1270 m at its confluence with the Paria River. Climate is semiarid, though there is considerable variation as a function of elevation. Weather stations at Lees Ferry, AZ (elev. 978 m), Kanab, UT (1494 m), and Bryce Canyon (2413 m) span the elevational range of the watershed and report mean annual temperatures of 62.9 F, 54.6 F, and 41.5, F, respectively. Mean annual precipitation values for the same sites are 168 mm, 381 mm, and 419 mm, respectively (Western Regional Climate Center). Most precipitation can be categorized into three seasonal storm regimes: late winter mid-latitude cyclones, summer monsoonal thunderstorms, and early fall tropical cyclones (Figure 3-2). Differences between the sites illustrate a strong orographic amplification of precipitation.

Vegetation varies accordingly, with a mixed conifer forest in the highlands grading into Pinyon/Juniper and sagebrush steppe in the lowlands and floodplains.

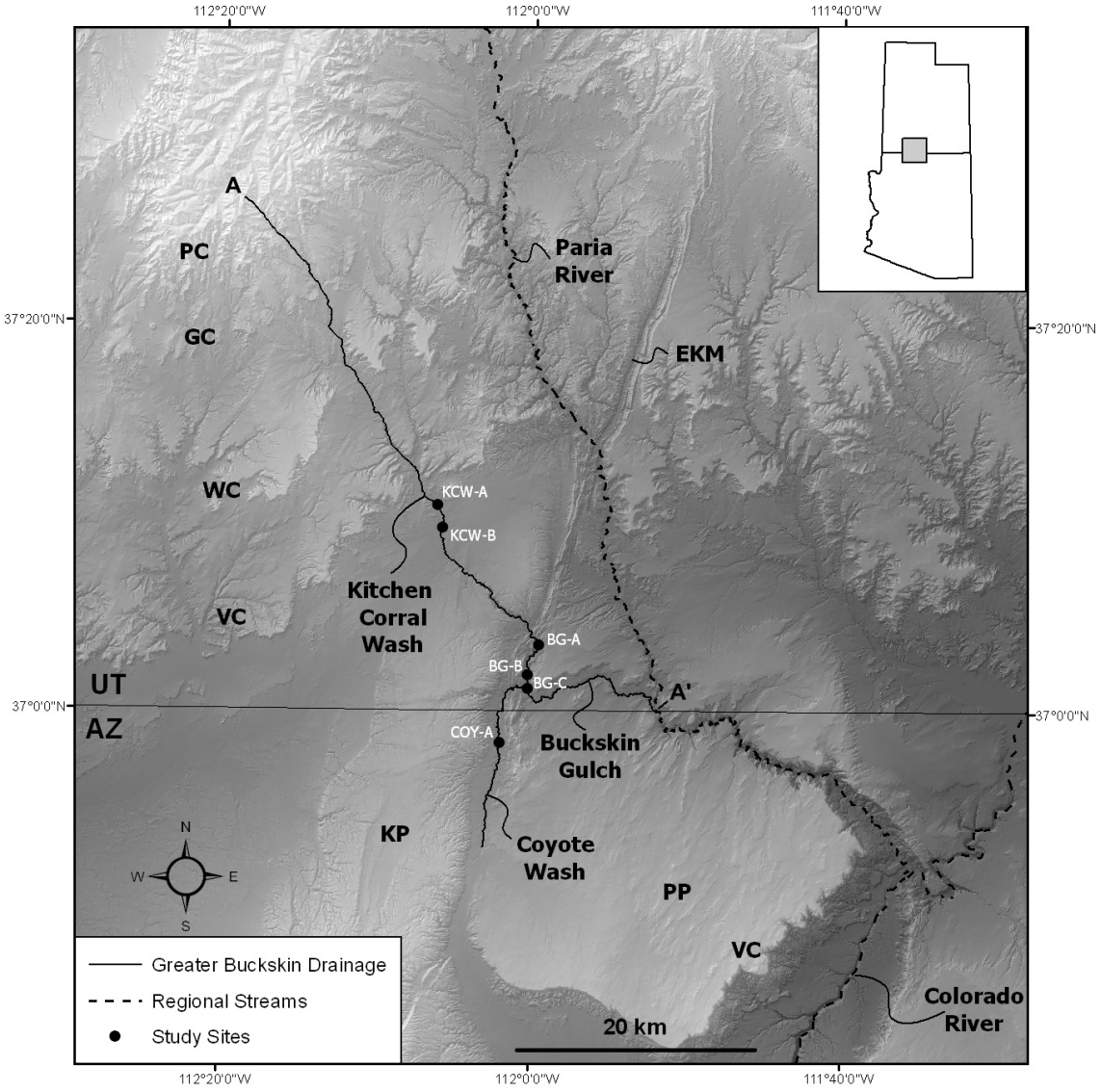

Figure 3-1 – Map of study area showing study site locations and topography. KP-Kaibab Plateau, PP-Paria Plateau, VC-Vermillion Cliffs, WC-White Cliffs, GC-Gray Cliffs, and PC-Pink Cliffs, EKM-East Kaibab Monocline.

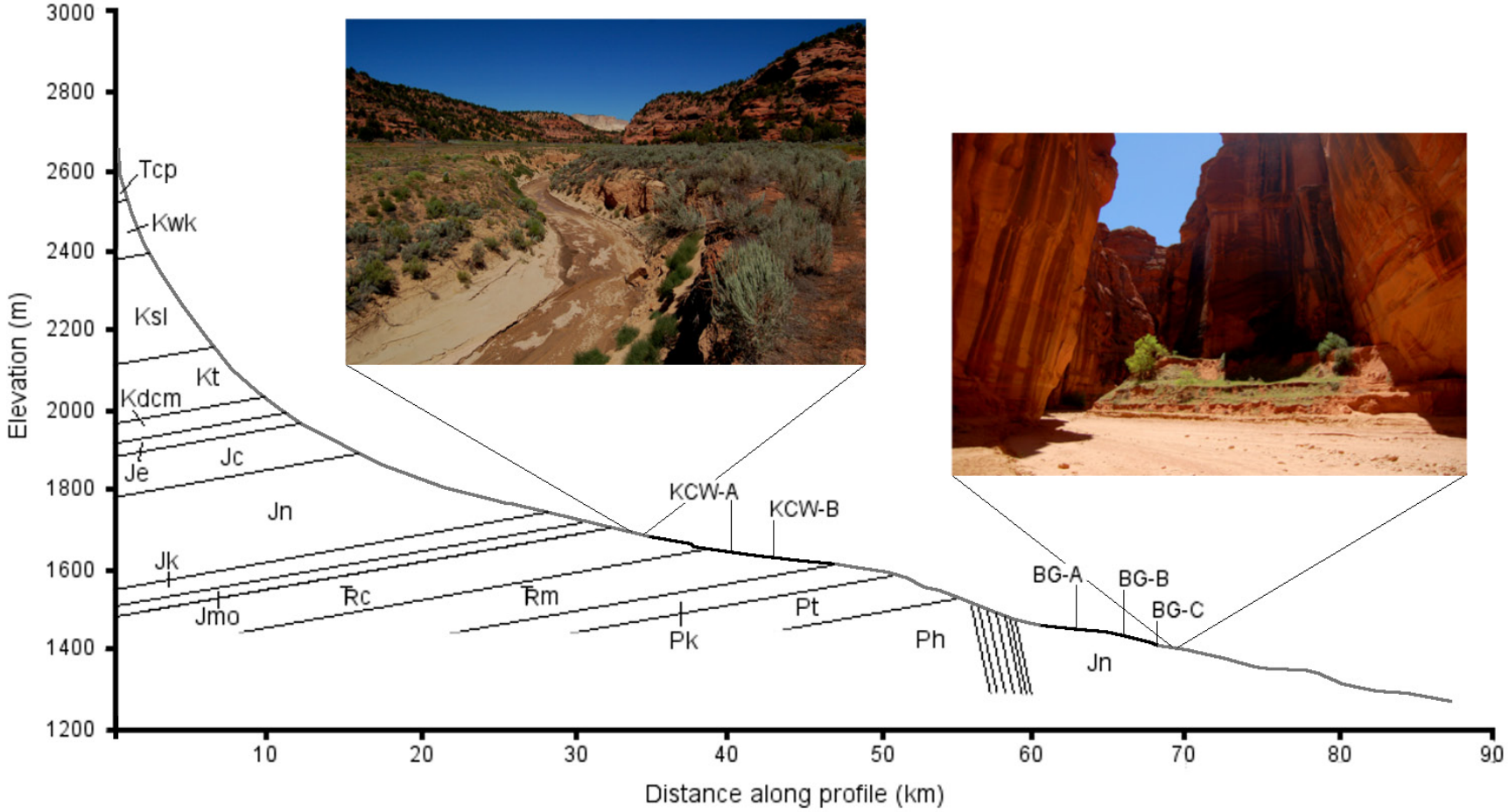

Figure 3-2 – Longitudinal profile of the greater Buckskin drainage, along line A-A' (Figure 3-1). Profile constructed from field survey data (dark) and a 5-m DEM (light). Representative valley geometries are shown for Kitchen Corral Wash (a) and Buckskin Gulch (b). Bedrock representations are approximate and are based on Doelling and Davis (1989). See Table 3-1 for key to lithologies. Vertical Exaggeration = ~25x.

Table 3-1 – Key to lithologies in the study area (Doelling and Davis, 1989)

Symbol	Formation/Unit name
Tcp	Claron Fm
Kwk	Wahweap/Kaiparowitz Fm
Ksl	Straight Cliffs Fm
Kt	Tropic Shale
Kdcm	Dakota Sandstone/Mancos Shale
Je	Entrada Sandstone
Jc	Carmel Fm
Jn	Navajo Sandstone
Jk	Kayenta Fm
Jmo	Moenave Fm
TRc	Chinle Fm
TRm	Moenkopi Fm
Pk	Kaibab Limestone
Pt	Toroweap Fm
Ph	Hermit Shale

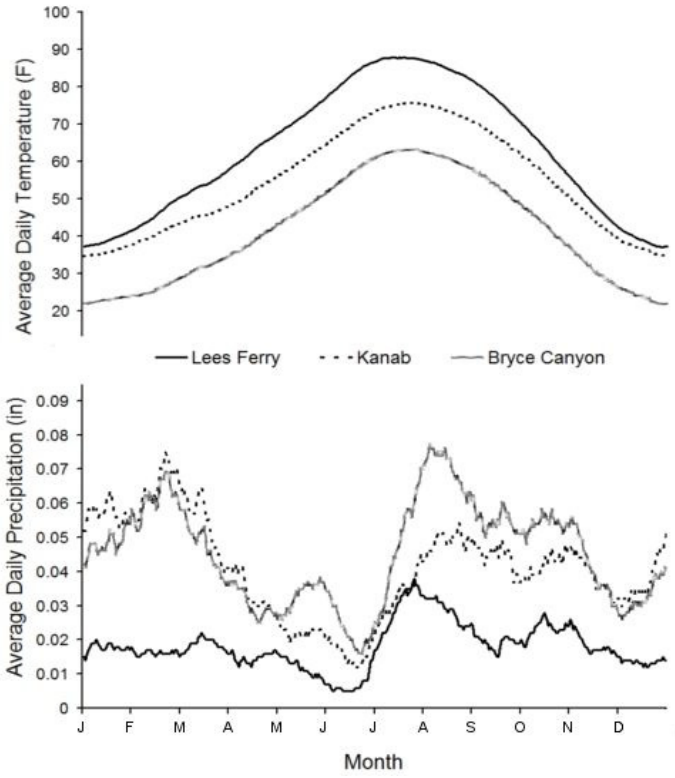

Figure 3-3 – Seasonal temperature and precipitation patterns across the study area. Data from Western Regional Climate Center; period of record: 1970-2000 AD.

Kitchen Corral Wash, Coyote Wash, and most of the tributaries of the upper catchment flow through alluvial valleys between 100 – 400 m wide, bounded on either side by bedrock cliffs and/or high gravelly terraces. Within these active alluvial valleys, the modern streams flow through a continuous arroyo system incised 2-10 meters below the surrounding valley fill. This arroyo network was cut most recently between ~1880 and 1910 AD (Gregory and Moore, 1931, Webb, 1985, Hereford, 1986). Larger tributaries have cut their own arroyos, probably in response to the base level fall associated with the cutting of the mainstem arroyo. Earlier visitors to the area, including the Dominguez-Escalante mission of the late 1770s, observed streams flowing in broad, shallow channels on the surface of grass-covered alluvial valleys (Reagan, 1924; Webb, 1985). Though the cause of the historic arroyo-cutting is debated, a combination of floodplain alteration and the propagation of steep knickpoints during a series of exceptionally large floods was observed in several regional streams at the time (Cooke and Reeves, 1976; Webb, 1985; Webb et al., 1991). Since the arroyo entrenchment at the turn of the century, up to 2 m of sediment has been deposited on the bottom of the arroyo network beginning during the mid-century drought 1940-1980 AD (Leopold, 1976; Hereford, 1986). Field observations during this study indicated that modern floods are once again actively aggrading these in-arroyo floodplains.

After crossing the East Kaibab monocline, the alluvial valley becomes increasingly confined between bedrock walls of Navajo Sandstone before plunging into the true slot canyon of Buckskin Gulch. In this transitional reach, a single, prominent fill terrace ~3 – 5 m high stretches from the channel to the bedrock walls on either side, which vary between ~10 and ~200 m apart. Rounded gravels and boulders as well as and

abundant sand dunes mantle the bedrock topography above the alluvial valley, supplying sediment via small tributaries and hillslopes. The smaller of these tributaries debouche onto the valley-fill terrace as low-relief alluvial fans whereas larger tributaries have incised into the main terrace. Inset into the main terrace and lining much of the channel is an active floodplain 1.5 - 2 m high, analogous to that found upstream.

The constricted reach of Buckskin Gulch has a markedly different valley geometry than the reaches described above. Here, the stream is confined between ~vertical bedrock walls 10s-100s of meters high and 2-10 m apart. The streambed alternates between sandy and bouldery reaches; the coarser reaches tend to have steeper gradients. In Wire Pass, the slot canyon through which Coyote Wash enters Buckskin Gulch, 1-3 m boulders form knickpoints up to 3 m high. Deeper into Buckskin Gulch, large rockfalls form a series of major knickpoints on the order of 10-15 m high. The lowermost reaches of Buckskin Gulch are relatively flat and sandy, and maintain a spring-fed baseflow year-round. The only alluvial deposits to speak of in Buckskin Gulch are found in rare expansions and alcoves, forming sandy terraces ~9-12 m above the modern wash. Inset into these higher deposits at the two largest expansions is a 1-2 m high low-flow floodplain not unlike the modern floodplains upstream. The statement by Graf et al. (1991) that these floodplains did not exist in Buckskin Gulch indicates that these channel-margin deposits have either formed since 1991, or that that their existence had not been groundchecked at the time.

PREVIOUS WORK

Several previous research efforts in the Buckskin-Kitchen Corral watershed demonstrate the end-member approaches to alluvial reconstructions. Working in the broad alluvial reaches of the Paria River basin, Hereford (1986) investigated the cutting and subsequent refilling of the historic arroyos and relations to climate change. He described the stratigraphy of the in-arroyo floodplains mentioned above and dated its components using repeat photography and dendrochronology. He constrained the age of these deposits to a period of floodplain building between 1940 and 1980 AD. This work was followed up by Graf et al. (1991), who used historical records to determine the role of climate, sediment load, and hydrology in building the in-arroyo floodplains. They confirmed that a decrease in magnitude and frequency of floods took place beginning around 1940. At the time of publication, they stated that no floods had topped the floodplains since 1980. They suggested that temporary storage of sediment on floodplains in the alluvial reaches of the Paria basin were related to decreased sediment loading to the Colorado River downstream.

In a later contribution, Hereford (2002) studied the valley-fill stratigraphy along both Kitchen Corral Wash and Coyote Wash to document the episode of aggradation that preceded the historic arroyo cutting. Several buried juniper trees and samples of organic material were radiocarbon-dated to constrain the timing of this aggradational package from roughly 1350 AD to 1880 AD. He deemed this valley-fill the “Settlement” alluvium, and correlated it to several other aggradational packages in the southern Colorado Plateau of similar age, including the “Naha” alluvium from the Black Mesa

region of Arizona (Hack 1942), the "post-Bonito" alluvium of the Chaco Canyon region (Hall, 1977), and the "Settlement" Alluvium of the Virgin River (Hereford, 1996). He argued that fine-grained material derived from hillslopes in tributary catchments was the source for this valley fill, as evidenced by interfingering tributary and mainstem alluvium exposed in arroyo walls. A regional cooling during the Little Ice Age and increase in granular disintegration was cited as the causal factor for the increase in hillslope sediment yield and resulting alluviation of stream valleys (Hereford, 2002).

As part of a regional paleoflood reconstruction, Ely (1992) studied two sites in the Buckskin Gulch slot canyon near and at the confluence of Coyote Wash and Kitchen Corral Wash. She interpreted the alluvial deposits at both sites as a series of paleoflood slackwater deposits, and recorded the number of large floods they represent. She constrained the ages of flood units with radiocarbon dates, though a stratigraphic reversal and potential coal contamination limited their utility at one of the sites. The better-dated paleofloods were then incorporated into a broader regional Holocene flood record (Ely, 1997). A major conclusion of the flood chronology was that large floods tend to cluster into particular intervals over the Holocene; some of which can be correlated to positive-index ENSO events. This work has been heavily cited, as it is one of very few efforts to summarize several paleoflood chronologies into a single regional chronology with paleoclimatic implications. Both of Ely's Buckskin Gulch study sites are revisited in this study.

Webb et al. (2002) likewise examined nearby deposits in the narrow constrictions of the Paria River canyon downstream of its confluence with Buckskin Gulch. All three of their study sites are located in alcoves in the Navajo Sandstone canyon walls. They

described the general stratigraphy of the deposits therein and constrained the ages with radiocarbon and ^{137}Cs (post-bomb) analysis. After surveying channel geometry through a lengthy reach of the canyon, they used step-backwater modeling to estimate the discharges of paleofloods preserved in the alcove deposits. The resulting paleoflood record, combined with the modern instrumented record, consisted of a 4000-year long series of flood events ranked by discharge. Noting geologic evidence for ~20 m of incision since ~20 ka, they recognized that paleostage indicators may have been emplaced when the stream grade was higher. Though the authors accounted for the possibility of steady incision when reconstructing paleodischarges, they did not discuss the possibility or impact of subsequent aggradational episodes and/or temporary sediment storage over the Holocene.

Finally, Topping (1997) studied historic changes along the Paria River between Cannonville, UT and the Colorado River by thoroughly analyzing USGS discharge, sediment load, and climate data. He concluded that there has been effectively no change in the hydrology of the Paria River over the period of record (1923 - 1995), in contrast to the results of Hereford (1986) and Graf et al. (1991). Instead, he argues that the changes observed by previous authors can be explained by changing gaging methods employed by the USGS. He argues that observed channel changes could be solely the result of shifts between "equivalent hydraulic geometries." These shifts are internal adjustments that result in temporary changes in channel slope and geometry, such as the cutoff of a large meander bend or shift in location of the confluence of the Paria and Colorado Rivers.

The two previous efforts most germane to this study are those by Hereford (2002) and Ely (1992), classic examples of the contrasting approaches to interpretation of

dryland alluvial archives. Yet, here within the same greater drainage, these previous studies lack sufficient temporal resolution and sedimentological detail for comparison and reconciliation. Hereford (2002) constrained the ages of prehistoric and historic arroyo-cutting to ~600-750 cal yr BP (1200-1350 AD) and ~50-70 cal yr BP (1880 – 1900 AD), respectively. Just downstream, Ely (1992) dated the base of one of the younger paleoflood packages to <350 cal yr BP (< 1600 AD). Her regional synthesis shows peaks in the frequency of large floods around 2000-1600 BC and 1600 AD to the present. The latter peak corresponds with the later stages of deposition of the "Naha" alluvium and correlative units in many southwestern drainages (Hereford, 2002). It also overlaps the period of arroyo entrenchment and subsequent refilling in those same drainages which are understood to have occurred over a matter of decades. Clearly, the 200 year bins used in Ely's study are too large to resolve such decadal-scale episodes. Webb et al. (2002) recorded the largest floods on the Paria River over the past 4000 yr, though, unlike in Ely's study, they did not highlight any particular episodes of frequent, high magnitude flooding.

Despite these previous efforts throughout the basin, there is insufficient information to determine whether deposition and erosion is correlated, anticorrelated, or just non-correlated across the contrasting geomorphic reaches. This deficiency may be improved greatly with the utilization of diverse geochronometers like OSL, short-lived isotopes, archaeology, and dendrochronology. An additional deficit is the lack of detailed sedimentology required to link the units in the alluvial archives to depositional process. We improve upon these earlier studies by filling these gaps.

METHODS

Stratigraphy

In order to define the stratigraphy of the alluvial reaches of the watershed, three study sites that record the best exposures of valley-fills and paleoarroyos were chosen based on surficial mapping and reconnaissance. Sites KCW-A and KCW-B are located along an alluvial reach of Kitchen Corral Wash upstream of the Kaibab Plateau and COY-A is located in the alluvial reach of Coyote Wash (Figure 3-1). Similarly, three study sites were chosen in the constricted reach. BG-A is located in upper Buckskin Gulch where the volume of the valley fill is markedly less than the alluvial reach upstream, yet channel form is not as constricted by bedrock walls as in the slot canyon just downstream. Sites BG-B and BG-C are located in short expansions within the constricted slot canyon of Buckskin Gulch and correspond to 'Site 2' and 'Site 1' of Ely (1992), respectively.

In order to capture more information than a vertical stratigraphic section, detailed photographic panels were constructed for entire exposures at each site. Beds representing individual stream flow events were easily distinguished, thanks to striking color contrasts, mud partings, and abrupt changes in sedimentology between beds. Rapid changes in the characteristics of a single event can produce two adjacent beds that appear to be separate events, however, this uncertainty was likely limited to very few instances. Depositional units were mapped onto the panels, described, and associated with one of twelve sedimentary facies (Table 3-2). Special attention was given to identifying bounding surfaces, buried soils, and other forms of evidence for depositional hiatuses.

These include obvious surfaces that truncate stratal packages, as well as less-obvious nonconformities marked only by evidence of prolonged surface exposure, including soil development, the presence of rhizoliths, and bioturbation from roots and burrowing organisms. These features helped guide the choice of targets for geochronology, which was aimed at constraining the timing of major shifts in stream behavior.

Geochronology

Age control was provided by a combination of Optically-Stimulated Luminescence (OSL) dating, Accelerated Mass Spectroscopy (AMS) radiocarbon dating, and ^{137}Cs Analysis. In a few places, rough age constraints from ring counts on buried trees and cultural artifacts were also available. Using this suite of independent geochronometers allows verification of methods against one another and provides a more thorough geochronology than would be provided by any individual method alone.

OSL dating provides an estimate of the age of a particular depositional event. Its success depends on full exposure (bleaching) of quartz grains to sunlight during transport, and undisturbed burial since deposition. After burial, defects in the crystal lattice begin to accumulate as a result of β- and γ-rays emanating from radiogenic isotopes in the material immediately surrounding the sample. These defects act as photon traps, the bulk of which release their photons when again exposed to light—a luminescence response. By measuring the luminescence response to a sample of quartz grains upon exposure to a controlled amount light in the laboratory, an age of burial can be derived. For more information about the theoretical basis for OSL dating, the reader is referred to Aitken (1998).

Water-lain sediments are challenging for OSL dating because fluvial transport can result in partial bleaching of quartz grains prior to burial (Bailey et al., 1997). When a deposit contains partially-bleached grains, residual luminescence is inherited from prior burial events, resulting in an age-overestimation. Samples collected initially in this study showed clear signs of partial bleaching, so subsequent target beds included only those that exhibited sedimentary structures indicative of a depositional process favoring more complete bleaching of sand grains. Such facies include subcritical ripple cross-lamination and lower-flow regime plane beds, as they are the product of relatively low sediment loads and flow velocities. Beds with sedimentary structures indicative of high sediment concentration, such as massive, poorly sorted sands and supercritically climbing ripples were avoided, as turbidity greatly reduces penetration of sunlight into the water column (Berger, 1990). In addition, beds exhibiting significant soil development or bioturbation were also avoided, as vertical movement of quartz grains in a sediment column can lead to mixing of units of different ages.

A total of 12 OSL samples were collected and subject to at least initial analyses. Samples were collected in aluminum tubes, opened under darkroom conditions, and processed at the Utah State University Luminescence Lab. Early processing steps included wet-sieving to isolate the 90-150 μm grain size and soaking in HCl and H_2O_2 to remove carbonates and organic material, respectively. Samples were then floated and centrifuged in a Sodium Polytungstate ($3Na_2WO_4 \cdot 9WO_3 \cdot H_2O$) solution to remove heavy minerals. Floated samples were given HF treatment to remove feldspars and remaining non-quartz minerals and to etch the quartz grains for analysis. Samples were then dried and sieved to remove the <75 μm portion.

Processed samples were mounted onto steel disks and analyzed using the single aliquot regenerative-dose (SAR) protocol reviewed by Murray and Wintle (2003). For each sample, this involves exposing dozens of aliquots containing ~15-100 grains to blue light (470 nm) and measuring the natural luminescence response with a Riso TL/OSL-DA-20 reader. Increasing artificial doses of radiation are then given to each aliquot, measuring the luminescence response after each dose. These data are used to construct a signal-response curve for each aliquot. This allows interpolation of the equivalent dose (D_e), or the amount of radiation necessary to force the same luminescence response that was measured initially. Plots showing the distribution of D_e values were constructed for each sample. A positive skew in such a plot was used as an indicator of partial bleaching (Wallinga, 2002). Dose rates (R_d) are calculated for each sample by collecting a representative sample of surrounding material and analyzing its bulk chemistry.

Ages are calculated as:

$$\text{Age (kyr)} = D_e \text{ (Gy)} / R_d \text{ (Gy/kyr)}$$

Usually, the D_e is taken from the mean of >20 accepted aliquots for the age calculation. Results reported here are considered preliminary, as they are usually based on <20 accepted aliquots. Therefore, they do not yet have the precision and meaningful errors of finalized ages. Where partial-bleaching of sand grains is evident, it has been shown that using only the "leading edge," or lower end of the De distribution provides more accurate results than the mean (Fuchs et al., 2007). Due to the extended timescale required to accumulate the necessary number of aliquots, ages reported here for samples showing signs of partial bleaching have been corrected by simply removing those

aliquots that clearly lie outside the expected Gaussian distribution. Because this is a conservative approach to dealing with partial bleaching, all ages from partially-bleached samples should be interpreted as maximum ages. A more statistically rigorous analysis of the distribution of De values will be undertaken before finalized ages are published in external literature.

To provide an alternative source of age constraints and to verify OSL results, a total of 11 radiocarbon samples were collected and analyzed. Detrital charcoal is somewhat common in the study area, though potential ~10^2 yr residence times of this material in the landscape can inhibit confident age determinations, especially in younger deposits (Webb et al., 2002). Where possible, we targeted detrital plant litter such as twigs, berries, and seeds, with a negligible residence time in the landscape. Samples were sent to Beta Analytic Inc. for AMS-radiocarbon dating. Resulting radiocarbon ages were converted to calendar ages using the INTCAL04 calibration by Reimer et al. (2004). Multiple intercepts on the calibration curve for dates of < 350 BP lead to high uncertainties in calendar ages in this age range. Hence, both OSL and radiocarbon methods suffer from significant uncertainty in the younger age range (younger than ~ 500 years).

To provide age control for younger deposits that could not be constrained by OSL or radiocarbon, five samples were analysed for the presence of ^{137}Cs, an isotope whose measurable presence in the atmosphere began with atomic bomb testing around 1950 AD (Grootes, 1983). Work by Ely and Webb (1992) showed that such a test could accurately distinguish flood events that occurred before ~1950 AD from those that occurred after. It is possible for ^{137}Cs to be absent from a post-1950 flood deposit if the majority of the

material in transport came from places shielded from atmospheric fallout, but these instances are rare. Samples were collected by excavating ~500 g of material from the lower half of each sampled unit. This method reduces the possibility of contamination of units by rain and groundwater tainted with ^{137}Cs. Bulk sediments were analyzed at Arizona State University for the presence of the isotope, however, results are only available in terms of counts per minute (cpm). This limits our ability to define a specific threshold like the detection limit of 0.05 pCi/g used by Ely and Webb (1992); however, the presence and absence of ^{137}Cs can still be determined rather confidently.

Finally, relative age determinations from archeological materials and buried junipers provided additional age constraints. A buried suite of potsherds at site KCW-A can be associated with a particular formative period in Puebloan history. Ring counts on buried, living juniper trees provide maximum ages of units burying the germination horizon. Uncertainties associated with false or missing rings are significant, but probably do not exceed ~ 10% of a given tree's age (Hereford, 2002). Two cores each were taken from two partially-buried juniper trees at study site BG-B in Buckskin Wash. Cores were mounted onto wooden blocks and sanded to expose rings for counting under magnification.

Surveying

The longitudinal profile of the modern streambed (Figure 3-3) was extracted from a 5 m autocorrelated digital elevation model (DEM) provided by the Utah AGRC (http://agrc.utah.gov). The drainage line along which the profile was extracted was drawn manually and is labeled as "Kitchen Corral Wash" in Figure 3-1. Due to the

narrow constrictions of the slot canyon, the DEM was unable to accurately capture the elevation of the streambed. Those areas were removed from the dataset and bounding points were connected with straight lines. Hence, the profile should not be scrutinized too carefully downstream of site BG-C. To provide a higher level of detail around the study sites, a 6 km reach of Kitchen Corral Wash and a 4 km reach of Buckskin Gulch were surveyed manually with a Topcon RTK GPS. At a precision of ± 1-2 cm in vertical and horizontal, the survey data provide details obscured by the coarse resolution of DEM coverage. GPS points were taken along the channel thalweg and valley-fill surface for each reach to determine downstream changes in terrace heights. Where the GPS signal was obstructed by slot-canyon walls, a handlevel and rangefinder were used. In addition to longitudinal profiles, a series of cross-sections were surveyed in representative reaches of both Kitchen Corral Wash and Buckskin Gulch in order to document modern valley geometries and provide boundary conditions for future hydraulic modeling efforts.

RESULTS

Sedimentology and Stratigraphy

Depositional Facies

A wide range of sedimentary facies are preserved in the alluvium at the study sites. Despite this variability, nearly all units could be classified into one of ten lithofacies designations (Table 3-2; Figure 3-4). These classifications were made to assist in characterizing the hydraulic environment of deposition for comparison across valley geometries.

The sediment that composes the valley fills in the watershed is primarily fine to coarse sand. This reflects the dominance of eolian and fluvial sandstone in the bedrock of the watershed. Coarser facies include both massive and imbricated clast-supported gravels (Gcm, Gci), and rounded, intraclastic gravels (Gmr). Gravels come primarily from Pleistocene fill terraces that bound the alluvial valley and mantle the bedrock in the constricted reach (Figure 3-3). These coarse facies represent higher-energy environments that probably only occur during larger floods. Sandy facies are primarily laminated (Sl), and trough- or ripple-crossbedded (Spx, Srx), but are occasionally massive (Sm, Sma). Finer-grained, muddy facies are less common and are usually quite thin and bioturbated (Ssm, Mcg). In some locations, many thin beds of Ssm and Mcg with mudcracked upper surfaces can be found in sequence.

Throughout the study area, mainstem deposits can be distinguished from tributary and local slope deposits by sorting, composition, and hue. Mainstem sands are typically light yellowish brown, well sorted, and dominated by medium-coarse, well rounded sand from the White Cliffs (Navajo Sandstone). Tributary and local slope sediments have a variety of characteristics depending on the local lithology. At the Kitchen Corral Wash and Buckskin Gulch study sites, tributary sediment is typically reddish-brown, silty fine to medium sand, reflecting a source area in the Kayenta, Moenave and lower Navajo Sandstones. In Coyote Wash, tributary alluvium ranges from calcareous gray clay to 3 m boulders derived from the Kaibab Limestone, light reddish brown sand from the Vermillion Cliffs/Coyote Buttes, and multi-colored shale pebbles from the Petrified Forest member of the Chinle Formation. Pleistocene terraces along much of the studied

reaches contribute coarse boulders and sand directly into the channel and onto the valley bottom via hillslope and debris flow processes.

The range of facies found in valley fills can be assembled into broad depositional facies associations representing particular settings along the drainage (Table 3-3). We define three facies associations as follows: channel-bottom (CB), channel-margin (CM), and valley surface (VS). These associations manifest themselves in different, reach-specific manners, but are linked by a common locale of deposition. Channel-bottom deposits include those facies that can be associated with deposition in or near the thalweg on the channel bed. Facies in this association reflect the energy of the depositional event, and therefore range from coarse (e.g. Gcm, Gci) to muddy (e.g. Mcg, Ssm) facies.

Table 3-2 – Facies codes used in the text.

Lithofacies Code	Description
Gcm	massive, matrix- to clast-supported gravels
Gci	imbricated, crossbedded clast-supported gravels
Gmr	rounded mud intraclasts and reworked bank material
Sl	fine-coarse sand with planar to subhorizontal laminae
Sm	fine-coarse sand, massive due to bioturbation.
Spx	poorly sorted coarse sand-pebbles with trough crossbedding
Ssm	thin red and tan massive silty fine sand
Srx	fine-medium sand with sub- to supercritical climbing ripples
Sma	massive, poorly sorted sand ± floating angular clasts
Mcg	tabular gray calcareous clay ± mudcracks

Table 3-3 – Depositional facies associations.

Channel-bottom	Channel-margin	Valley-surface
Gcm	Sl	Ssm
Gci	Spx	Sm
Gmr	Sm	Mcg
Spx	Ssm	
Ssm	Srx	
Sm	Sma	
Mcg		

Facies that are generally unique to this environment include gravels (Gcm, Gci, and Gmr), and trough-crossbedded pebbly sands (Spx). These grain sizes and bedforms can only be produced under high flow velocities, and in the modern channel are

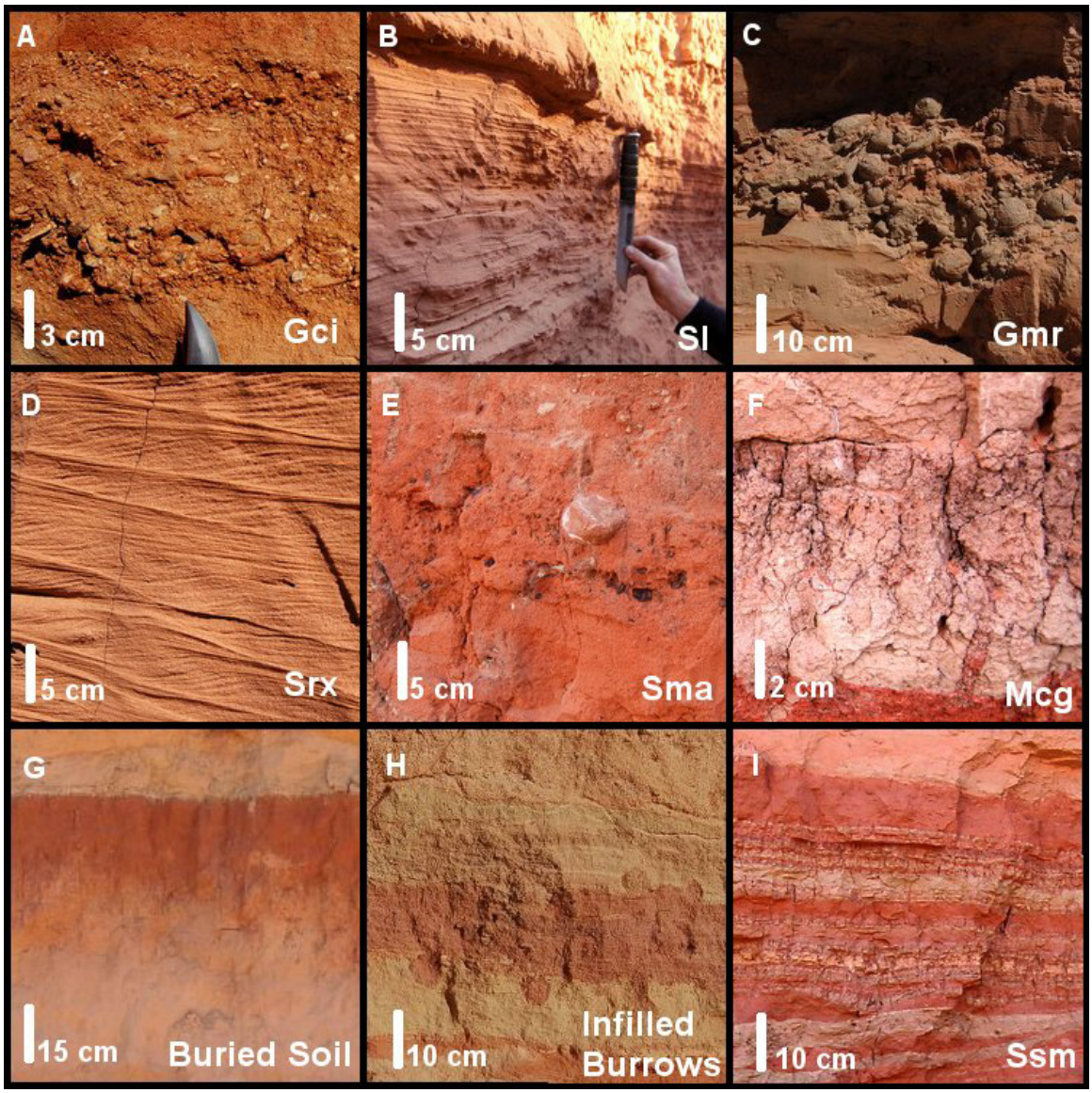

Figure 3-4 – Representative facies: A) Gci - imbricated sandy gravel; B) Sl - planar laminated medium-coarse sand; C) Gmr – rounded intraclastic gravels D) Srx – medium sand with upstream-climbing ripples; E) Sma - poorly-sorted coarse sand with suspended shale pebbles; F) Mcg – tabular calcareous gray clay; G) buried inceptisol; H) Infilled burrows; and I) Ssm – massive fine-medium sand.

only found in the thalweg. Bed geometries in this facies association are usually lenticular or discontinuous, suggesting frequent scour and refilling. This association is similar to the "older channel alluvium" described by Hereford (1986).

Channel-margin deposits are indicative of deposition within the channel system but away from the thalweg; for example, vertical accretion on in-arroyo floodplains and in slackwater zones. Facies in this environment are fine to coarse sands with ripple cross-lamination or plane-bed laminae. These sedimentary structures result from the migration of 2-d and 3-d ripples and lower- and upper-flow regime plane beds. Because of the lateral continuity of the locations of deposition, channel-margin deposits have more tabular bed geometries as compared with the mostly lenticular channel-bottom deposits.

Valley-surface deposits include tributary, hillslope, and eolian facies deposited on the surface of the alluvial valley as well as overbank mainstem facies that overtop arroyo walls and spread onto the alluvial valley. In this setting, width of flow is greatly increased and depth and velocity are greatly decreased. Thus these facies are generally finer-grained (Ssm, Mcg). Prolonged exposure on the surface of the valley bottom also results in significant bioturbation, eolian reworking, and disturbance by prehistoric and modern humans, often resulting in massive textures and disruption of original sedimentary structures.

Stratigraphy of Study Sites

KCW-A

Site KCW-A is located on a west-facing, nearly vertical cutbank that is actively eroding into the modern channel (Figure 3-5). Large slump blocks in the channel

indicate ongoing undercutting and failure of arroyo walls, and provide fresh surfaces for study. The arroyo in this reach is about 10 m deep and 30 m wide. A ~2 m high floodplain occupies much of the arroyo bottom, pinning the channel against the cutbank.

Four distinct stratal packages are present, separated by four bounding surfaces that crosscut depositional units (Figure 3-6). Package I is stratigraphically lowest, contains 39 depositional units, and is more than 6.5 m thick, with a base somewhere below modern stream grade. Package II lies above an unconformity that truncates the upper 29 units of package I. It contains 68 units, is about 7.0 m thick, and overtops package I by ~0.5 m. Most of package II is truncated by another bounding surface that soles out at depth. Package III was deposited above this unconformity and overtops package II by ~1.2 m. It is 6.5 m thick and contains 31 units, all of which are truncated by a third bounding surface. Package IV fills in and slightly overtops this surface, therefore underlying a portion of the valley surface in this reach. The complex nature of this youngest package prohibits an accurate count of beds representing individual events, but at least 80 individual events are represented in the outcrop.

The basal units of package I are obscured by slumped material. The lowest visible units are primarily laminated (Sl) and massive sand (Sma). Thin, finer interbeds (Ssm, Mcg) often drape these lower units. Overlying these basal units and forming the bulk of the package thickness is a series of mostly tabular, medium- to thick-beds of fine-coarse sand that are massive to planar laminated. Several thin interbeds of Ssm and Mcg are found throughout the package. Especially in the upper half of the package, many exposure surfaces are present, marked by bioturbated upper contacts, abundant rhizoliths,

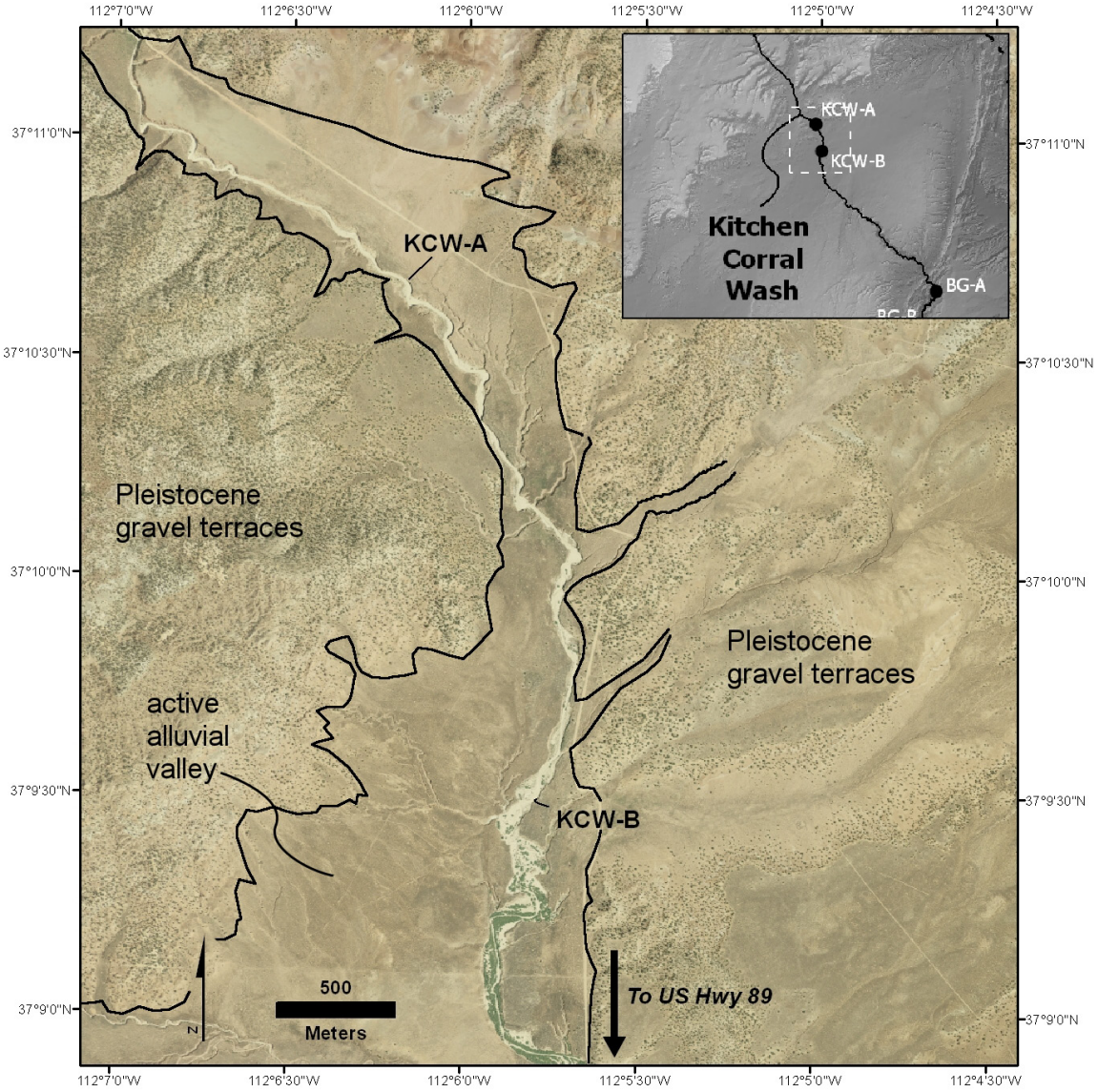

Figure 3-5 – Location map of study sites KCW-A and KCW-B.

and clay-lined pores. The uppermost of these tabular beds caps the unit and has a weak, reddish-brown entisol developed on its surface. We interpret these tabular beds as representing the in-arroyo floodplain environment. The dominance of horizontal, planar laminae and tabular bed geometries are consistent with the 2-meter high deposits that currently fill much of the arroyo bottom.

The basal units of package II, where exposed, are composed of lenticular beds of massive to imbricated gravels (Gcm, Gci) and trough-crossbedded coarse sands (Spx). Beds are normally-graded and often laterally truncate each other. The coarse texture and lenticular geometries of these basal units suggest deposition as gravelly bars in a channel-bottom environment on the bottom of a paleoarroyo. Finer interbeds record lower-energy events in the same channel setting. These coarse sands and gravels are overlain by medium to thick, tabular, sandy beds with thin, finer-grained interbeds. These upper units interfinger with massive, disorganized wedges of sandy alluvium (Sma) that can be traced to the paleobank truncating package I. Where these wedges of slopewash alluvium occur, they overlie the weakly-bioturbated upper surface of the unit below. This configuration suggests that after deposition of a tabular channel-margin deposit, prolonged exposure allows colonization of the newly-formed surface by plants and accumulation of material eroded from adjacent arroyo walls. The uppermost of these yellowish-brown, tabular sands is ~1.5 m thick, and is massive due to very heavy bioturbation throughout. This package is capped by a sequence of 6-8 reddish-brown silty sands (Ssm) that are heavily bioturbated. We interpret these capping units as recording a variety of depositional processes taking place on the surface of the alluvial valley, including tributary fans, eolian reworking, and slopewash. A 3-4 m wide infilled semicircular cavity crosscuts these upper valley-surface (VS) deposits and is infilled by a massive, reddish-brown, clay- and silt-rich, disorganized fill that is difficult to explain geologically. Potsherds, charcoal, and out-of-place chert found in and on these capping units indicate that the surface of package I was occupied by pre-Puebloan cultures, suggesting an anthropogenic origin of the infilled cavity.

The basal unit of package III is a thick bed of gravel intraclasts (Gmr) and another of massive, disorganized sandy sediment. These lenticular units represent the reworking of material that slumped into a paleoarroyo from the arroyo walls, an interpretation supported by the abundant slumps in the modern arroyo with varying degrees of reworking. These basal units are overlain by several thin to thick beds of laminated sand (Sl) and massive, reddish-brown silty sand (Ssm). These units are somewhat bioturbated throughout, with irregular contacts and infilled burrows and root casts. Wedges of disorganized sediment (Sma) can be traced to the surface bounding package II. A thick bed of massive sand overtops the surface of package II. This unit is overlain by a series of reddish-brown silty sands similar to those that cap package II. Like in packages I and II, this sequence records the vertical accretion of an in-arroyo floodplain, with enough time passing between events to allow occupation of the floodplain surface by vegetation and burrowing organisms and the introduction of material washed of the walls of the paleoarroyo. Eventually these floodplains aggraded to the point where subsequent floods overtopped the walls of the paleoarroyo.

Package IV contrasts with the three older packages. Whereas the others are dominated by mainstem alluvium, the facies in package IV are quite silty and mostly reddish-brown, consistent with a tributary draining the Vermillion Cliffs. Thin lenses of gravelly Gcm, Gci, Spx, Sma, and Ssm abut the bounding surface, and interfinger in the upstream direction with thicker, more tabular units of Ssm and Sl sand. Bed geometry suggests that these facies record the ~simultaneous deposition of channel-bottom and channel-margin deposits, respectively. Relatively yellow-gray lenses probably represent

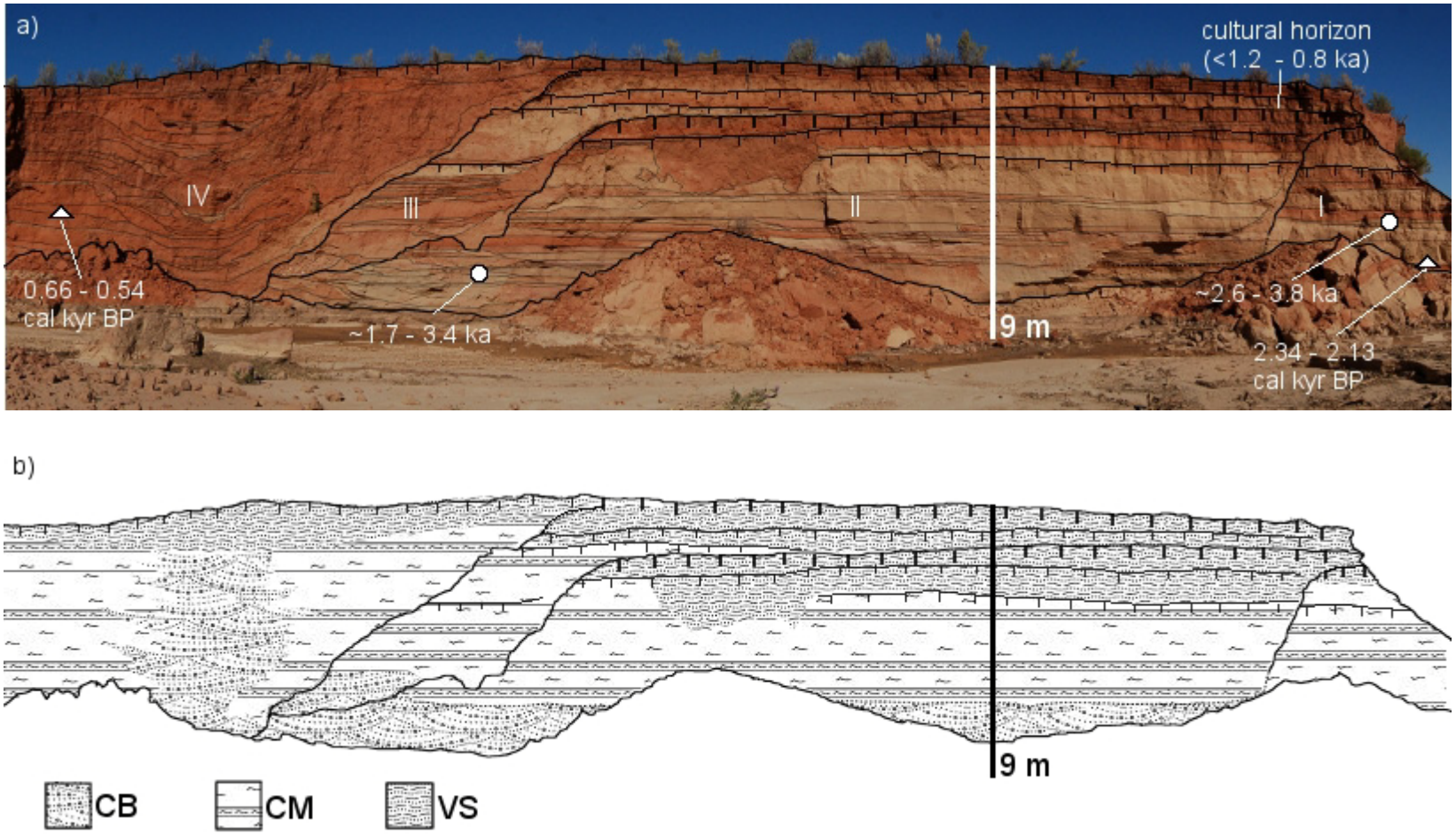

Figure 3-6 – Chronostratigraphy (a) and facies associations (b) for study site KCW-A. White circles and triangles are OSL and ^{14}C samples, respectively. Facies associations: CB = channel-bottom, CM = channel-margin, VS = valley-surface.

the backflooding of the tributary arroyo bottom by mainstem flows. Wedges of Sma interfinger with these units and extend from the unconformity into the paleochannel. This lateral facies sequence changes little upsection, until the upper two meters, where lenticular thin beds are replaced by tabular thin beds of Ssm. These units are similar to those capping package II and III, and are more consistent with the valley-surface facies association. Bioturbation by plant rooting and rodent burrowing is evident throughout the package, but no particular buried soils are present.

In summary, packages I-III are each interpreted to record the cutting and subsequent filling of a mainstem arroyo. Entisols developed on the bounding surfaces of each package record extended exposure during subsequent incision, as described by Hack (1942) and Karlstrom (1988). Package IV records in cross-section the infilling of a tributary arroyo as tabular channel-margin deposits that can be traced laterally to coarse lenses of channel-bottom deposits. This lateral facies transition is preserved in package IV in part because this tributary arroyo was probably narrower and had less lateral mobility than the mainstem arroyo it was graded to. Gravelly channel-bottom deposits are found up to 7 m above the modern arroyo bottom in package IV, clear evidence of aggradation of the fluvial system between arroyo-cutting events.

KCW-A geochronology

A sample of detrital charcoal from the base of package I yields an age of 2235 +/- 105 cal yr BP (2.2 – 2.4 ka), while an OSL sample 1 m above it gives a maximum age of (~2.6 – 3.8 ka). Another OSL sample at the base of package II gives a maximum age of (~1.7 – 3.4 ka). These two samples are partially bleached (Appendix A), and the true age

of the samples is probably closer to the younger end of the given age ranges (Table 3-4). Potsherds found eroding from the buried surface at the top of package II suggest that it was occupied around ~1.2 – 0.8 ka. A radiocarbon sample of detrital twigs from the base of package IV yields an age of 600 +/- 60 cal yr BP (0.6 – 0.7 ka). Finally, two radiocarbon samples collected from the base of packages II and III were rejected, as one was clearly contaminated with coal and the other was the result of recent rooting into the outcrop wall (Table 3-5).

KCW-B

Site KCW-B is located about 1.7 km downstream of KCW-A, also on a west-facing cutbank that is actively eroding into the arroyo (Figure 3-5). In fact, between the time of initial fieldwork and the time of this writing, a recent slump has obscured much of the outcrop. Modern channel geometry is similar to KCW-A, with ~2 m of deposits filling much of the arroyo bottom and pinning the channel against the cutbank. The surface of the alluvial valley here is only 5 m above the modern wash, suggesting that the grade of the modern wash converges with the tread of the valley-fill terrace in a downstream direction.

Four packages separated by bounding surfaces are exposed at KCW-B (Figure 3-7). Package I is 4.0 m thick and contains 33 units. All but the lowest are truncated by a surface that soles out with depth. Package II is exposed on the upstream side of this surface, and consists of 17 units that fill up to the same height as package I. Package III is a narrow channel-shaped package that again fills up to a similar height at I and II. This shared surface is buried by six units that form the upper 1.5 m of the outcrop, referred

Table 3-4 – Results of optically stimulated luminescence analyses.

Site	Sample Number	Lab Number	Depth (m)	# disks run	# disks accepted (used)	De (Gy)	Rd (Gy/kyr)	Age (ka)	Age Range (ka)	Position
KCW-A**	JHKCW6	USU 530	8.0	45	36 (21)	3.9 ± 1	1.52 ± 0.07	2.61 ± 0.87	1.7 - 3.4	Base of II
KCW-A**	JHKCW7	USU 531	4.0	41	33 (23)	6.9 ± 1.5	2.21 ± 0.10	3.13 ± 0.71	2.6 - 3.8	Middle of I
KCW-B**	JHKCW3	USU 389	4.0	45	33 (23)	4.8 ± 1.7	0.96 ± 0.05	4.99 ± 1.81	3.1 - 6.8	Base of II
KCW-B**	JHKCW2	USU 388	4.0	43	27 (20)	9.16 ± 2.8	2.06 ± 0.09	4.35 ± 1.36	3.0 - 6.9	Base of I
COY-A*	CWOSL2	USU 136	3.2	25	16	19.1 ± 5.6	1.50 ± 0.07	12.78 ± 3.84	9.0 - 16.6	Base of II
COY-A	CWOSL1	USU 135	5.8	25	13	19.9 ± 2.4	1.14 ± 0.05	17.50 ± 2.50	15.0 - 20.0	Base of I
BG-A**	JHBG6	USU 385	3.0	33	20 (11)	4.3 ± 1.8	1.84 ± 0.08	2.34 ± 1.00	1.3 - 3.3	Middle of II
BG-A**	JHBG5	USU 384	3.6	20	15 (5)	10.1 ± 3.4	2.09 ± 0.09	4.82 ± 1.67	3.1 - 6.5	Base of I
BG-B*	JHBG11	USU 523	6.0	15	8	4.0 ± 1.8	1.73 ± 0.08	2.32 ± 1.03	1.3 - 3.3	Middle of II
BG-B**	JHBG10	USU 522	9.0	15	7 (6)	3.2 ± 1.9	1.76 ± 0.08	1.81 ± 1.06	0.8 - 2.9	Base of II
BG-B**	JHBG9	USU 521	5.5	35	24 (14)	4.0 ± 1.0	2.29 ± 0.10	1.74 ± 0.43	1.3 - 2.2	Middle of I

*sample has significant partial bleaching

** sample has significant partial bleaching; only younger population of accepted disks used in De calculation

Table 3-5 – Results of radiocarbon analyses.

Site	Sample Number	Lab Number	Depth	Material	14C Age (yr BP)	Calibrated 2σ age range (yr BP)*	Position
KCW-A	RCKCW2	Beta - 256838	6.8	twigs	610 ± 40	660 - 540	Middle of IV
KCW-A	RCKCW7	Beta - 256841	6.0	rotting root	101.5 +/- 0.4 pMC	modern	Middle of II
KCW-A	RCKCW3	Beta - 256839	9.0	charcoal (coal)	> 44800	∞	Base of II
KCW-A	RCKCW4	Beta - 256840	6.3	charcoal	2220 ± 40	2340 - 2130	Middle of I
COY-A	RCCW1	Beta - 244295	2.0	charcoal	4890 ± 40	5670 - 5590	Middle of II
BG-A	RCBG2	Beta - 248726	2.5	woody debris	440 ± 40	530 - 460	Middle of II
BG-B	RCBG7	Beta - 256838	9.5	charcoal (coal)	> 44800	∞	Base of II
BG-B†	RCBG3	Beta - 256834	3.5	tree litter	150 ± 40	290 - 0	> base of II
BG-B	RCBG6	Beta - 256836	5.5	charcoal	1250 ± 40	1280 - 1070	Middle of I
BG-B	RCBG5	Beta - 256835	8.2	charcoal	1780 ± 40	1820 - 1600	Base of I
BG-C	RCBG1	Beta - 248725	9.4	woody debris	180 ± 40	300 - 0	Base of I

* Reimer et al. (2004)
† From correlative unit upstream of main outcrop

to here as package IV.

The base of package I is composed mostly of tabular thin to medium beds of sandy Spx, Sl, and Sm. These are topped by 12-15 tabular thin beds of muddy Ssm and Mcg that alternate between reddish brown and light yellowish brown. This finer sequence is overlain by several medium to thick, tabular beds of the sandy Sm facies. The uppermost is almost 60 cm thick and is capped by a buried, reddish-brown entisol. Many of the lower beds contain infilled burrows and root traces, though they become coarser and more abundant upward. The sandy texture, tabular bed geometry, and position in outcrop are consistent with the channel-margin facies association. The fine-grained, thin-bedded sequence above the basal units was noted in many other outcrops along the wash, and is interpreted to represent the deposition of silt and mud from floodwater pooled in depressions on the surface of the in-arroyo floodplain. Modern analogs are found in many places along Kitchen Corral Wash. The uppermost thick sandy beds represent higher-energy flows, probably after some degree of channel aggradation and lateral movement of the channel back toward the outcrop location. The bounding surface that truncates package I is a cutbank of a paleoarroyo incised into package I. Package II was deposited above this bounding surface as several thick, tabular beds of Spx and Sl with irregular contacts. These units represent channel-margin deposits filling the paleoarroyo cut into package I. Again, several medium beds of Sm cap the package. Package III overlies a downstream-sloping unconformity that truncates the upper 3 m of package II. It is composed of a series of lenticular beds of Gmr, Sl, and Spx that interfinger with wedges of hillslope colluvium extending from the bounding surfaces along its margins. These irregularly-shaped beds are overlain by five lenticular,

thin to medium beds of Ssm and Mcg with light yellowish-brown and reddish-brown hues. Package III represents the filling of a channel that was incised into the channel-margin deposits of package II and subsequently abandoned. A reddish-brown, medium bed of Ssm caps package III and buries I and II. The event that deposited this unit represents the valley-surface facies association, as it marks the overtopping of the walls of the paleoarroyo and spreading out onto the greater alluvial valley. An entisol developed on this unit before burial by package IV. This buried soil likely corresponds to a period of channel incision between the deposition of packages III and IV, though no paleochannels of this speculative incision are preserved here. Package IV consists of six beds that overlie the buried on packages I, II, and III. The lower three of these are thin lenses of bioturbated sand and mud (Mcg and Sm). These are overlain by two tabular beds of reddish-brown Sm facies. Capping the outcrop is a hummocky, light yellowish-brown bed of Sm between 60 and 100 cm thick. Interpretation of these uppermost units is difficult due to the geometry of preservation. Their tabular geometries and sandy textures suggest channel-margin deposition, though they may have been large enough events that the entire valley surface became the channel margin. The capping unit is especially thick, probably due to eolian reworking and inflation of the upper fluvial deposit in this position downwind of the arroyo. The upper 20-30 cm of this bed has a reddish brown stain that appears to infill many very coarse root traces and burrows throughout the bed. It is likely due to eolian sand reworked and introduced from the redder locally-derived sediment on the valley surface. The disorganized, hummocky nature of the bed could also be due to anthropogenic alteration. This possibility is not

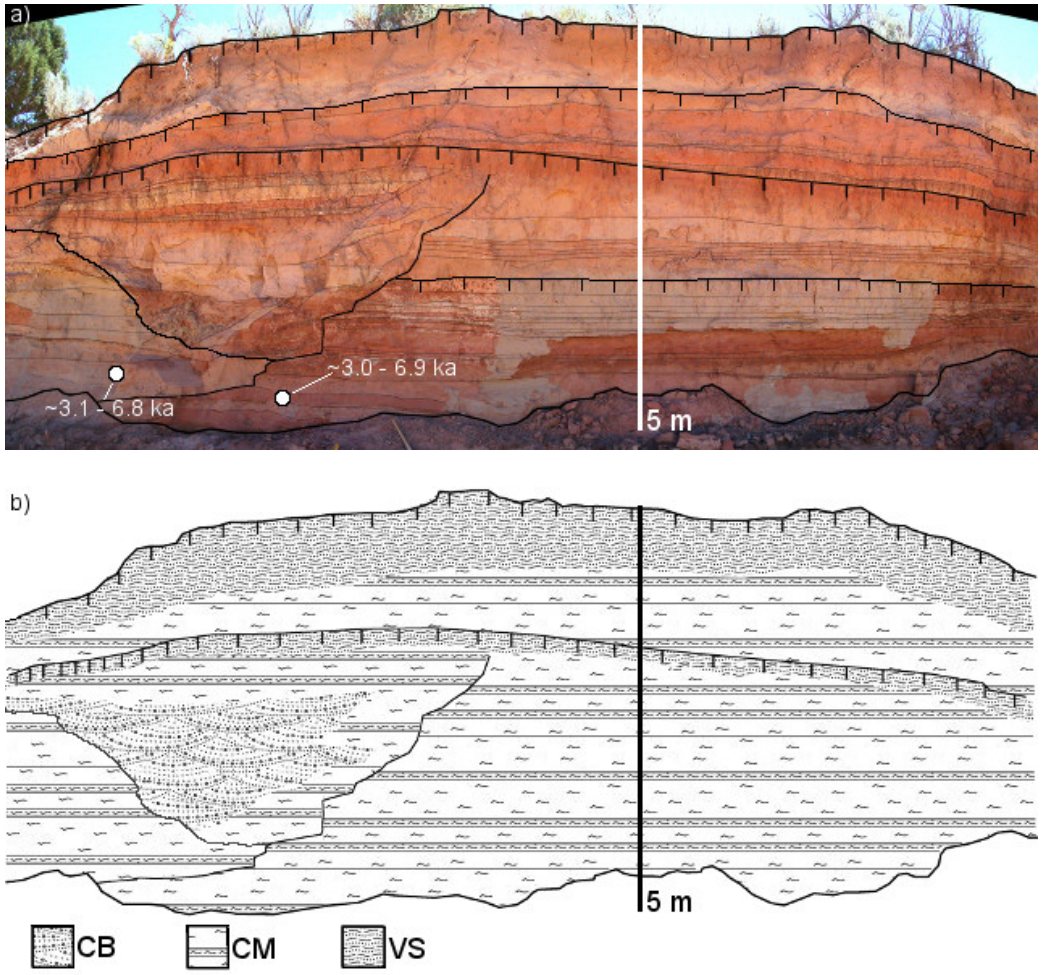

Figure 3-7 – Chronostratigraphy (a) and facies associations (b) for study site KCW-B. White circles represent OSL samples. Facies associations: CB = channel-bottom, CM = channel-margin, VS = valley-surface

outrageous, as the valley at Kitchen Corral Wash has been subjected to land uses such as farming and grazing since the late 1800s (Johnson, pers. comm.).

KCW-B Geochronology

OSL samples from the base of packages I and II give preliminary ages of ~3.0 - 6.9 ka and ~3.1 - 6.8 ka, respectively. Again, both samples suffer from partial bleaching (Appendix A); thus, they are considered to be overestimates. These two samples were collected early in the campaign from relatively coarse, poorly-sorted, trough-crossbedded sand, a facies representing higher-energy deposition by sediment-rich flows; and environment not ideal for maximizing the proportion of bleached grains. These relatively weak age constraints prohibit confident correlation to packages at KCW-A, though landscape position suggests that package IV correlates to package IV upstream.

COY-A

Much of the strike valley that Coyote Wash occupies is covered by a high alluvial slope underlain by cobbly to bouldery alluvial gravel shed from the Kaibab Plateau to the West. The east side of the valley is underlain by a dissected alluvial slope composed of sand and silt derived from Coyote Buttes and the Paria Plateau. This surface is graded to the same level as the dominant terrace on the west side of the valley. This suggests contemporaneous deposition, likely during the late Pleistocene. Inset tens of meters into these older surfaces is the Holocene alluvial valley (Figure 3-8). The COY-A study site is located along a west-facing arroyo wall along Coyote Wash. Here the arroyo is 10-30 m wide and relatively shallow, with a ~2-3 m high terrace lining much of the modern

arroyo. This surface is inset into a deposit, the height of which above the wash depends on where the wash has intersected its sloping surface (Figure 3-9). The modern arroyo bottom at this locality is the site of a bouldery, multi-threaded knickzone with vegetated islands.

Three stratal packages are exposed, separated by two bounding unconformities (Figure 3-9). Package I underlies the higher terrace, which is 6.5 m high here. A steep buttress unconformity truncates its entire exposed thickness, and massive, sandy hillslope deposits blanket this contact with the inset package II. Reworked slump blocks from package I are incorporated into and overtopped by package II. The ~3-4 m thick exposed package II is itself capped by a buried soil that slopes gently westward toward the wash and merges eastward with the soil capping package I. Subsequently, package III was deposited as a channelward-thickening wedge that disconformably overlies the sloping surface of II and underlies the lower, 2.5 m high terrace, mapped by R. Hereford (pers comm.) as the "settlement alluvium".

The alluvium at COY-A is notably different from that found in Kitchen Corral Wash, the other alluvial study reach. The base of package I is a series of thick beds of massive, poorly-sorted light reddish coarse sand (Sma), which contains suspended, angular shale pebbles. The color of the sand and composition of the pebbles indicates that it was derived from a tributary draining the incised piedmont on the east side of the wash. This facies diminishes and is increasingly interbedded upward with a series of 5-15 cm-thick tabular beds of grey calcareous clay (Mcg). Despite having continuous, planar contacts, these units are densely penetrated by infilled mud cracks, root traces, and

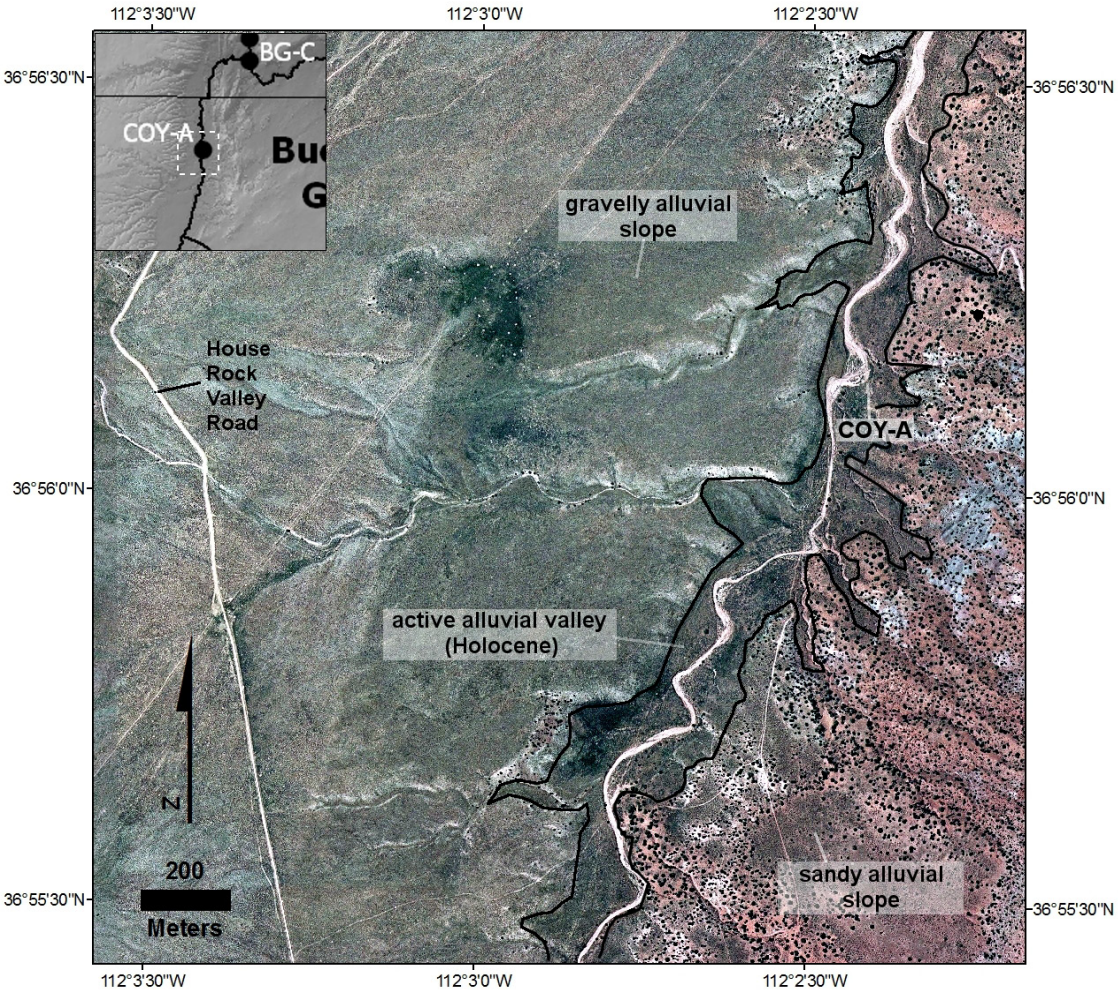

Figure 3-8 – Location map for study site COY-A.

burrows. Thick, massive, light reddish brown sands (Sm) overlie these finer units and underlie the terrace. The alternating silty clay and coarse sand facies preserved in package I indicate impulsive high-energy deposition periodically interrupting long periods of incremental deposition of silty clay in a low-energy setting like a marshy valley bottom. The density of root casts suggests abundant riparian vegetation. These are characteristics of a ciénega, a swampy, vegetated wetland that was a common sight in the Southwest during cooler, wetter periods (Hendrickson and Minckley, 1985).

However, the mudcracks indicate that perhaps the wetland was subject to seasonal drying and subaerial exposure. This is an indication that the source for the water may have been related to groundwater. The wetland was repeatedly injected by disorganized, concentrated flows from a nearby east-derived tributary. Suspended shale pebbles are derived from the Chinle Formation, which field observations indicate supplies a great deal of sediment to valleys incised into it. The above depositional environments are difficult to classify into a particular facies association considering how different the paleoenvironment was from the modern. However, VS is probably the best choice, as it includes those deposits that are emplaced outside of an entrenched channel.

Package II consists mostly of massive, bioturbated, poorly-sorted silty Sma. Individual units are distinguishable only in the base of the outcrop. Lenses of angular, massive to imbricated, matrix- to clast-supported gravel (Gci) support deposition in a channel-bottom environment. Gravel clasts are primarily Kaibab limestone, but the matrix is primarily sand derived from the Mesozoic rocks to the east. This supports the interpretation that these units were derived in the mainstem. These coarser lenses are inset into and overlain by tabular thin to medium beds of massive mainstem and tributary sand (Sma) and silty sand (Ssm). These facies represent the upward transition from channel-bottom gravel bars to channel-margin sandbars and finally broader floodplains. These units grade upward into the rest of the outcrop which is mostly massive, brown silty sand with few floating angular Kaibab clasts. These disorganized deposits represent severely bioturbated channel-margin and valley-surface environments. Material eroding from the high terrace riser inflates this terrace toward the unconformity. A gently sloping, partially-buried entisol with a recognizable A horizon is developed on its

surface. The presence of clay throughout the upper ~2-3 m of the package suggest that downward translocation of clays has occurred, though not in a narrow horizon.

Package III is a thin wedge of alluvium disconformably overlying this buried soil. This youngest package can be correlated according to stratigraphy and landscape position to the predominant ~2.5 m-high terrace that covers the west side of the alluvial valley here. The beds underlying this surface are very similar to the better-preserved facies in package II, containing an upward transition from coarse lenses of channel-bottom deposits (Gci and Gcm) to thinner beds of channel-margin and valley-surface deposits (Sma and Ssm). In contrast to this trend, however, are the several thin beds of reddish brown Spx with angular Kaibab pebbles that cap the unit. The presence of such coarse clasts 2-3 m above the modern wash implies deposition during a series of very high energy events, or, alternatively, significant downcutting since deposition. We favor the later interpretation, and, as with package II, we interpret this package as recording lateral and vertical accretion during an aggradational episode.

COY-A geochronology

An OSL sample from the base of package I yields a preliminary age of ~15-20 ka, roughly coincident with the Last Glacial Maximum. A preliminary OSL age from the base of package II suggests that it began to be deposited around 9 - 16 ka. However, this sample appears to be very partially bleached, resulting in an almost flat histogram of De's (Appendix A). Because there is no skew to the data, standard minimum-age models are difficult to apply. The youngest aliquots are ~6 - 7 ka; which represents the minimum

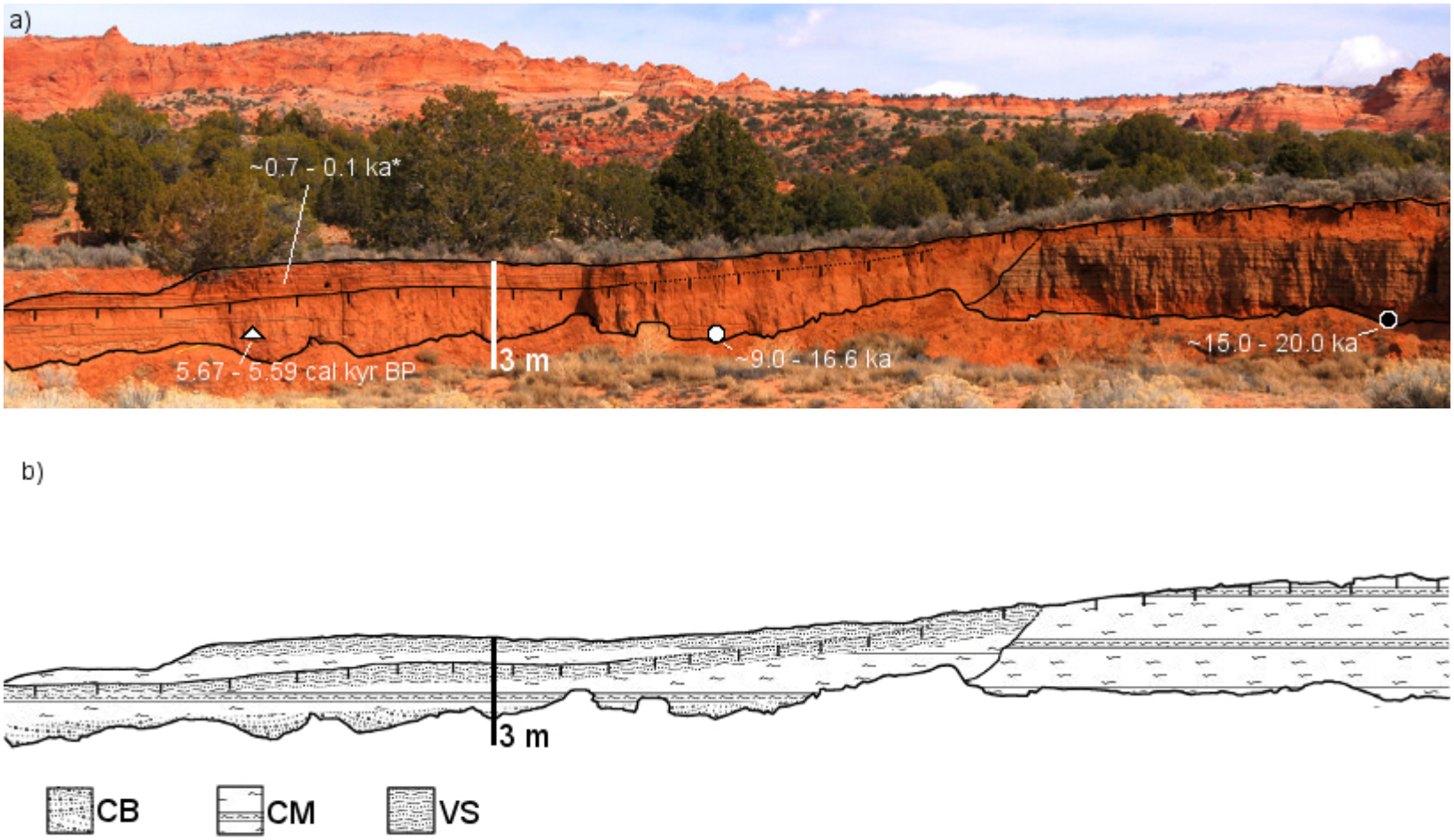

Figure 3-9 – Chronostratigraphy (a) and facies associations (b) for study site COY-A. White circles and triangles are OSL and ^{14}C samples, respectively. Asterisk indicates correlative age constraint by Hereford (pers. comm.). Black circle is OSL sample from correlative unit outside of pictured outcrop. Facies associations: CB = channel-bottom, CM = channel-margin, VS = valley-surface.

age for that sample. A radiocarbon sample from what appears to be the burnt rootball of a bush below the top of the package dates to 5600 – 5680 cal. yr BP. Together, Packages I and II are the oldest Holocene alluvial packages identified in this study. Package III was not dated here, having been mapped as the "settlement" alluvium by Hereford (2002). Over a dozen radiocarbon dates on buried Juniper trees along the Coyote drainage and its tributaries constrain the start of its deposition to ~1350 – 1400 AD (Hereford, unpublished data). It was likely still aggrading as of 1776 AD, when the Dominguez-Escalante mission passed through the area ~4 km downstream and described the wash as a marshy wetland (Hereford, 1993).

BG-A

This reach represents a transitional geometry between the broad alluvial valley near the Buckskin trailhead and the constrictions of the slot canyon downstream. Bedrock controls the width of the alluvial valley, which ranges from ~10 m in two short constrictions to expansions as wide as 100 m (Figure 3-10). A single, sparsely vegetated valley-fill terrace dominates the valley bottom. It is ~3-4 m high through the entire reach, inflated in places by eolian activity and tributary fans. A 2 m high vegetated floodplain underlain by modern channel-margin deposits is inset into this higher surface, and lines much of the stream. At BG-A, an active point bar and cutbank along the channel indicate some degree of recent lateral mobility. Just downstream of the site is one of the two 10 m wide constrictions in this reach. This bedrock control may exert a slight backwater effect during higher flows.

Two packages are present here, both extending to an unknown depth below modern stream grade (Figure 3-11). The first is thinly-bedded and difficult to record because it contains more than 50 thin depositional units. The entire exposed package is truncated by a buttress unconformity. Package II is inset into package I, contains 20-30 units, and laps directly onto a knob of Navajo sandstone just downstream. The entire outcrop is capped by a very weak entisol.

The base of package I includes 3-5 medium beds of sandy Sl and Spx interbedded with thin beds of silty Ssm and Mcg. The units generally thin and fine upward into a sequence dominated by Ssm, Sm, and Spx. These upper tabular beds range in thickness from 2 to 10 cm, and have generally wavy contacts. The finer-grained beds commonly preserve mudcracks, organic litter, and infilled root casts and burrows, suggesting incremental deposition in low-energy, shallow water. The reddish brown units suggest that the dominant source is the surrounding slopes of Navajo Sandstone, in the form of slopewash, shallow alluvial fans, and thin eolian sheets deposited on the valley bottom. The absence of mainstem material in the upper part of the package suggests that most mainstem events did not overtop the surface, though large mainstem floods probably contributed the thicker, coarser, tan beds seen in the base of the package. Because of the dominance of fine overbank deposits interbedded with eolian and slopewash sands, this package is interpreted as almost entirely valley-surface deposits. The basal unit of package II is a thick bed of gravelly Spx that coarsens upward into matrix-supported gravel with clasts < 5 cm. Above this unit, five medium-thick beds of Spx dip gently into the paleochannel, paralleling the underlying bounding surface (Figure 3-11). Crossbedding parallels contacts between these lower beds, and both contacts and

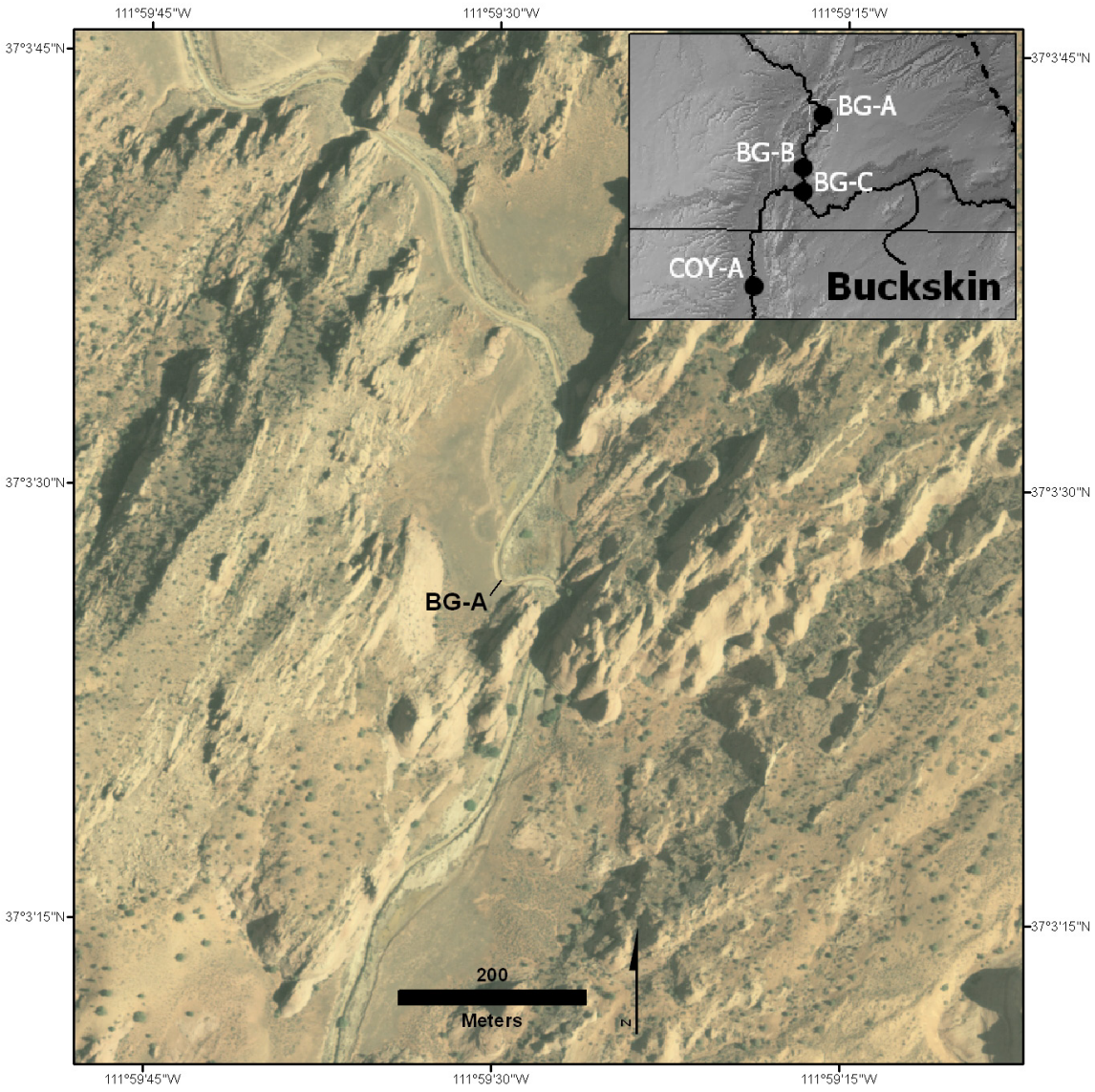

Figure 3-10 – Location map for study site BG-A.

crossbedding become horizontal upsection. These beds are overlain by a fining-upward sequence of 15-20 lenticular silt- and clay-rich units (Ssm, Mcg). Contacts are smooth, and bioturbation is limited to the uppermost beds. The base of package II is interpreted as one of a sequence of channel-margin lateral bars growing into the paleochannel cut

into package I. These channel-bottom deposits transition into what is interpreted as channel-margin and valley-surface deposits that accreted up to the rim of the unconformity that truncates package I. The fining-upward, channel-bottom to valley-surface sequence of facies associations suggests that the main channel migrated away from the locality as aggradation of the valley bottom continued, just like in packages I-III at KCW-A. Incipient soil development and bioturbation across the top of both packages prevents determination of whether or not II actually overtops package I, but the two share a common terrace surface.

BG-A geochronology

A sample of detrital woody material from the middle of package I yields an age of 530 – 460 cal yr BP (~0.5 – 0.6 ka). An OSL sample collected from the base of package I yields an age of ~9-15 ka, though its broad scatter in equivalent done suggests that the majority of its grains were not bleached during sediment transport. Such a strong skew toward higher equivalent doses could be the result of transport at night, or transport in very turbid waters over a short distance. An OSL sample collected from the base of package II also suffers from a partial bleaching, though the spread in equivalent dose is not nearly as large. It yields an age of and ~1.4 – 1.9 ka. The developing desert soil on the terrace surface that dominates the valley indicates that it has not been overtopped in modern times. If we trust the radiocarbon age from package I, the whole of the package must have been deposited between about 1400 AD and 1920 AD, indicating that some degree of downcutting did indeed occur through this reach during the historic arroyo cutting.

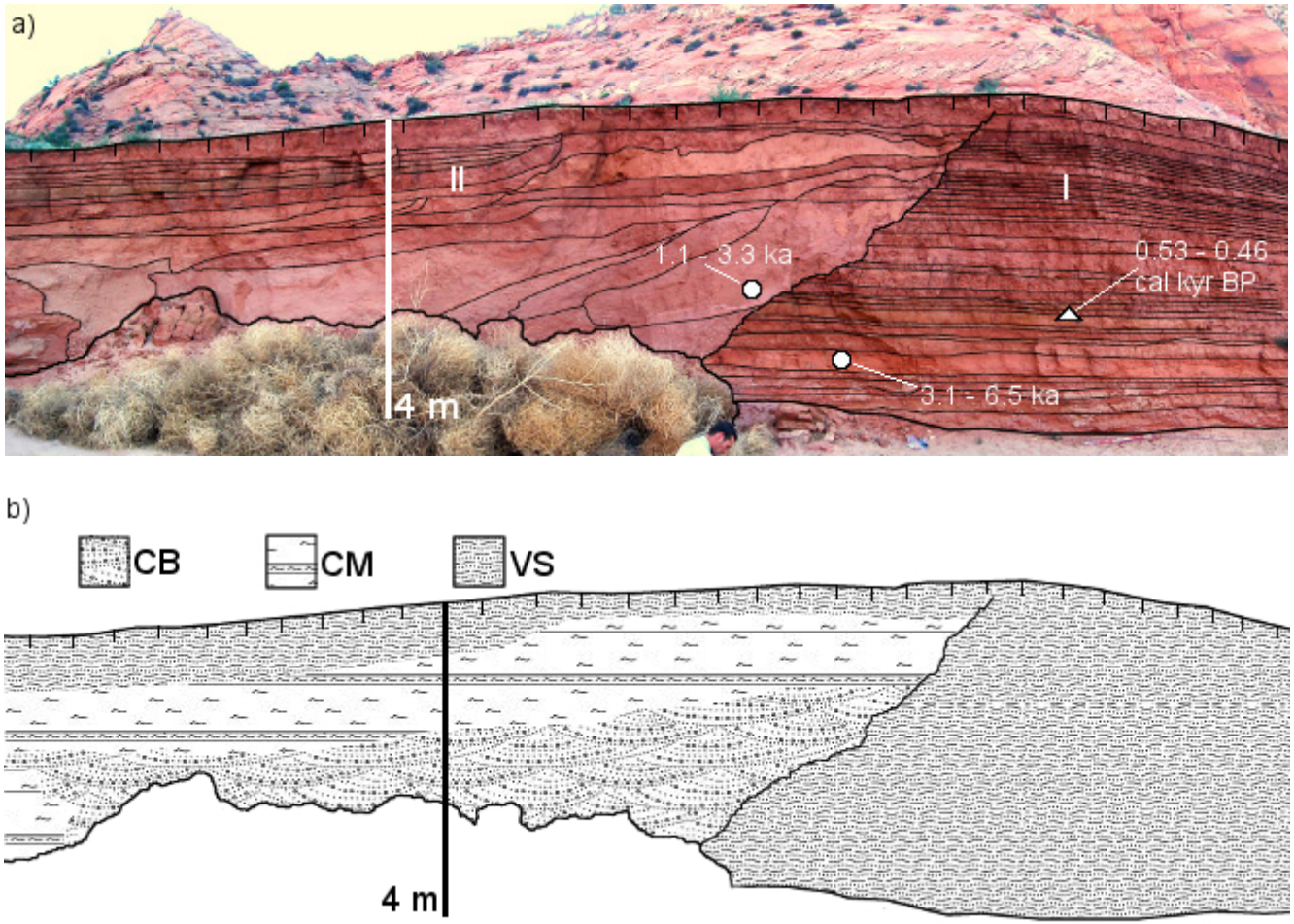

Figure 3-11 - Chronostratigraphy (a) and facies associations (b) for study site BG-A. White circles and triangles are OSL and ^{14}C samples, respectively. Facies associations: CB = channel-bottom, CM = channel-margin, VS = valley-surface.

BG-B

Site BG-B is located at the head of a steeper channel reach where the walls of Navajo Sandstone converge to constrict the channel (Figure 3-3 and Figure 3-12). Just upstream of the site, the stream flows through an initial, short notch where undulating bedrock walls are 6-10 m apart. The studied outcrop is located on the west face of a 10 m high fill terrace in an expansion between this initial slot and the first severe, continuous constriction of Buckskin Gulch ~100 m downstream. This terrace surface is roughly concordant with the top of the constricting walls downstream, suggesting that the deposits at this location are related to a backwater effect of the constriction (Ely, 1992). Correlative deposits drape the bedrock topography along the approach leading into the main constriction. Inset against the high terrace are ~1 m high channel-margin deposits that cover much of the valley bottom. These are similar in appearance and sedimentology to the historic floodplain described in the reaches upstream of this site by Hereford (1986), and for other southwestern streams by Leopold (1976). Here, these deposits act to channelize lower flows and form a vegetated buffer zone between the higher deposits and the thalweg.

The deposits underlying the fill terrace here were first studied by Ely (1992). Five stratigraphic packages are present, separated by buttress unconformities (Figure 3-13). Package I is ~6 m thick, contains 15 depositional units, and forms the core of the deposit. Package II is inset into and overtops package I by ~2 m and contains 19 units. Package III consists of 8 units that fill in two steep gullies eroded into the face of Package II. Though it fills up to a point nearly as high as the top of Package II, it does not overtop it. Packages IV and V continue the trend of filling in void space above

downstream-dipping unconformities with 9 and 6 units, respectively. Each successively younger package forms a cut-and-fill sequence downstream of the preceding package. Because of the length and awkward geometry of the outcrop, two separate panels are required to show all five packages.

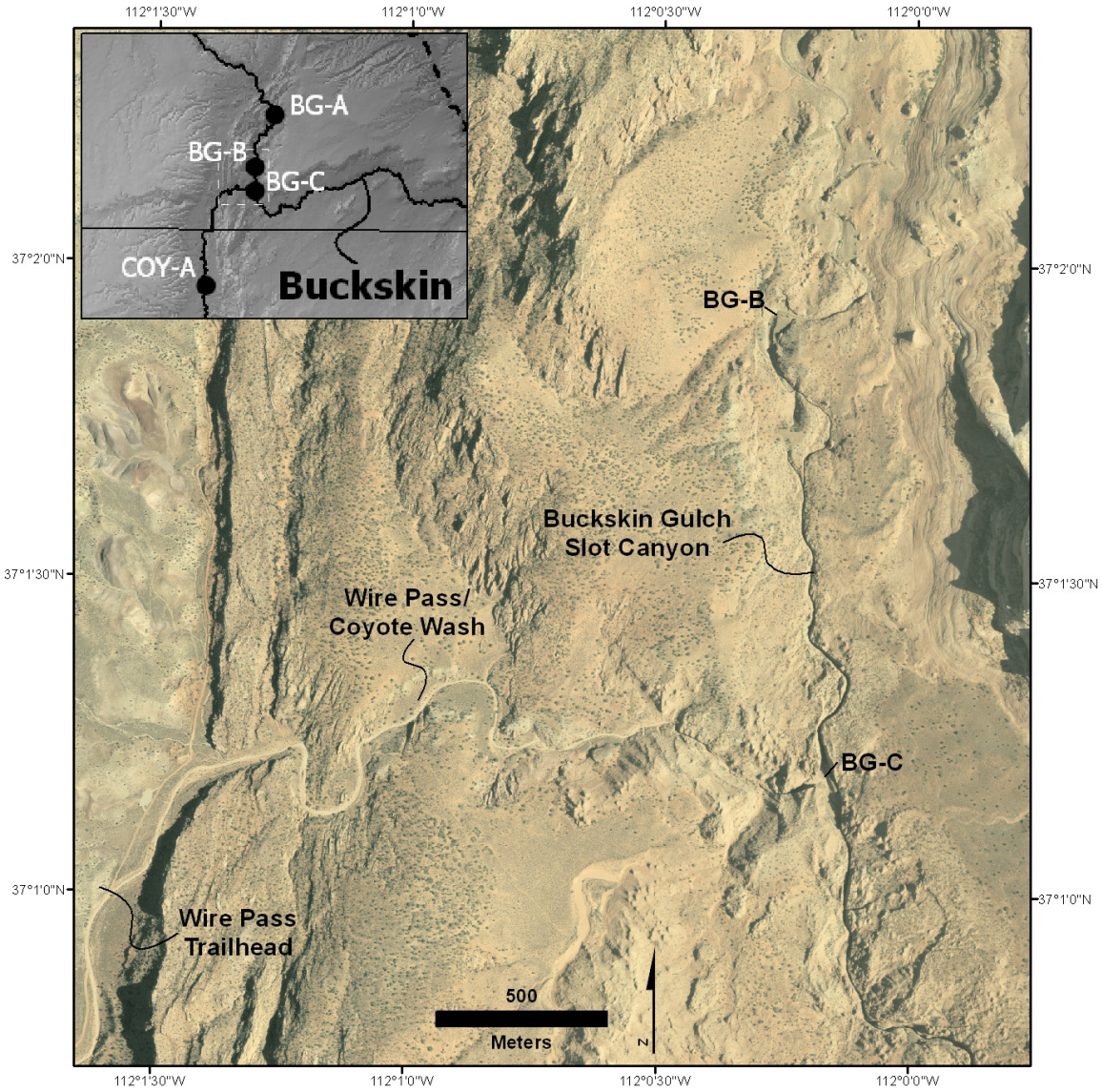

Figure 3-12 – Location map for study sites BG-B and BG-C.

Sedimentologically, package I is a series of medium to thick beds of silty medium to coarse sand. Beds are mostly tabular and laterally continuous. Though some are massive (Sm), the majority of beds contain clear horizontal planar laminae (Sl) (Figure 3-4). The coarse, sandy texture of these facies record deposition by high-energy events, though their tabular nature does not support a channel-bottom setting. They probably represent a channel-margin environment, preserved here on the inside of a ninety-degree bend in the channel. Because the entire valley bottom here is probably ponded during high-stage floods, the channel-margin and valley-surface deposits are essentially the same. There is evidence for several hiatuses and three buried entisols within this package. The first is developed upon unit 6, about 3 m from the base of the package. Weak A and Btk horizons are present, as well as abundant rhizoliths, burrows, and root casts. The second buried soil is found on the irregular, eroded surface of unit 8, which could be an eolian wedge deposited over the soil on unit 6. It is less developed and preserved than the first, yet features a weak reddish stain and infilled root traces and burrows. The third, best-developed soil is found along the upper surface of the 2 m-thick unit of massive, medium-coarse sand capping package I. This represents exposure for a relatively significant period of time, as it is heavily bioturbated, contains abundant rhizoliths, and has a strong reddish stain, likely a result of incorporation of slopewash from nearby bedrock hillslopes into the unit via infiltration and translocation processes. Correlation by stratigraphy and landscape position across the wash to other exposures indicates that this marker surface had numerous junipers germinated on it that are now buried (Figure 3-13). Two of these buried trees are still living, and are the target of tree-ring counts described below.

Package II overlies a wedge of sandy hillslope colluvium along the unconformity that truncates package I. Its basal units are four medium beds of well-cemented, massive, yellowish-brown sands (Sm) that pinch out against the bounding surface between I and II. These are overlain by a 2 m thick bed of yellowish-brown Spx, which fills much of the void left by the erosion of Package I. A series of 14 downstream-thickening beds of reddish brown and light yellowish brown Sl and Srx compose the upper 4 m of the deposit overtopping package I and burying the junipers germinated on its surface. Several of these units preserve climbing ripples that range from sub- to supercritical and variable directions of climb. This requires very high sedimentation rates and changing paleocurrent direction during a single flood event. In this case, deposition was probably in a recirculating eddy that formed downstream of the paleoslope of package I. Contacts between all units are smooth and free of bioturbation, indicating that the entire package was deposited rather quickly and that successive units were passively draped over existing deposits. Where package II has overtopped package I, planar laminae (Sl) dominate, marking a transition to more shallow, laminar flow no longer controlled by the obstruction of package I.

During high-stage floods, the majority of the valley is the wetted perimeter. However, observation of the present-day system allows us to distinguish locales of deposition. For instance, the modern channel bottom contains coarse sand to boulders while the low channel-margin floodplain is vegetated and consists of silty sand with planar, horizontal laminae and interbedded mats of detrital organic litter. There are no channel-bottom deposits preserved in the studied outcrop. Most units in each package feature a reverse- then normal-grading, which suggests deposition during both the rising

and falling limb of flood events. Such complete preservation of events suggests deposition in a protected zone away from the thalweg, such as an eddy or backwater.

BG-B geochronology

A sample of detrital charcoal from just below the lowest paleosol in package I yields an age of 1820 - 1600 cal yr BP. A similar sample taken six units above this gives an age of 1280 - 1070 cal yr BP. An OSL sample taken between the two returns a preliminary age of ~1.3 – 2.2 ka, consistent with the radiocarbon results. A radiocarbon sample of tree litter found on the buried hillslope between packages I and II constrains the age of package II to less than 290 cal yr BP. Additional OSL samples were taken from the base and middle of package II. Though they are consistent with late Holocene ages, initial results reveal that they suffer from major partial bleaching and therefore return unreliably older ages (Table 3-3). Our radiocarbon samples and those from Ely (1992) consistently argue that package II is younger than 290 cal yr BP.

A living juniper tree buried by the uppermost 4-5 units of package II is exposed near the head of a gully on stream right (Figure 3-14). A tree-ring count on a core collected ~2-3 m above the tree's germination horizon places a minimum age of ~85 years on the tree, a maximum age for overlying units. A second living, buried Juniper on top of package II across the valley yields a tree-ring count of ~110 years. The depth to the germination horizon on this tree is unknown, as the wilderness status of the study area precludes extensive excavation. However, this tree very likely germinated on the same horizon as did the others observed in the area (Figure 3-14). These data suggest that the upper portion of package II and the whole of packages III, IV, and V were deposited in

the last 150 years, which arouses suspicion that at least some of these higher flood deposits were emplaced during the cutting of arroyos upstream.

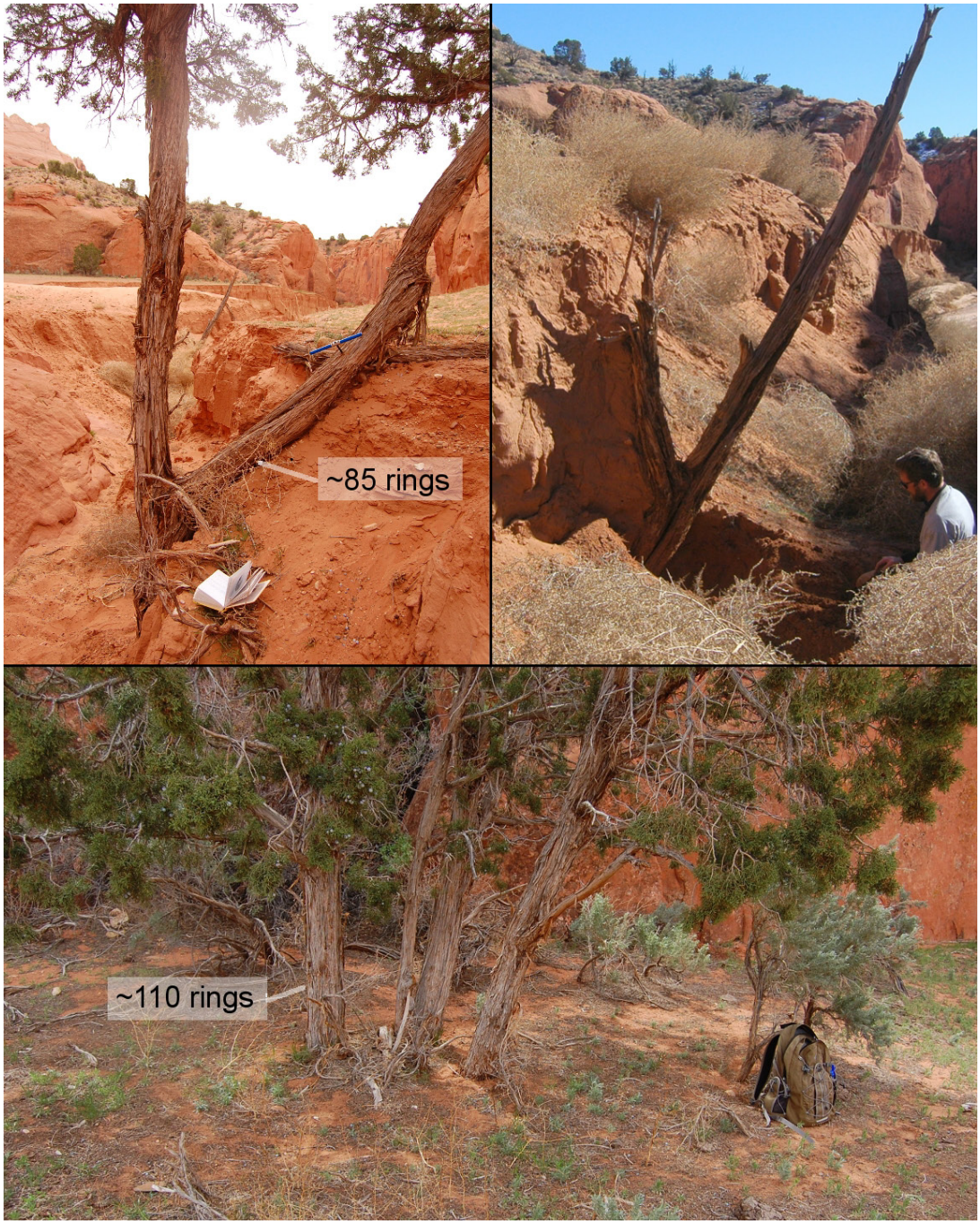

Figure 3-13 – Buried juniper trees at site BG-B. The two living trees (top left and bottom) produced cores; the dead tree in top right did not.

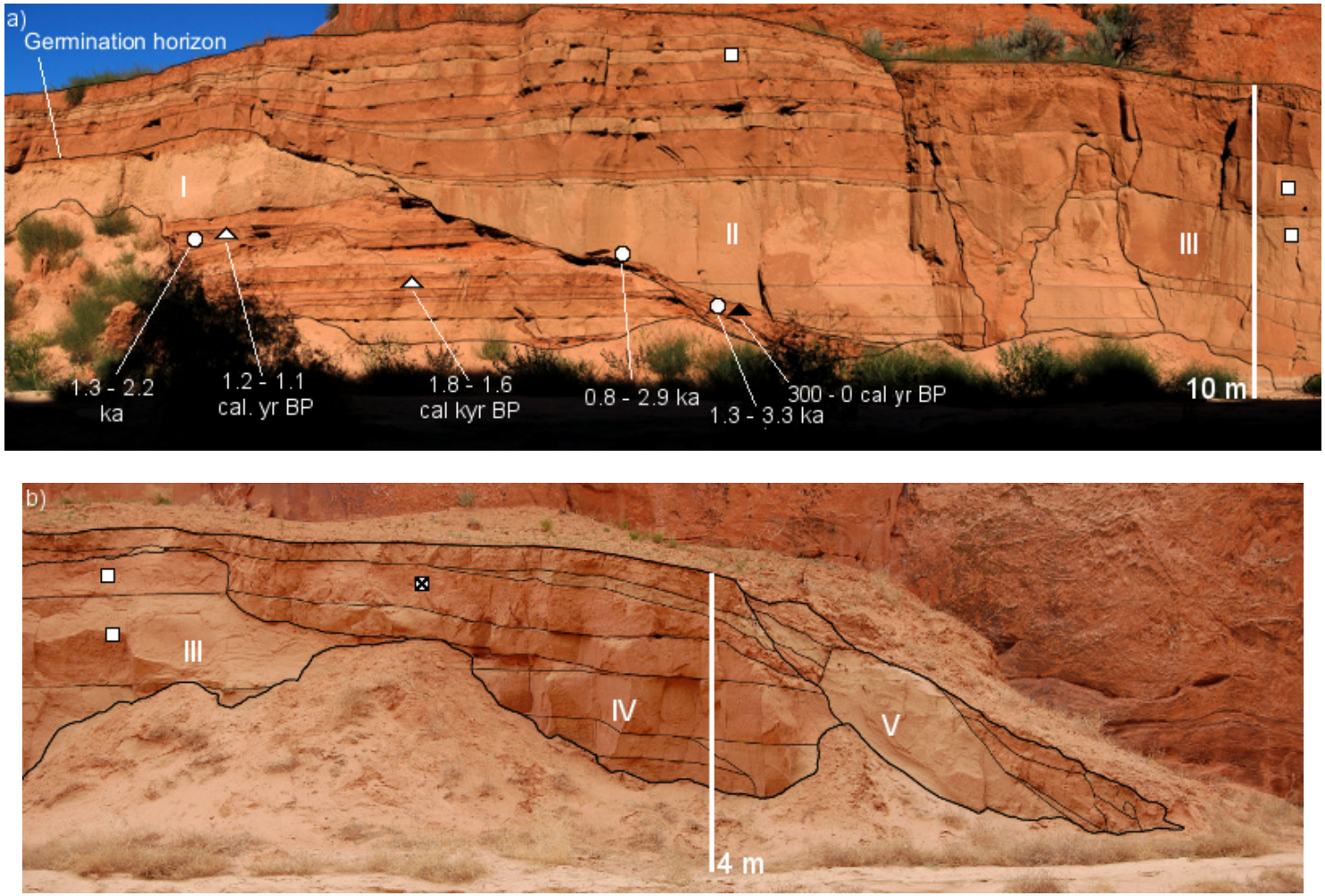

Figure 3-14 - Chronostratigraphy for study site BG-B. White circles and triangles are OSL and ^{14}C samples, respectively. Where black, sample was from correlative unit outside of outcrop. Squares show units sampled for ^{137}Cs, closed where ^{137}Cs was detected. All units are interpreted as part of the CM (channel-margin) facies asiation.

Finally, five units at site BG-B were analyzed for the presence of post-bomb ^{137}Cs (Figure 3-13). No ^{137}Cs was detected in packages II or III. A minimal amount (0.0092 ± 5% counts/second) was detected in the middle of package IV, whereas a significant amount (0.053 ± 5% counts/second) was detected near the top of package IV. This suggests that bomb testing occurred sometime near the end of deposition of package IV. Hence, all stratigraphically older units were deposited before around 1950 AD. These data, combined with the tree-ring data, argue that packages II, III, and IV were rapidly deposited between ~150 and 50 years ago.

BG-C

Site BG-C is located in the first expansion encountered downstream of site BG-B. Here, Coyote Wash meets Buckskin Gulch from the west in a spectacular gorge confined between sheer bedrock walls over 30 m high. At the downstream end of this ~100 m-long expansion is yet another severe constriction that inevitably causes a backwater to form during moderate and larger floods. As in site BG-B, a steep, bouldery knickzone marks the entrance into this downstream constriction. Famous petroglyphs on a southwest wall of this expansion are partially buried by the active channel bed, suggesting some aggradation since their creation.

The best exposure is found along the east flank of this expansion, and is the same one studied by Ely (1992). The majority of the deposit consists of a single sequence of deposits passively draped over one another, though the lowermost 2 m of the section is composed of four sub-packages inset against one another (Figure 3-15). Because the relief on these surfaces is much less than the relief of the outcrop and they are not

Figure 3-15 - Chronostratigraphy for study site BG-C. White triangles are 14C samples. Asterisk indicates that sample is from Ely (1992). All units are interpreted as part of the CM (channel-margin) facies association.

traceable to an exposure surface, we describe the sequence as if it were a single stratal package. The base of the deposit is composed of 15 thin- to medium-bedded units that truncate and overlie each other in a complex relationship. These units are mostly massive coarse sand (Sm) though a few show ripple cross-stratification (Srx). The geometry of these beds and their contacts indicates that existing deposits were scoured and refilled by later floods, preserving evidence of lateral accretion in the downstream direction. The rest of the deposit is a series of 16 tabular medium to thick beds composed of Sl, Spx, and Srx; the same facies that compose package II at site BG-B. Though individual beds have different observed thicknesses at this locality, the two packages are clearly correlative. Thus, we interpret the two packages to share a common origin, a conclusion that is corroborated by age control. Packages III and IV from site BG-B do not have correlatives here, but a deposit that could be correlative to package V from BG-B is locally smeared against the main outcrop. This suggests that in recent history, the hydraulics at BG-C have effectively preserved only those floods that overtop existing deposits. Again, no deposits recording a channel-bottom environment were seen in the outcrop.

BG-C geochronology

Radiocarbon-dated woody debris in package I suggests that the entire overlying package is younger than <290 cal yr BP (Figure 3-15). This determination is corroborated by a similar sample and consistently younger ages in stratigraphically younger units from Ely (1992). Two OSL samples were collected from the near the base and near the top of the package, though initial signs of strong partial bleaching

combined with first-order results of sub-400 year old ages led us to abandon these samples in favor of those with higher information potential. A deep gully that bisects the main terrace at BG-C, an ideal locale for preservation of high-stage flood deposits, has not been infilled by any floods. This suggests that this seemingly decades-old gully post-dates the floods that emplaced packages III, IV, and V at BG-B, suggesting that those units are at least several decades old.

Summary of Chronostratigraphy

Testing our hypothesis requires detailed chronostratigraphy to compare the timing of deposition across reaches of contrasting valley geometry. In this study, this goal has been met partially, with most temporal constraints from two of the six study sites. At each site, we have divided the alluvium into discrete packages separated by bounding surfaces. To summarize, six distinct alluvial packages were identified in the alluvial reaches of the watershed (Figure 3-17). The two oldest, identified only in Coyote Wash, were deposited sometime around the last glacial maximum and the early Holocene. Three younger packages were identified only in Kitchen Corral Wash. The first was deposited ~3 - 2 ka. The next two packages had to have been deposited between ~2.0 and 0.8 ka, separated from each other by an additional period of arroyo-cutting and soil formation. The youngest package was identified in both Coyote and Kitchen Corral Wash and was deposited from ~0.7 ka until historic arroyo cutting around 0.11 ka. Two packages were identified in the study site within the transitional reach, both deposited since ~0.6 ka. This correlates with deposition of the youngest package in the alluvial reaches. However, age control at this locality is

sparse. Five stratal packages separated by bounding surfaces are present in two outcrops within the constricted reaches of the watershed. The distinctive first package was deposited ~2 - 1 ka, and the next three packages were deposited between ~0.15 and 0.05 ka. The final package was deposited after 1950 AD.

In addition to those bounding unconformities that crosscut strata and represent periods of erosion, depositional hiatuses recorded in the alluvial records are important stratigraphic markers. These can be classified into two groups: 1) short-lived hiatuses manifested by rhizoliths, bioturbation, and introduction of eolian and slopewash material; and 2) longer-lived diastems marked by all of the above, as well as the presence of buried A and/or Bw soil horizons. In the alluvial reaches, these longer diastems mark the boundary between each cut-and-fill package. Each package contains multiple short-lived hiatuses within the channel-margin and valley-surface facies associations, usually in the upper parts of the package. In the constricted reach, a diastem separates the oldest package (I) from package II, and represents close to 1000 years based on geochronology and buried-tree evidence. Two shorter hiatuses are present in the upper-middle of this oldest package; but, importantly, none are present in the four younger packages.

Though we are somewhat limited by an incomplete geochronology, some interesting patterns have emerged in the last millennium of the records. Our primary result in terms of geochronology is that packages II and III at BG-B, which form the bulk of the stored sediment at that locality, are indeed broadly correlative with historic arroyo cutting in the alluvial reaches upstream. Additionally, the notable hiatus in preserved flood deposition between packages I and II in the constricted

reach is correlative with the aggradation of the Naha or 'settlement' fill terrace (Hereford, 2002) in the alluvial reaches upstream (Figure 3-16).

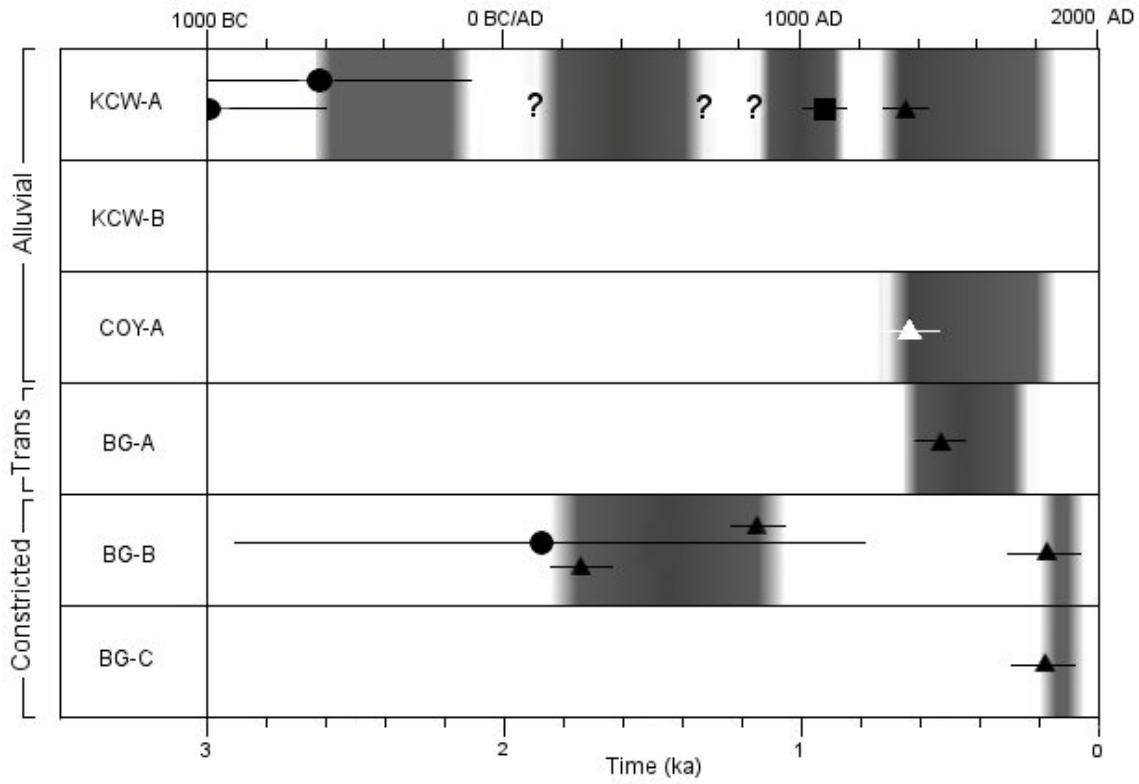

Figure 3-16 – Temporal comparison of deposition at all six study sites. Black circles and triangles are OSL and radiocarbon ages from this study, respectively. Closed square represents a constraint from cultural material. White triangle represents over a dozen radiocarbon ages from Hereford (pers. comm.).

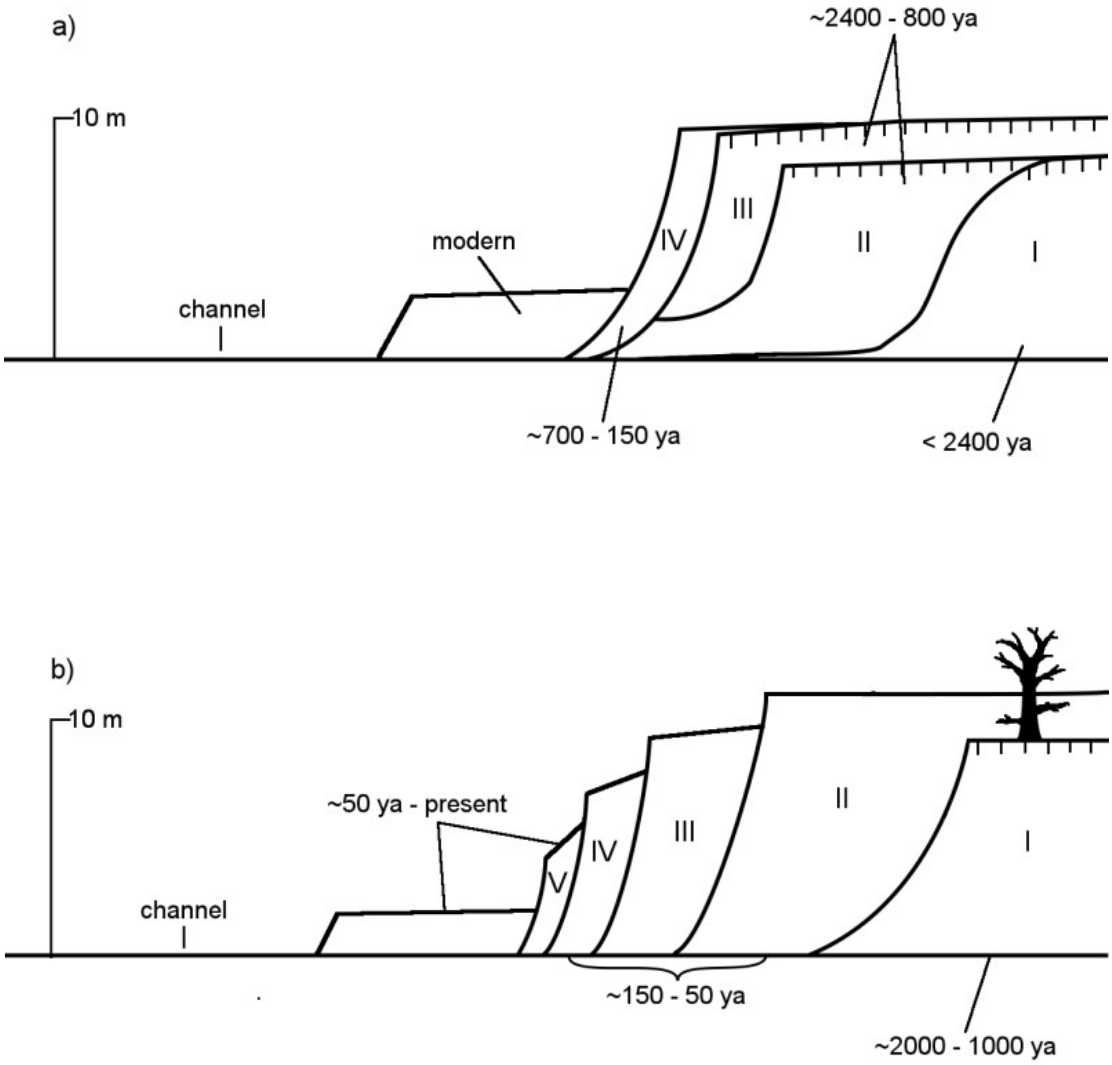

Figure 3-17 – Summarized chronostratigraphy of the greater Buckskin drainage: a) alluvial reaches, b) constricted reach.

DISCUSSION

In the greater Buckskin drainage, two end-member valley geometries exist: 1) broad alluvial reaches where the channel is free to migrate laterally between bedrock walls hundreds of meters apart, and 2) constricted reaches where bedrock walls effectively form the lateral channel boundaries during high flows. Because these valley geometries control channel geometry, they influence sediment transport and storage during floods and ultimately the alluvial record stored within a given reach. The most informative exposures in these two reaches were found at study sites KCW-A and BG-B. Thus, the following discussion is based primarily on observations from these two sites.

Contrast of alluvial and constricted reach deposits

In the alluvial reach, accommodation space and preservation potential are relatively high. Stored sediment consists of interfingering mainstem, local-slope, and tributary deposits. The facies of these deposits can usually be associated with deposition in three main environments within the alluvial valley: CB – the bottom of the channel where flow depths and velocities are highest, CM – the margins of the channel, where flow depths and velocities are reduced relative to the thalweg, and VS – the broad, flat surface of the alluvial valley where flow width is greatly increased and velocity and depth are greatly decreased.

The arrangement of depositional units within these facies associations in the studied outcrops provides clues about changes in late Holocene stream grade. Channel-bottom deposits at the base of each package at KCW-A record quasi-braided

streams with coarse bedload and high flow velocities at the base of newly-incised and widening arroyos. In packages I, II, and III, these channel-bottom deposits are overlain by thick sequences of voluminous channel-margin deposits distinguished by thin- to thick tabular beds of planar to ripple cross-laminated sand. These are in turn overlain by thin caps of valley-surface deposits, characterized by increasingly bioturbated, massive, silty sands with weakly developed soils.

Though this fining-upward sequence is similar to that described for lateral accretion in a meandering stream, such deposits should not be much thicker than typical channel depths unless significant channel aggradation has taken place. Thus, the late Holocene history of Kitchen Corral Wash can be characterized by cycles of arroyo cutting and filling. As additional evidence, in package IV, lenticular channel-bottom deposits accreted vertically in tandem with adjacent channel-margin deposits up to 8 m above the modern wash. Hence, we argue that aggradation of the channel bottom must have coincided with lateral and vertical accretion on channel-margin floodplains to accomplish the filling and overtopping of paleoarroyos with such thick stratal packages.

In the constricted reach, accommodation space is minimal and preservation potential is therefore lower. Three components similar to those in the alluvial reach were recognized in this constricted depositional system: 1) the channel-bottom; 2) the areally-extensive channel-margin floodplain; and 3) the high valley-surface terrace. The same facies associations found in the alluvial reach can be applied to these sites of deposition, with some variations. At site BG-B, the geometry and facies composing the modern channel-margin floodplain are quite similar to its analog in

Kitchen Corral Wash. Indeed, field observations following the largest flood of 2008 showed that in both the alluvial and constricted reaches, floodwaters barely overtopped this landform and deposited a thin wedge of laminated sand. This suggests that, at such flows, processes of deposition and erosion are not greatly influenced by local valley geometry. In contrast, during rarer, higher-discharge events, the constricted valley geometry begins to control spatial patterns of deposition and erosion. As evidence, the prominent high terrace here is present only in those areas where flow separation is expected to occur during high-stage floods, such as the inside of sharp channel beds, tributary confluences, and alcoves in the wall of the otherwise narrow slot canyon.

Though the units that compose the higher deposits at BG-B are similar in landscape position to the primary terrace of the alluvial reach, they are sedimentologically distinct. These deposits lack tributary and local-slope facies, indicating that this location preserves only mainstem depositional events. The thickness and geometry of beds are broadly similar to the deposits of the channel-margin facies association that compose the bulk of the packages at KCW-A. However, more subtle differences suggest a different environment of deposition. Increased abundance of silt in the constricted reach deposits suggests a lower-velocity environment while wavy parallel laminae draping lower contacts suggest faster rates of deposition. Additionally, the deposits of the constricted reach lack channel-bottom facies preserved any higher than the grade of the modern wash, in contrast to the trough-crossbedded coarse sands and imbricated gravels in the alluvial reach. The massive, poorly-sorted, yellowish brown units in package II at BG-B do contain a few

suspended pebbles and granules, but tabular bed geometry and lack of sedimentary structures suggests that these units were deposited out of suspension on the smooth surface of the pre-existing slackwater deposits. These larger grains could have been carried in suspension by a concentrated or hyperconcentrated flow, a conclusion supported by the disorganized, massive structure.

The deposits at BG-B also differ in their internal stratigraphy from those underlying the valley fill at KCW-A. Though four downstream-dipping unconformities and a diastem representing ~900 years of missing time are present at site BG-B, they are of different character than those surfaces bounding aggradational cycles at KCW-A. Whereas each bounding unconformity at KCW-A can be linked to a buried entisol atop the truncated package, only the one that truncates package I at BG-B can be associated with a buried soil. Instead, those unconformities separating packages II, III, IV, and V are associated with, at the very most, weakly bioturbated surfaces that represent a much shorter period of exposure. Additionally, the rarity of zones of bioturbation *within* a given package in the constricted reach suggests that the units in each were deposited in rather quick succession. This contrasts sharply with the frequent bioturbation of surfaces within packages in the alluvial reaches. Hence, the packages of the constricted reach appear to represent much shorter periods of time than the aggradational packages of the alluvial reach.

Chronostratigraphic Interpretation

Chronostratigraphy results reveal two major clusters of flood deposition preserved at BG-B: deposition of package I from ~2 - 1 ka and the more rapid

deposition of packages II – V from ~0.15 - 0.05 ka. Under the paradigm of paleoflood hydrology, one might suggest that these deposits preserve two distinct, climatically-significant clusters of increased flood frequency and magnitude, separated by a ~900 year absence of significant flooding. This interpretation is difficult to accept for multiple reasons. First, a ~900-year absence of large floods followed by the occurrence of ~40 such floods within a 100-year period is hydroclimatically unlikely. Such a drastic transition in the hydrology of the system has not been noted in any other regional paleohydrologic records. Second, the pattern of sedimentation in the constricted-reach packages contrasts with that of a typical paleoflood sequence, which is usually biased toward rarer, larger floods up-section. In that scenario, one would expect increasing abundance of exposure surfaces toward the top of the section, reflecting the increasing period of time between floods large enough to overtop existing deposits. Instead, the absence of exposure surfaces and consistent bedding character suggests that the whole sequence was deposited rather rapidly with no increasing selectivity up-section.

We argue that instead of just hydroclimatic changes, the deposits in the studied constricted reaches of Buckskin Gulch represent episodes of increased preservation potential. This is more consistent with the character of the sedimentary packages as well as the known paleohydrological record. Importantly, the timing of deposition of the bulk of the constricted reach deposits does indeed correlate to historic arroyo cutting in the alluvial reach upstream. This large-scale excavation of valley-fill alluvium upstream certainly resulted in extreme sediment loads downstream, as documented by historic records on nearby Kanab Creek (e.g. Webb et

al., 1991). We argue that the transfer of such large amount of alluvium overwhelmed the system and altered the preservation potential of floods in the Buckskin slot canyon. This could be accomplished by changing the stage-discharge relation in the constricted reach via deposition of large volumes of sediment along channel margins. As the arroyo headcut migrated upstream during successive floods, additional sediment-laden floods would have been easily preserved without necessarily being of abnormally high discharge.

This interpretation is supported by the modern geometry of the deposits in the constricted reach. The deposits are actively slumping into the modern wash, and probably have been since the cessation of arroyo cutting upstream. This suggests that they once extended farther into the channel than they do today. In a stream with such a low width-to-depth ratio, a logical result of these voluminous deposits being emplaced so rapidly would have been an altered stage-discharge relationship. In turn, this altered relationship served to rapidly emplace and preserve deposits of many moderate, perhaps climatically-insignificant floods atop the channel margin deposits. Hence, we argue that the majority of the deposits in the constricted reach of Buckskin Gulch represent those major pulses of alluviation that resulted from the upstream migration of arroyo headcuts during historic arroyo cutting. The slow removal of these deposits over the past few decades represents the 'relaxation' of the system to its background state and the reduction of preservation potential to where it was before arroyo cutting.

This conceptual model also explains why no floods were preserved in the constricted reach during the deposition of the settlement alluvium upstream over the

several hundred years preceding historic arroyo cutting. While significant floods may have occurred this period, they were evidently not large enough to induce arroyo cutting. Hence, they carried less sediment downstream, avoiding the conditions that would have enhanced their preservation. During this time, it is likely that the unconsolidated deposits in the constricted reach (Package I from BG-B) were instead slowly removed by lateral erosion.

Thus, we suggest that the original hypothesis is broadly correct – upstream alluviation and constricted reach deposition are temporally anti-correlated over the past 700 years. However, we do not link this anticorrelation to the conclusion that abnormally frequent and high-magnitude floods caused arroyo cutting. Instead, paleoflood deposits at the studied sites in Buckskin Gulch are subject to preferential preservation and are not truly representative record of flood magnitude and frequency through time.

The temporary episodes of sediments storage that affect the constricted reach record are consistent with the work of Graf (1987). He described the different patterns of sediment transport and storage as a function of drainage size, i.e. position within drainage. In particular, local streams (drainage area = 1 – 1,000 km^2) alternatingly stored and evacuated sediment over centennial timescales in response to allogenic influences. Regional streams (drainage area = 1,000 – 10,000 km^2) alternatingly stored and evacuated sediment mostly in response to events upstream. Buckskin Gulch, with a drainage area of ~1000 km^2, lies right at the boundary between these two stream classifications, and appears to store and evacuate sediment as a function of both climatic changes and upstream influences. Pederson (2000),

working in another bedrock canyon in the Colorado Plateau, showed that episodic sediment input from tributaries controlled the the alluvial records of Lake Canyon. He argued that these episodes of sediment storage were climate-driven. These examples from other studies bolster our argument that upstream geomorphic changes can significantly impact downstream alluvial records.

CONCLUSIONS

1) Depositional processes in the greater Buckskin drainage are a function of valley geometry. In broad alluvial valleys, valley-fill alluvium consists of interfingering mainstem- and tributary-derived gravels, sands, and silts, preserving deposition in channel-bottom, channel-margin, and valley-surface environments. In constricted bedrock reaches, stored sediment is strictly silty fine to coarse sand, representing slackwater deposition in a channel-margin environment.

2) Late Holocene alluvial deposits in the alluvial reach upstream of Buckskin Wash are composed of at least four aggradational packages since ~3.0 ka. The youngest was deposited from ~0.7 – 0.1 ka and correlates regionally with the Naha alluvium, while the older packages are related to the more complex Tsegi and Jeddito alluvia described elsewhere in the Southwest. The constricted reach contains two main clusters of deposition: one from ~2.0 to 1.0 ka, and another from ~0.15 to ~0.05 ka. The younger cluster of deposits correlates to the incision of the Naha or “settlement” alluvium in the late 1800s and early 1900s. The preceding several-hundred year

hiatus in constricted-reach deposition correlates roughly with the aggradation of that same valley fill upstream.

3) OSL samples from both the alluvial and constricted reaches consistently suffer from partial bleaching due to rapid, turbid transport processes in the drainage. This is problematic, especially for samples younger than ~1 ka. Workers in similar environments should target those beds resulting from eolian or clear-water fluvial transport and avoid those that show characteristics of disorganized, concentrated flows. A higher number of aliquots should be analyzed with the SAR method in order to minimize the uncertainties introduced by partial bleaching, though single-grain OSL dating may more do a better job of isolating the population of fully-bleached grains.

5) Paleoflood records in tightly-constricted bedrock canyons may not be a representative sample of flood magnitude and/or frequency. Instead, the record in Buckskin Wash strongly suggests preferential preservation of flood deposits during episodes of very high sediment supply from arroyo cutting upstream. Temporary sediment storage in backwaters during these episodes should significantly alter local stage-discharge relations and produce rapid sequences of high-stage deposits. Thus, paleoflood sequences in slot canyons may not be solely a function of paleohydrology, but may also be a function of geomorphic changes upstream.

REFERENCES

Aitken, M.J., 1998, An introduction to optical dating: Oxford, Oxford University Press, 267 p.

Bailey, R. M., Smith, B. W., and Rhodes, E. J., 1997, Partial bleaching and the decay form characteristics of quartz OSL: Radiation Measurements, v. 27, p. 123-126.

Berger, G. W., 1990, Effectiveness of natural zeroing of the thermoluminescence in Sediments: Journal of Geophysical Research, v. 95, p. 12,375 - 12,397.

Cooke, R.U., and Reeves, R.W., 1976, Arroyos and environmental change: Oxford, Clarendon Press, 213 p.

Doelling, H.H., and Davis, D.D., 1989, The geology of Kane County, Utah: Salt Lake City, Utah Geological and Mineral Survey Bulletin 124, 8 plates, 192 p.

Ely, L. L., 1992, Large Floods in the Southwestern United States in Relation to Late-Holocene Climatic Variations [Ph.D. dissertation]: Tucson, University of Arizona, 326 p.

Ely, L. L., 1997, Response of extreme floods in the southwestern United States to climatic variations in the late Holocene: Geomorphology, v. 19, p. 175–201.

Ely, L. L., and Webb, R. H., 1992, Accuracy of post-bomb ^{137}Cs and ^{14}C in dating fluvial deposits: Quaternary Research, v. 38, p. 196-204.

Fuchs, M., Woda, C., and Burkert, A., 2007, Chronostratigraphy of a sediment record from the Hajar mountain range in north Oman: Implications for optical dating of insufficiently bleached sediments: Quaternary Geochronology, v. 2, p. 202-207.

Graf, J. B., Webb, R. H., and Hereford, R., 1991, Relation of sediment load and flood-plain formation to climatic variability, Paria River drainage basin, Utah and Arizona: Geological Society of America Bulletin, v. 103, p. 1405-1415.

Graf, W. L., 1983, The arroyo problem—Paleohydrology and paleohydraulics in the short term *in* Gregory, K.G., ed., Background to paleohydrology: New York, John Wiley and Sons, p. 279-302.

Graf, W.L., 1987, Late Holocene sediment storage in canyons of the Colorado Plateau: Geological Society of America Bulletin, v. 99, p. 261–271.

Graf, W.L., 1988, Fluvial processes in dryland rivers: New York, Springer-Verlag, 346 p.

Gregory, H.E., and Moore, R.C., 1931, The Kaiparowits region, a geographic and geologic reconnaissance of parts of Utah and Arizona: U.S. Geological Survey Professional Paper 164, 161 p.

Grootes, P. M., 1983, Radioactive isotopes in the Holocene, *in* H. W. Wright, Jr., ed., Late Quaternary Environments of the United States. Volume 2, the Holocene, Minneapolis, University of Minnesota Press, p. 86-105.

Hack, J.T., 1942, The changing physical environment of the Hopi Indians of Arizona: Peabody Museum Papers, v. 25, no. 1., 85 p., 12 plates.

Hall, S.A., 1977, Late Quaternary sedimentation and paleoecologic history of Chaco Canyon, New Mexico: Geological Society of America Bulletin, v. 88, p. 1593–1618.

Hereford, R., 1986, Modern alluvial history of the Paria River drainage basin: Quaternary Research, v. 25, p. 293–311.

Hereford, R., 1993, Paleoflood Hydrology of the southern Colorado Plateau: AMQUA field trip guide, p. 17-18.

Hereford, R., Jacoby, G.C., and McCord, V.A.S., 1996, Late Holocene alluvial geomorphology of the Virgin River in the Zion National Park area, southwest Utah: Geological Society of America Special Paper 310, 41 p.

Hereford, R., 2002, Valley-fill alluviation during the Little Ice Age (ca. A.D. 1400-1880), Paria River basin and southern Colorado Plateau, United States: Geological Society of America Bulletin, v. 114, p. 1550-1563.

Karlstrom, T. N. V., 1988, Alluvial chronology and hydrologic change of Black Mesa and nearby regions, *in* Gumerman, G. J., ed., The Anasazi in a Changing Environment: Cambridge, Cambridge University Press, p. 45-91.

Leopold, L.B., 1976, Reversal of erosion cycle and climatic change: Quaternary Research, v. 6, p. 557-562.

Murray, A. S., and Wintle, A. G., 2003, The single aliquot regenerative dose protocol: potential for improvements in reliability: Radiation Measurements, v. 37, p. 377-381.

Pederson, J. L., 2000, Holocene paleoloakes of Lake Canyon, Colorado Plateau: Paleoclimate and landscape response from sedimentology and allostratigraphy: Geological Society of America Bulletin, v. 112, p. 147-158.

Reagan, A. B., 1924, Recent changes in the plateau region: Science, v. 60, p. 283-285.

Reimer, P. J., Baillie, M. G. L., Bard, E., Bayliss, A., Beck, J. W., Bertrand, C. J. H., Blackwell, P. G., Buck, C. E., Burr, G.S., Cutler, K. B., Damon, P.E., Edwards, R. L., Fairbanks, R. G., Friedrich, M., Guilderson, T. P., Hogg, A. G., Hughen, K. A., Kromer, B., McCormac, F. G., Manning, S. W., Ramsey, C. B., Reimer, R.W., Remmele, S., Southon, J. R., Stuiver, M., Talamo, S., Taylor, F. W., van der Plicht, J., and Weyhenmeyer, C. E., 2004, IntCal04 terrestrial radiocarbon age calibration, 26–0 ka BP: Radiocarbon, v. 46, p. 1029–1058.

Topping, D. J., 1997, Physics of flow, sediment transport, hydraulic geometry, and channel geomorphic adjustment during flash floods in an ephemeral river, the Paria River, Utah and Arizona [Ph.D. Thesis]: Seattle, University of Washington, 405 p.

Wallinga, J., 2002, Optically stimulated luminescence dating of fluvial sediments: A review: Boreas 31, 3003–3322.

Webb, R.H., 1985, Late Holocene flooding on the Escalante River, south-central Utah [Ph.D. thesis]: Tucson, University of Arizona, 204 p.

Webb, R. H., Smith, S. S., and McCord, V. A. S., 1991, Historic channel change of Kanab Creek, southern Utah and northern Arizona: Grand Canyon Natural History Association Monograph 9. 91 pp.

Webb, R.H., Blainey, J.B., and Hyndman, D.W., 2002, Paleoflood hydrology of the Paria River, southern Utah and northern Arizona, USA, *in* House, P.K., Webb, R.H., Baker, V.R., and Levish, D.R., eds., Ancient Floods and Modern Hazards: Principles and Applications of Paleoflood Hydrology: American Geophysical Union Water Science and Application Series, v. 5, p. 295–310.

Western Regional Climate Center [online] available at: http://www.wrcc.dri.edu/

CHAPTER 4

SUMMARY AND IMPLICATIONS

In Chapter II, I described the distinction between the approaches taken by paleoflood hydrologists and those reconstructing arroyo cut-and-fill cycles in drylands. To reconcile these approaches and their resulting records, I advocated focused chronostratigraphic studies of both record types in a single drainage. In Chapter III, I reported the results of such a study in Buckskin Wash, a classic example of a dryland stream featuring a broad alluvial valley that grades into a narrow bedrock canyon. Using detailed sedimentology, stratigraphy, and geochronology, I compared the composition of the major valley-fill terraces in the two end-member reaches of the watershed.

The broad valley fills in the alluvial reaches of the study area are composed of multiple aggradational packages bound by erosional surfaces. The aggradational packages are composed of three broad depositional facies associations: channel-bottom, channel-margin, and valley-surface. Channel-bottom deposits contain mostly lenticular sandy gravels and trough-crossbedded coarse sands deposited in a high-energy environment. These are generally overlain by the thick, tabular sands of the channel-margin facies association. These for the most part represent the in-arroyo floodplains that effectively filled the paleoarroyos. The valley surface facies association includes those mainstem floods that overtop arroyo walls as well as eolian, slopewash, and tributary deposits that accumulate on the surfaces of entrenched valleys. Four late Holocene aggradational packages were emplaced in the

alluvial reach since 3.0 ka. The latest was deposited from ~0.7 – 0.1 ka, and is correlative to the Naha alluvium found throughout the Southwest. These packages generally record centennial-scale episodes of valley-bottom aggradation punctuated by decadal-scale episodes of incision.

In the slot canyon downstream, the valley-fill terrace contains similar packages bound by erosional surfaces. Composed of tabular, medium to thick beds of silty sand, they primarily record slackwater deposition during paleofloods. In contrast to the aggradational packages upstream, these constricted-reach deposits do not necessarily record cycles of streambed aggradation and entrenchment. These deposits are composed of five distinct stratal packages. The oldest of these was deposited from ~1.9 – 1.1 ka; notably 1500 years earlier than previously thought. After a ~1000 year hiatus in deposition, the next four packages were deposited in a matter of several decades between 150 and 50 years ago.

Importantly, these younger deposits are broadly contemporaneous with historic arroyo-cutting upstream. This correlation provides support for the hypothesis that deposition is anticorrelated across the two end-member reaches. The floods that accomplished arroyo cutting carried enormous volumes of sediment downstream (e.g. Webb et al., 1991). Temporary storage of this sediment in backwaters likely changed local stage-discharge relationships such that floods could much more easily overtop existing deposits and be preserved in the alluvial record. Hence, the paleoflood record in the constricted reach of Buckskin Wash is not simply a function of hydroclimatic changes. The alternative interpretation presented here suggests that in dryland streams, paleoflood sequences in constricted bedrock canyons may not be

insulated from the geomorphic changes associated with arroyo cutting and filling upstream.

An important conclusion of our interpretation is that paleoflood hydrologists working constricted canyons downstream of entrenched alluvial valleys should be careful to consider the influence of temporary sediment storage from upstream arroyo cutting events on local stage-discharge relationships. Such an influence may exert greater control over the preservation of particular floods than discharge, artificially inflating the frequency of high-discharge events during and following the event. Both slot canyon study sites in this study were affected to the point that they are not reliable paleoflood records. However, other deposits observed farther downstream may be less sensitive to geomorphic changes upstream because they were not located immediately upstream of a major constriction. It would be worthwhile to examine the ages of deposits in this alternative hydraulic setting to determine if the arroyo cutting signal overwhelms these deposits as well. In general, this source of uncertainty in paleoflood reconstructions could simply be eliminated by avoiding sites downstream of broad alluvial valleys subject to periodic excavation.

Future efforts in the study area should attempt to produce a more complete geochronology. A major gap in this study's geochronology is the timing of the arroyo-cutting events that followed aggradation of packages I and II in Kitchen Corral Wash. If the timing of these events could be established, it would allow comparison with the timing of deposition of package I in Buckskin Gulch. If deposition across the two reaches was anticorrelated during those episodes as it was in the last ~800 years, it would lend further support to our hypothesis that the constricted reach

records are related to periods of sediment transport from the alluvial reach into the constricted reach.

The best approach for constraining the age of older (> 300 yr) units is to utilize both OSL and radiocarbon methods. Such a hybrid approach allows validation of either method and highlights instances where uncertainties such as partial bleaching or old carbon resulted in inaccurate ages. Though difficulties were encountered with OSL dating in the study area, targeting only those units that have been thoroughly bleached, such as eolian beds, would improve precision and accuracy. For fluvial units, single-grain OSL dating has the potential to overcome the uncertainties introduced by partial bleaching, though this method will be limited at the younger age range, where weak luminescence signals become problematic.

It would be worthwhile to more precisely constrain the timing of the younger (<300 yr) flood units in the constricted reach. For the youngest units, ^{137}Cs is a relatively cheap and reliable method to determine if a bed was deposited before or after bomb testing (~1950 AD). Care should be taken to avoid units that could be contaminated by in-situ deposition of meteoric ^{137}Cs. Despite the irregular growth patterns exhibited by Juniper trees, they provide additional high-precision age estimates. Again, such a hybrid approach could allow independent age estimates that could be compared against each other. Though all living trees at site BG-B were cored in this study, observations made during a through-hike of the Buckskin Gulch slot canyon identified several additional deposits downstream of the study area that may host candidate trees.

Another aspect of the problem worth further investigation is the uncertain hydraulic environment of the constricted reach during large floods. Because direct measurement would be extremely difficult, characterization of the hydraulics through the constricted reaches at sites BG-B and BG-C must be accomplished through modeling. Survey data collected from these reaches during this study could be used to parameterize a 1- or 2-dimensional flow model such as HEC-RAS. This would allow rough estimation of flood discharges necessary to overtop existing surfaces through these reaches. It would also allow exploration of the effect that changes in cross-sectional morphology would have the stage of a flood with a given discharge, having direct implications for its preservation potential. Another application of the modeling approach would be to better characterize the distinction and transition between end-member valley geometries. For example, during a flood of a given discharge, estimates of shear stress in the arroyo reach could be compared with estimates from the constricted reach. Such an exercise would help quantify the effects that bedrock constrictions have on the behavior of individual floods, with implications for the types of records that may be stored in a given reach. Unfortunately, the current generation of hydraulic models is not yet capable of accurately modeling the complex flow conditions involving irregular bedrock walls, rapid expansions and contractions, and unsteady flow conditions. Hence, the results of the above proposed studies would serve as only rough estimates until more powerful models are produced.

APPENDICES

Appendix A. Optically Stimulated Luminescence Data

Table A-1 – Results of optically stimulated luminescence analyses.

Site	Sample Number	Lab Number	Depth (m)	# disks run	# disks accepted (used)	De (Gy)	Rd (Gy/kyr)	Age (ka)	Age Range (ka)	Position
KCW-A**	JHKCW6	USU 530	8.0	45	36 (21)	3.9 ± 1	1.52 ± 0.07	2.61 ± 0.87	1.7 - 3.4	Base of II
KCW-A**	JHKCW7	USU 531	4.0	41	33 (23)	6.9 ± 1.5	2.21 ± 0.10	3.13 ± 0.71	2.6 - 3.8	Middle of I
KCW-B**	JHKCW3	USU 389	4.0	45	33 (23)	4.8 ± 1.7	0.96 ± 0.05	4.99 ± 1.81	3.1 - 6.8	Base of II
KCW-B**	JHKCW2	USU 388	4.0	43	27 (20)	9.16 ± 2.8	2.06 ± 0.09	4.35 ± 1.36	3.0 - 6.9	Base of I
COY-A*	CWOSL2	USU 136	3.2	25	16	19.1 ± 5.6	1.50 ± 0.07	12.78 ± 3.84	9.0 - 16.6	Base of II
COY-A	CWOSL1	USU 135	5.8	25	13	19.9 ± 2.4	1.14 ± 0.05	17.50 ± 2.50	15.0 - 20.0	Base of I
BG-A**	JHBG6	USU 385	3.0	33	20 (11)	4.3 ± 1.8	1.84 ± 0.08	2.34 ± 1.00	1.3 - 3.3	Middle of II
BG-A**	JHBG5	USU 384	3.6	20	15 (5)	10.1 ± 3.4	2.09 ± 0.09	4.82 ± 1.67	3.1 - 6.5	Base of I
BG-B*	JHBG11	USU 523	6.0	15	8	4.0 ± 1.8	1.73 ± 0.08	2.32 ± 1.03	1.3 - 3.3	Middle of II
BG-B**	JHBG10	USU 522	9.0	15	7 (6)	3.2 ± 1.9	1.76 ± 0.08	1.81 ± 1.06	0.8 - 2.9	Base of II
BG-B**	JHBG9	USU 521	5.5	35	24 (14)	4.0 ± 1.0	2.29 ± 0.10	1.74 ± 0.43	1.3 - 2.2	Middle of I

*sample has significant partial bleaching

** sample has significant partial bleaching; only younger population of accepted disks used in De calculation

Figure A-1 – OSL data from sample JHKCW6.

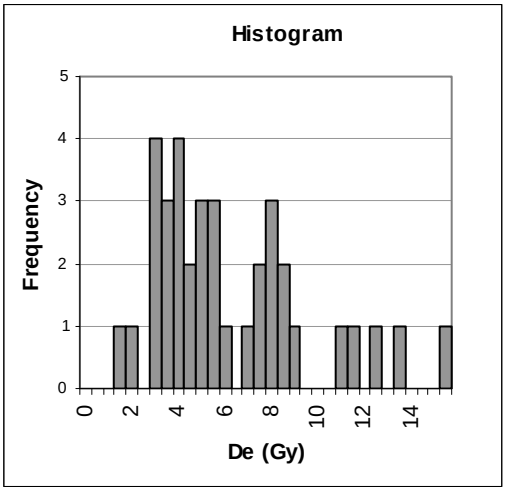

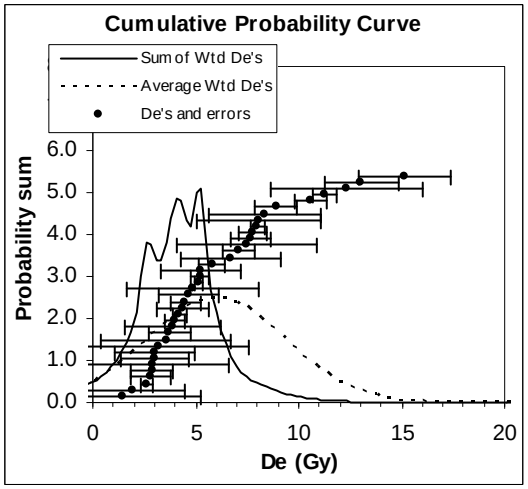

JHKCW6 **Base of I, KCW-A** **Individual Aliquot Data**
USU530

	De (Gy)	±		Age (ka)	±
wt Mean =	**3.98**	**1.30**		**2.61**	**0.87**
manual fit=	2.900	1		**1.90**	**0.63**
n =	**21**	**Aliquots**			
Median =	4.58			3.0	1.0
Min =	1.44			0.9	0.3
Max =	7.99			5.2	1.7
S.D. =	1.30				
Standard error =	0.28				
Random Errors=	32.75	%			
Systematic Error=	6.12	%			
Total Error=	33.32	%			
Bin Width =	1	**Gy**			
		+/-			
dose rate=	**1.52**	**0.07**	**Gy/ka**		
U =	1.00	0.1	**ppm**		
Th =	3.20	0.3	**ppm**		
K2O =	1.25	0.03	**wt. %**		
Rb2O=	51.6	2.1	**ppm**		
H2O=	3.0	3.0	**wt. %**		
Cosmic=	0.07	**Gy/ka**			
depth =	8.0	**m**			
latitude=	37	**degrees (north positive)**			
longitude=	112.1	**degrees (east positive)**			
elevation=	1.65	**km asl**			

De (Gy)	±	Age (ka)	±
1.44	**3.84**	0.94	0.31
1.98	**2.50**	1.30	0.43
2.63	**0.29**	1.73	0.57
2.86	**0.97**	1.88	0.63
2.87	**1.03**	1.88	0.63
3.01	**1.65**	1.97	0.66
3.01	**1.91**	1.97	0.66
3.56	**3.12**	2.33	0.78
3.73	**1.01**	2.45	0.82
3.90	**2.33**	2.56	0.85
3.95	**0.50**	2.59	0.86
4.21	**0.35**	2.76	0.92
4.34	**1.25**	2.85	0.95
4.50	**0.76**	2.95	0.98
4.66	**1.50**	3.06	1.02
4.81	**3.20**	3.16	1.05
5.16	**0.22**	3.39	1.13
5.22	**0.45**	3.42	1.14
5.26	**1.97**	3.45	1.15
5.78	**0.62**	3.79	1.26
6.72	**2.44**	4.41	1.47

Notes: Quartz SAR OSL age (following Murray and Wintle, 2000)
Only youngest 23 of 36 accepted aliquots used in De calculation

Figure A-2 – OSL data from sample JHKCW7.

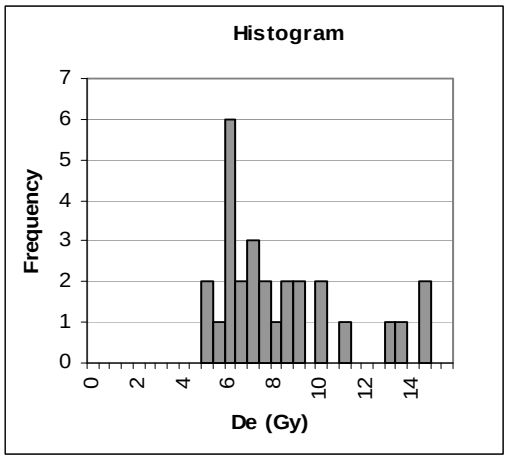

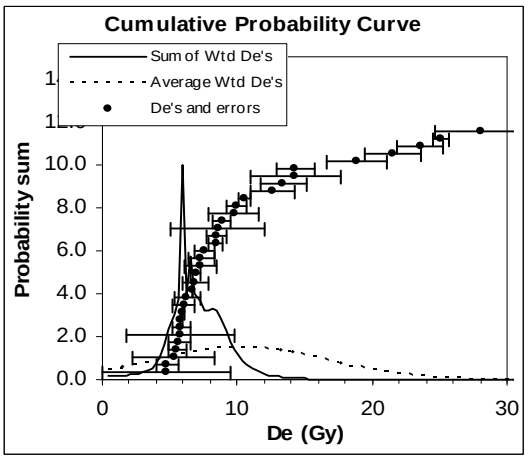

JHKCW7 **Middle of I, KCW-A** **Individual Aliquot Data**
USU-531

	De (Gy)	±	Age (ka)	±
wt Mean =	**6.90**	**1.51**	**3.13**	**0.71**
n =	**23**	**Aliquots**		
Median =	7.47		3.4	0.8
Min =	4.78		2.2	0.5
Max =	14.30		6.5	1.5
S.D. =	1.51			
Standard error =	0.31			
Random Errors=	21.97	%		
Systematic Error=	6.04	%		
Total Error=	22.79	%		
Bin Width =	1	**Gy**		

		+/-	
dose rate=	**2.21**	**0.10**	**Gy/ka**
U =	1.50	0.1	**ppm**
Th =	5.80	0.5	**ppm**
K2O =	1.67	0.04	**wt. %**
Rb2O=	68.9	2.8	**ppm**
H2O=	3.0	3.0	**wt. %**

Cosmic=	0.13	**Gy/ka**
depth =	4.0	**m**
latitude=	37	**degrees (north positive)**
longitude=	112.1	**degrees (east positive)**
elevation=	1.65	**km asl**

De (Gy)	±	Age (ka)	±
4.78	**4.72**	2.17	0.49
4.81	**0.80**	2.18	0.50
5.28	**3.01**	2.39	0.55
5.54	**0.65**	2.51	0.57
5.71	**0.80**	2.59	0.59
5.80	**4.03**	2.63	0.60
5.83	**0.65**	2.64	0.60
5.86	**0.10**	2.65	0.60
6.00	**0.10**	2.72	0.62
6.05	**0.81**	2.74	0.63
6.26	**0.96**	2.84	0.65
6.66	**0.05**	3.02	0.69
6.87	**0.99**	3.11	0.71
6.91	**0.41**	3.13	0.71
7.30	**1.16**	3.31	0.75
7.35	**0.90**	3.33	0.76
7.59	**0.78**	3.44	0.78
8.40	**0.54**	3.81	0.87
8.47	**0.68**	3.84	0.88
8.58	**3.51**	3.89	0.89
8.87	**0.65**	4.02	0.92
9.77	**1.88**	4.43	1.01
9.95	**0.81**	4.51	1.03

Notes: Quartz SAR OSL age (following Murray and Wintle, 2000)
Only youngest 23 of 33 accepted aliquots used in De calculation

Figure A-3 – OSL data from sample JHKCW3.

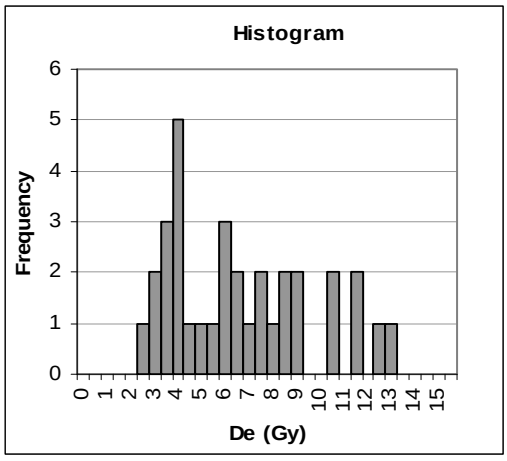

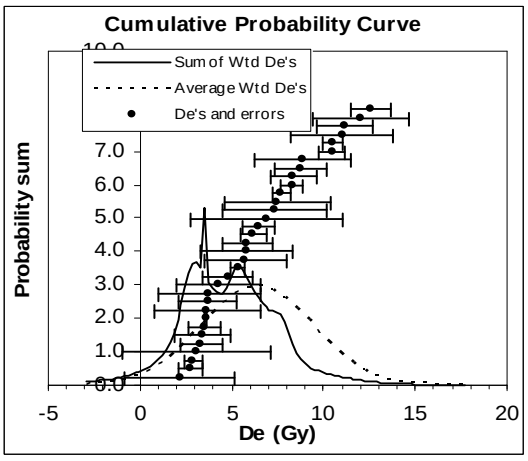

JHKCW3 **Base of II, KCW-B** **Individual Aliquot Data**
USU-389

	De (Gy)	±	Age (ka)	±
wt Mean =	**4.77**	**1.70**	**4.99**	**1.81**
n =	**23**	**Aliquots**		
Median =	5.84		6.1	2.2
Min =	2.16		2.3	0.8
Max =	10.47		10.9	4.0
S.D. =	1.70			
Standard error =	0.35			
Random Errors=	35.75	%		
Systematic Error=	5.74	%		
Total Error=	36.21	%		
Bin Width =	1	**Gy**		

		+/-	
dose rate=	**0.96**	**0.05**	**Gy/ka**
U =	0.60	0.1	**ppm**
Th =	1.90	0.2	**ppm**
K2O =	0.61	0.02	**wt. %**
Rb2O=	22.1	0.9	**ppm**
H2O=	3.0	3.0	**wt. %**

Cosmic=	0.20	**Gy/ka**
depth =	2.0	**m**
latitude=	37	**degrees (north positive)**
longitude=	-112	**degrees (east positive)**
elevation=	1.60	**km asl**

De (Gy)	±	Age (ka)	±
2.16	**2.97**	2.26	0.82
2.77	**0.68**	2.90	1.05
2.88	**0.48**	3.01	1.09
3.07	**4.05**	3.21	1.16
3.34	**1.14**	3.49	1.27
3.39	**1.51**	3.55	1.29
3.53	**0.88**	3.70	1.34
3.57	**0.04**	3.74	1.35
3.64	**2.91**	3.81	1.38
3.72	**1.59**	3.89	1.41
3.74	**2.79**	3.92	1.42
4.29	**2.25**	4.48	1.62
4.78	**1.36**	5.00	1.81
5.33	**0.41**	5.58	2.02
5.74	**2.28**	6.01	2.17
5.82	**2.51**	6.09	2.20
5.86	**1.35**	6.13	2.22
6.19	**0.68**	6.47	2.34
6.47	**0.90**	6.77	2.45
6.90	**4.16**	7.22	2.62
7.34	**2.82**	7.68	2.78
7.46	**2.88**	7.81	2.83
7.70	**0.47**	8.06	2.92

Notes: Quartz SAR OSL age (following Murray and Wintle, 2000)
Only 23 youngest of 33 accepted disks used in De calculation.

Figure A-4 – OSL data from sample JHKCW2.

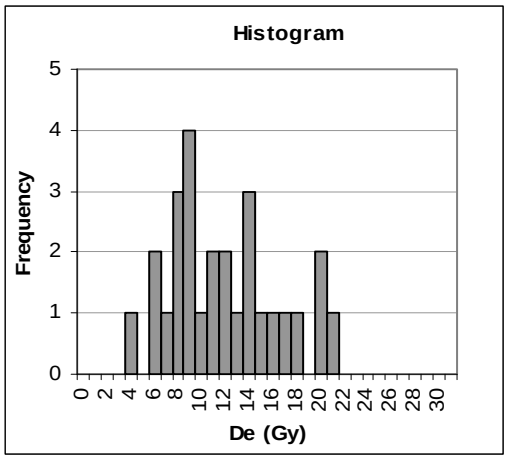

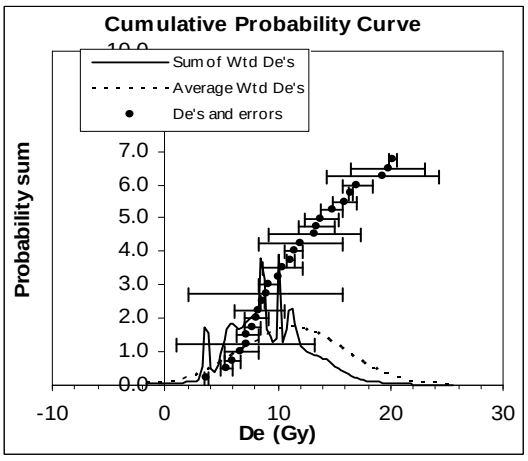

JHKCW2 **Base of I, KCW-B** **Individual Aliquot Data**
USU-388

	De (Gy)	±	Age (ka)	±
wt Mean =	**9.16**	**2.80**	**4.35**	**1.36**
n =	**20**	**Aliquots**		
Median =	10.40		4.9	1.5
Min =	3.68		1.7	0.5
Max =	20.25		9.6	3.0
S.D. =	2.80			
Standard error =	0.63			
Random Errors=	30.66	%		
Systematic Error=	6.11	%		
Total Error=	31.26	%		
Bin Width =	1	**Gy**		

		+/-	
dose rate=	**2.11**	**0.09**	**Gy/ka**
U =	1.00	0.1	**ppm**
Th =	3.30	0.3	**ppm**
K2O =	1.82	0.05	**wt. %**
Rb2O=	63.5	2.5	**ppm**
H2O=	3.0	3.0	**wt. %**

Cosmic=	0.20	**Gy/ka**
depth =	2.0	**m**
latitude=	37	**degrees (north positive)**
longitude=	-112	**degrees (east positive)**
elevation=	1.61	**km asl**

De (Gy)	±	Age (ka)	±
3.68	**0.22**	1.75	0.55
5.46	**0.57**	2.59	0.81
6.00	**0.63**	2.85	0.89
6.77	**1.52**	3.21	1.00
7.17	**6.16**	3.40	1.06
7.28	**0.98**	3.45	1.08
7.82	**0.70**	3.71	1.16
8.05	**1.07**	3.82	1.19
8.35	**2.22**	3.96	1.24
8.63	**0.18**	4.10	1.28
8.96	**6.79**	4.25	1.33
9.17	**0.87**	4.35	1.36
10.09	**0.07**	4.79	1.50
10.40	**1.74**	4.93	1.54
11.16	**0.35**	5.30	1.66
11.46	**0.85**	5.44	1.70
12.05	**3.77**	5.72	1.79
13.32	**4.12**	6.32	1.98
13.50	**1.57**	6.41	2.00
13.85	**1.52**	6.57	2.05

Notes: Quartz SAR OSL age (following Murray and Wintle, 2000)
Only youngest 20 of 27 accepted disks used in De calculation.

Figure A-5 – OSL data from sample CWOSL2.

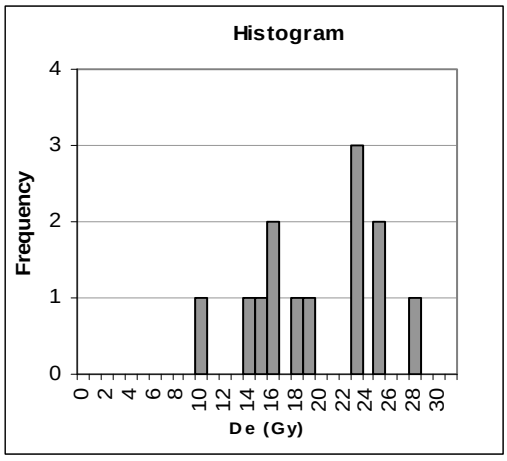

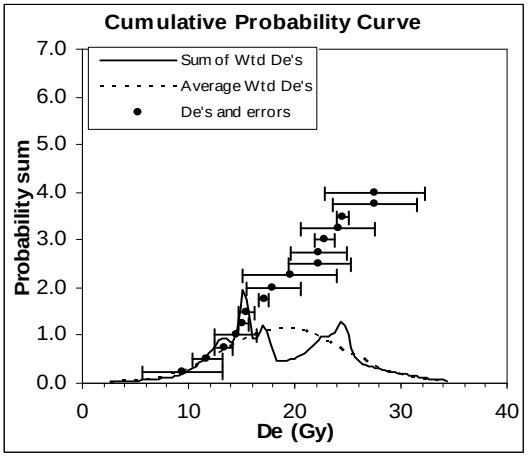

CWOSL2 **Base of II, COY-A** **Individual Aliquot Data**
USU-136

	De (Gy)	±	Age (ka)	±
wt Mean =	**19.10**	**5.60**	**12.78**	**3.84**
n =	**16**	**Aliquots**		
Median =	18.78		12.6	3.8
Min =	9.40		6.3	1.9
Max =	27.61		18.5	5.6
S.D. =	5.60			
Standard error =	1.40			
Random Errors=	29.45	%		
Systematic Error=	6.08	%		
Total Error=	30.07	%		
Bin Width =	1	**Gy**		

De (Gy)	±	Age (ka)	±
9.40	**3.78**	6.29	1.89
11.76	**1.38**	7.87	2.37
13.33	**0.80**	8.91	2.68
14.45	**1.94**	9.66	2.91
15.19	**0.39**	10.16	3.05
15.44	**0.70**	10.33	3.11
17.11	**0.52**	11.44	3.44
18.00	**2.47**	12.04	3.62
19.56	**4.45**	13.08	3.93
22.33	**2.88**	14.94	4.49
22.34	**2.65**	14.95	4.49
22.81	**0.99**	15.26	4.59
24.11	**3.51**	16.13	4.85
24.59	**0.59**	16.45	4.95
27.57	**3.96**	18.44	5.55
27.61	**4.72**	18.47	5.55

		+/-	
dose rate=	**1.50**	**0.07**	**Gy/ka**
U =	0.60	0.1	**ppm**
Th =	2.40	0.2	**ppm**
K2O =	1.29	0.03	**wt. %**
Rb2O=	48.1	1.9	**ppm**
H2O=	3.0	3.0	**wt. %**

Cosmic=	0.17	**Gy/ka**
depth =	3.2	**m**
latitude=	37	**degrees (north positive)**
longitude=	-112	**degrees (east positive)**
elevation=	1.60	**km asl**

Notes: Quartz SAR OSL age (following Murray and Wintle, 2000)
Collected by R. Hereford and J. Pederson in April 2006

Figure A-6 – OSL data from sample CWOSL1.

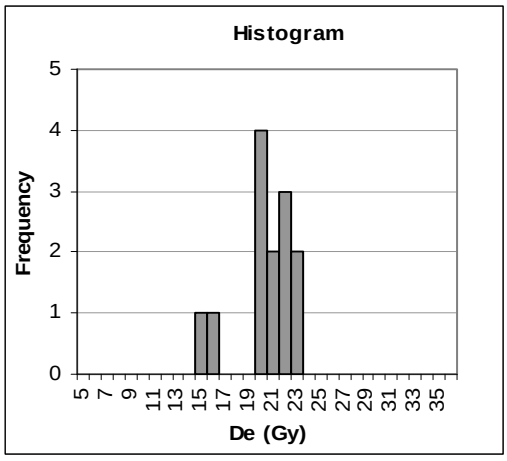

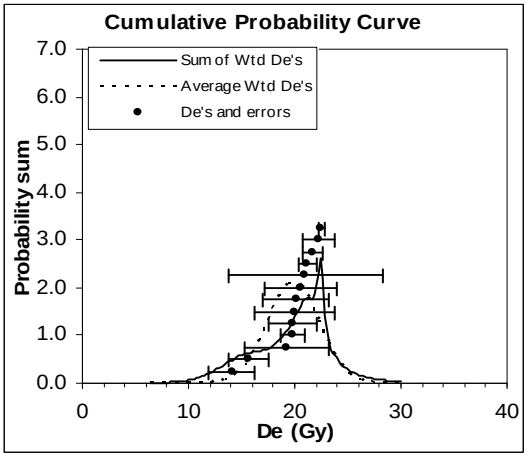

CWOSL1 **Base of I, COY-A** **Individual Aliquot Data**
USU-135

	De (Gy)	±	Age (ka)	±
wt Mean =	**19.86**	**2.44**	**17.47**	**2.46**
n =	**13**	**Aliquots**		
Median =	20.10		17.7	2.5
Min =	14.06		12.4	1.7
Max =	22.48		19.8	2.8
S.D. =	2.44			
Standard error =	0.68			
Random Errors=	12.62	%		
Systematic Error=	6.24	%		
Total Error=	14.08	%		
Bin Width =	1	**Gy**		

De (Gy)	±	Age (ka)	±
21.03	**7.29**	18.50	2.60
19.88	**2.25**	17.48	2.46
20.61	**3.44**	18.12	2.55
15.73	**1.89**	13.84	1.95
22.48	**0.29**	19.77	2.78
19.84	**1.15**	17.45	2.46
22.29	**1.57**	19.61	2.76
21.22	**0.89**	18.67	2.63
19.25	**4.02**	16.93	2.38
21.75	**0.98**	19.13	2.69
20.10	**3.18**	17.67	2.49
19.95	**3.80**	17.55	2.47
14.06	**2.17**	12.37	1.74

dose rate=	**1.14**	**+/- 0.05**	**Gy/ka**
U =	0.30	0.1	**ppm**
Th =	1.20	0.2	**ppm**
K2O =	1.10	0.03	**wt. %**
Rb2O=	32.6	1.3	**ppm**
H2O=	3.0	3.0	**wt. %**

Cosmic=	0.11	**Gy/ka**
depth =	5.8	**m**
latitude=	37	**degrees (north positive)**
longitude=	-112	**degrees (east positive)**
elevation=	1.60	**km asl**

Notes: Quartz SAR OSL age (following Murray and Wintle, 2000)
Collected by R. Hereford and J. Pederson in April 2006

Figure A-7 – OSL data from sample JHBG6.

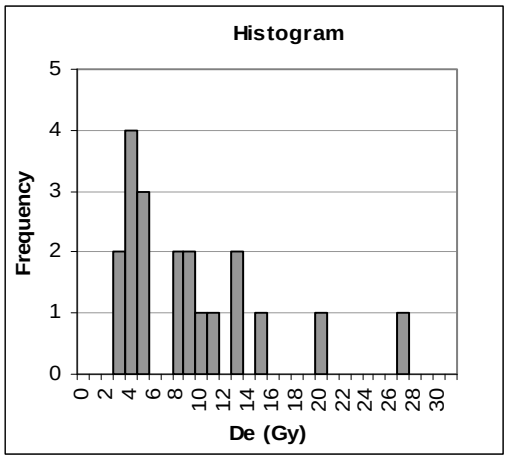

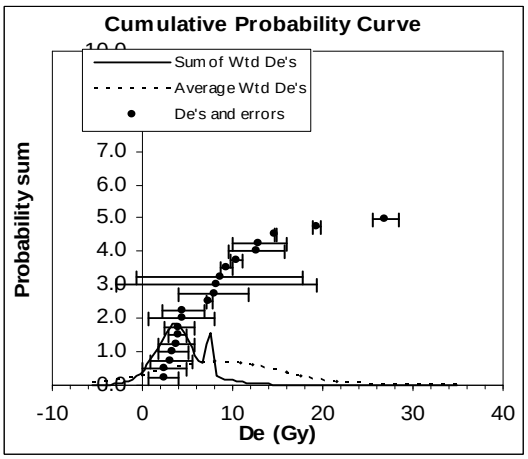

JHBG6 **Lower middle of II @ BG-A** **Individual Aliquot Data**
USU-385

	De (Gy)	±	Age (ka)	±
wt Mean =	**4.31**	**1.82**	**2.34**	**1.00**
n =	**11**	**Aliquots**		
Median =	7.68		4.2	1.8
Min =	2.34		1.3	0.5
Max =	26.96		14.7	6.3
S.D. =	1.82			
Standard error =	0.55			

De (Gy)	±	Age (ka)	±
2.34	**1.63**	1.27	0.54
2.41	**2.40**	1.31	0.56
3.21	**2.37**	1.75	0.75
3.43	**1.74**	1.86	0.80
3.72	**1.95**	2.02	0.86
3.91	**1.01**	2.12	0.91
4.10	**1.74**	2.23	0.95
4.35	**3.57**	2.36	1.01
4.54	**2.30**	2.47	1.05
7.43	**0.33**	4.03	1.72
7.94	**3.83**	4.31	1.84

Random Errors=	42.24	%
Systematic Error=	6.05	%
Total Error=	42.67	%
Bin Width =	1	**Gy**

		+/-	
dose rate=	**1.84**	**0.08**	**Gy/ka**
U =	0.90	0.1	**ppm**
Th =	3.20	0.3	**ppm**
K2O =	1.53	0.04	**wt. %**
Rb2O=	53.6	2.1	**ppm**
H2O=	3.0	3.0	**wt. %**

Cosmic=	0.20	**Gy/ka**
depth =	2.0	**m**
latitude=	37	**degrees (north positive)**
longitude=	-112	**degrees (east positive)**
elevation=	1.46	**km asl**

Notes: Quartz SAR OSL age (following Murray and Wintle, 2000)
Only youngest 12 of 20 accepted aliquots used in De calculation.

Figure A-8 – OSL data from sample JHBG5.

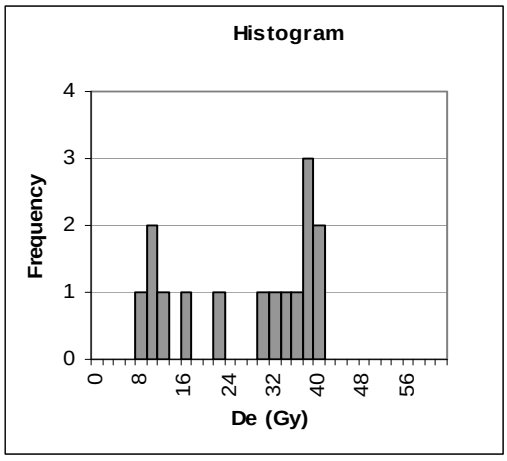

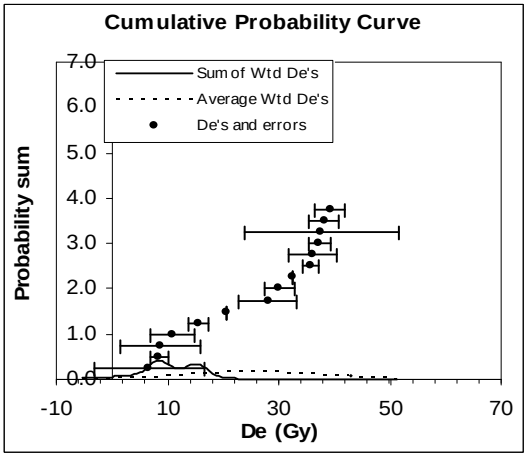

JHBG5 **Base of I, BG-A** **Individual Aliquot Data**
USU-384

	De (Gy)	±	Age (ka)	±	De (Gy)	±	Age (ka)	±
wt Mean =	**10.07**	**3.41**	**4.82**	**1.67**	**6.68**	**9.82**	3.20	1.11
					8.48	**1.59**	4.06	1.40
n =	**5**	**Aliquots**			**8.70**	**7.12**	4.17	1.44
					10.92	**4.12**	5.23	1.81
Median =	30.17		14.5	5.0	**15.55**	**1.72**	7.45	2.57
Min =	6.68		3.2	1.1				
Max =	39.26		18.8	6.5				
S.D. =	3.41							
Standard error =	1.53							
Random Errors=	34.00	%						
Systematic Error=	6.02	%						
Total Error=	34.53	%						
Bin Width =	2	**Gy**						

dose rate=	**2.09**	**+/- 0.09**	**Gy/ka**
U =	1.20	0.1	**ppm**
Th =	4.50	0.4	**ppm**
K2O =	1.64	0.04	**wt. %**
Rb2O=	61.4	2.5	**ppm**
H2O=	3.0	3.0	**wt. %**

Cosmic=	0.20	**Gy/ka**
depth =	2.0	**m**
latitude=	37	**degrees (north positive)**
longitude=	-112	**degrees (east positive)**
elevation=	1.46	**km asl**

Notes: Quartz SAR OSL age (following Murray and Wintle, 2000)
Only youngest 5 of 15 accepted aliquots used in De calculation.

Figure A-9 – OSL data from sample JHBG11.

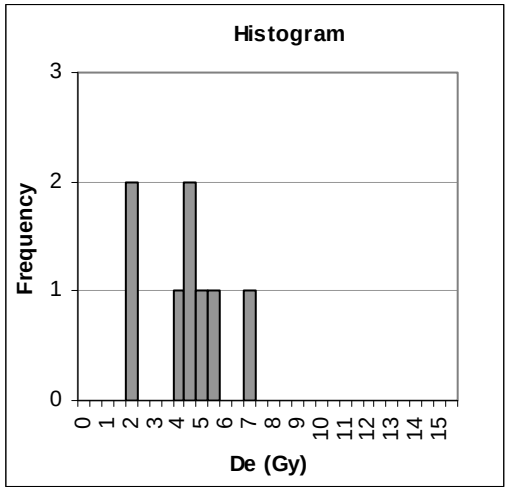

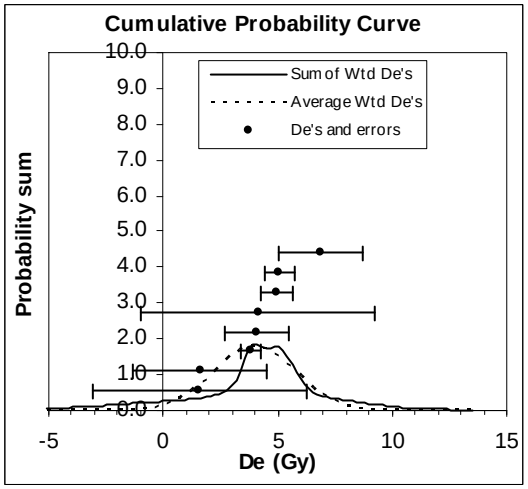

JHBG11 **Middle of II @ BG-B** **Individual Aliquot Data**
USU-523

	De (Gy)	±	Age (ka)	±	De (Gy)	±	Age (ka)	±
wt Mean =	**4.01**	**1.77**	**2.32**	**1.03**	**1.55**	**4.68**	0.90	0.40
					1.62	**2.91**	0.94	0.42
n =	**8**	**Aliquots**			**3.82**	**0.42**	2.21	0.99
					4.09	**1.42**	2.36	1.05
Median =	4.11		2.4	1.1	**4.13**	**5.11**	2.39	1.07
Min =	1.55		0.9	0.4	**4.95**	**0.67**	2.86	1.28
Max =	6.86		4.0	1.8	**5.07**	**0.67**	2.93	1.31
					6.86	**1.85**	3.97	1.77
S.D. =	1.77							
Standard error =	0.63							

Random Errors=	44.17	%
Systematic Error=	6.12	%
Total Error=	44.59	%

Bin Width =	1	**Gy**

		+/-	
dose rate=	**1.73**	**0.08**	**Gy/ka**
U =	1.10	0.1	**ppm**
Th =	3.10	0.3	**ppm**
K2O =	1.45	0.04	**wt. %**
Rb2O=	53.0	2.1	**ppm**
H2O=	3.0	3.0	**wt. %**

Cosmic=	0.11	**Gy/ka**
depth =	6.0	**m**
latitude=	37	**degrees (north positive)**
longitude=	-112	**degrees (east positive)**
elevation=	1.44	**km asl**

Notes: Quartz SAR OSL age (following Murray and Wintle, 2000)

Figure A-10 – OSL data from sample JHBG10.

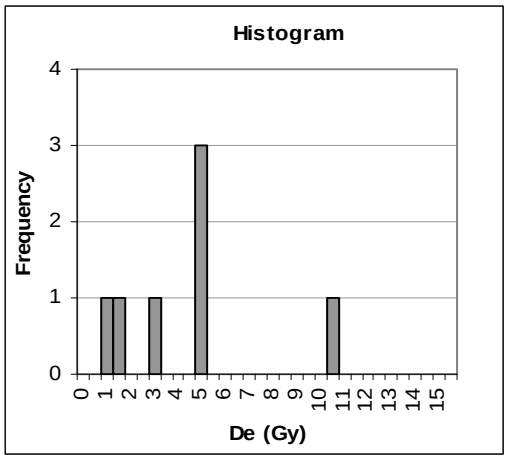

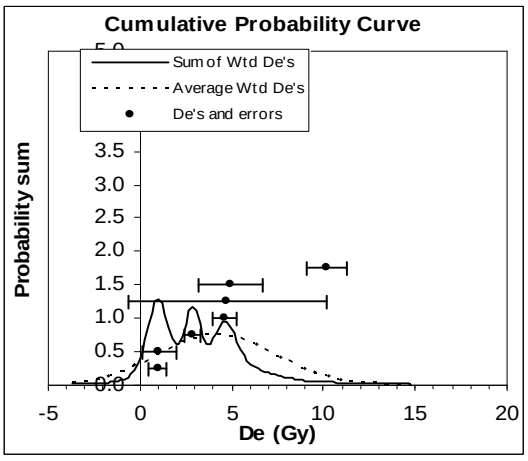

JHBG10 **in hillslope colluvium b/w** **Individual Aliquot Data**
USU-522 **I and II @ BG-B**

	De (Gy)	±	Age (ka)	±	De (Gy)	±	Age (ka)	±
wt Mean =	**3.21**	**1.86**	**1.81**	**1.06**	**0.97**	**0.52**	0.55	0.32
					1.05	**0.90**	0.59	0.35
n =	**6**	**Aliquots**			**2.88**	**0.43**	1.63	0.95
					4.62	**0.61**	2.62	1.53
Median =	4.62		2.6	1.5	**4.75**	**5.43**	2.69	1.57
Min =	0.97		0.5	0.3	**4.97**	**1.75**	2.82	1.64
Max =	10.17		5.8	3.4				
S.D. =	1.86							
Standard error =	0.76							
Random Errors=	58.01	%						
Systematic Error=	6.17	%						
Total Error=	58.34	%						
Bin Width =	1	**Gy**						

		+/-	
dose rate=	**1.77**	**0.08**	**Gy/ka**
U =	1.00	0.1	**ppm**
Th =	3.50	0.3	**ppm**
K2O =	1.53	0.04	**wt. %**
Rb2O=	56.8	2.3	**ppm**
H2O=	3.0	3.0	**wt. %**
Cosmic=	0.07	**Gy/ka**	
depth =	9.0	**m**	
latitude=	37	**degrees (north positive)**	
longitude=	-112	**degrees (east positive)**	
elevation=	1.44	**km asl**	

Notes: Quartz SAR OSL age (following Murray and Wintle, 2000)
Only youngest 6 of 7 accepted aliquots used in De calculation.

Figure A-11 – OSL data from sample JHBG9.

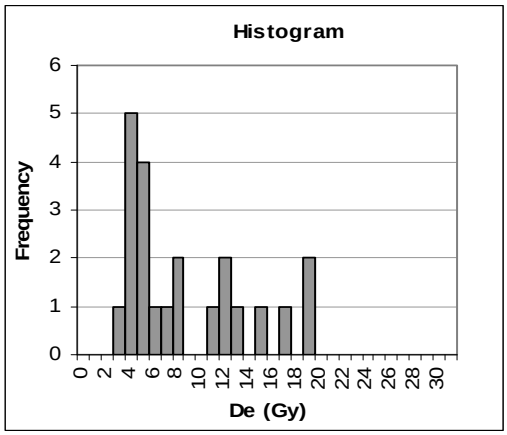

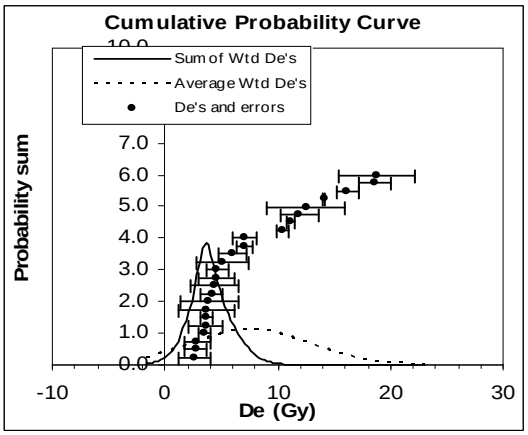

JHBG9 **Middle of I @ BG-B** **Individual Aliquot Data**

USU-521

	De (Gy)	±	Age (ka)	±	De (Gy)	±	Age (ka)	±
wt Mean =	**3.97**	**0.95**	**1.74**	**0.43**	**2.65**	**1.43**	1.16	0.29
					2.72	**0.95**	1.19	0.29
n =	**14**	**Aliquots**			**2.87**	**1.11**	1.25	0.31
					3.52	**0.61**	1.54	0.38
Median =	4.86		2.1	0.5	**3.62**	**1.48**	1.58	0.39
Min =	2.65		1.2	0.3	**3.71**	**0.57**	1.62	0.40
Max =	18.77		8.2	2.0	**3.71**	**2.52**	1.62	0.40
					3.89	**2.60**	1.70	0.42
S.D. =	0.95				**4.16**	**0.92**	1.82	0.45
Standard error =	0.25				**4.42**	**2.13**	1.93	0.48
					4.60	**1.66**	2.01	0.50
Random Errors=	23.98	%			**4.61**	**0.95**	2.01	0.50
Systematic Error=	6.11	%			**5.10**	**2.29**	2.23	0.55
Total Error=	24.75	%			**6.06**	**1.23**	2.65	0.66

Bin Width = 1 **Gy**

		+/-	
dose rate=	**2.29**	**0.10**	**Gy/ka**
U =	1.40	0.1	**ppm**
Th =	4.60	0.4	**ppm**
K2O =	1.90	0.05	**wt. %**
Rb2O=	68.1	2.7	**ppm**
H2O=	3.0	3.0	**wt. %**

Cosmic=	0.13	**Gy/ka**
depth =	4.5	**m**
latitude=	37	**degrees (north positive)**
longitude=	-112	**degrees (east positive)**
elevation=	1.44	**km asl**

Notes: Quartz SAR OSL age (following Murray and Wintle, 2000)
Only youngest 14 of 24 accepted disks used in De calculation.

Appendix B. Facies designations

This appendix contains tables showing the facies designations given to each bed of each study site. Beds are numbered in stratigraphic order.

Table B-1 – Facies codes and descriptions.

Lithofacies Code	Description
Gcm	massive, matrix- to clast-supported gravels
Gci	imbricated, crossbedded clast-supported gravels
Gmr	rounded mud intraclasts and partially reworked bank material
Sl	medium-coarse sand with planar to subhorizontal lamination
Sm	medium-coarse sand, massive due to bioturbation
Spx	poorly sorted coarse sand-pebbles with trough crossbedding
Ssm	thin red and tan massive silty fine sand
Srx	fine-medium laminated sand with climbing ripples
Sma	massive, poorly sorted sand ± floating angular clasts
Mcg	gray calcareous silty clay

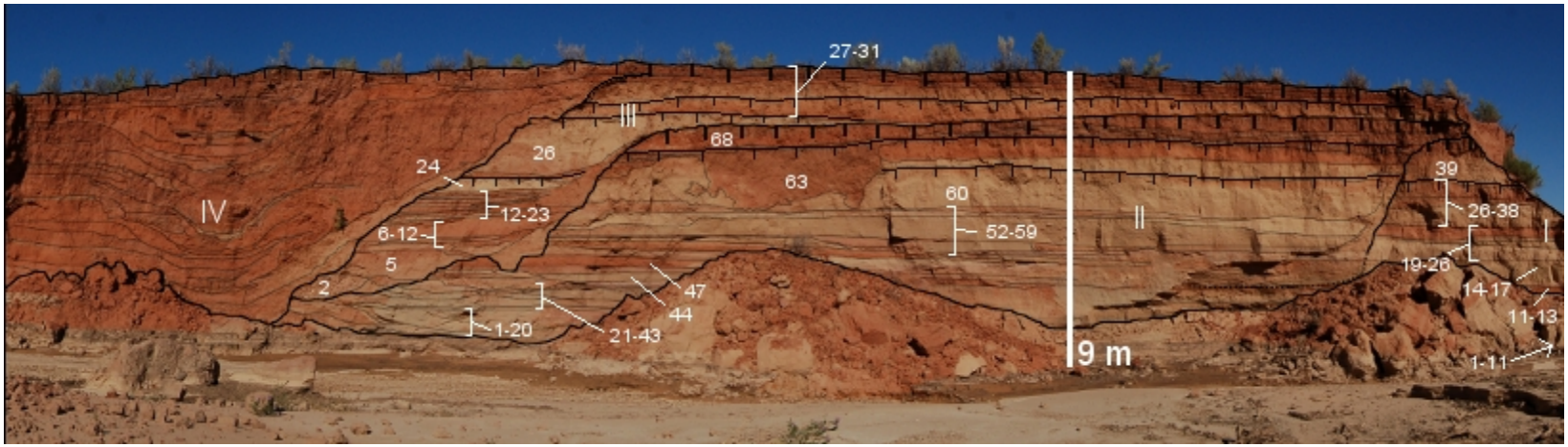

Figure B-1 – Key to units at study site KCW-A.

Table B-2 – Facies designations for study site KCW-A

Package	Unit	Facies Code
I	1	Sl
I	2	Sl
I	3	Sl
I	4	Mcg
I	5	Sl
I	6	Sm/Sma
I	7	Sl
I	8	Sm
I	9	Sm/Sma
I	10	Sm
I	11	Sl
I	12	Sm
I	13	Ssm
I	14	Spx
I	15	Sl
I	16	Sm
I	17	Srx
I	18	Sl
I	19	Sm
I	20	Sl
I	21	Sl
I	22	Spx
I	23	Srx
I	24	Sl
I	25	Sm
I	26	Spx
I	27	Ssm
I	28	Spx
I	29	Sm
I	30	Sm
I	31	Sm
I	32	Sm
I	33	Mcg
I	34	Ssm
I	35	Mcg
I	36	Sm
I	37	Sm
I	38	Ssm/Sm
I	39	Sl/Sm
II	1	Sl
II	2	Gcm
II	3	Sl
II	4	Sma
II	5	Gcm
II	6	Sma

II	7	Ssm
II	8	Sl
II	9	Sl
II	10	Sl
II	11	Spx
II	12	Sma
II	13	Sl
II	14	Srx
II	15	Ssm
II	16	Sl
II	17	Spx
II	18	Sl
II	19	Sl
II	20	Sma
II	21	Sl
II	22	Srx
II	23	Sma
II	24	Sma
II	25	Sl
II	26	Ssm
II	27	Sl
II	28	Spx
II	29	Sl
II	30	Sl/Sma
II	31	Spx
II	32	Sl
II	33	Sma
II	34	Mcg
II	35	Sl
II	36	Sl
II	37	Sl
II	38	Ssm
II	39	Sl
II	40	Sma
II	41	Sl
II	42	Sl
II	43	Spx
II	44	Sl
II	45	Sma
II	46	Sl
II	47	Sl
II	48	Sl
II	49	Sma
II	50	Ssm
II	51	Mcg
II	52	Srx
II	53	Srx
II	54	Sl
II	55	Mcg

II	56	Sl
II	57	Sl
II	58	Sl
II	59	Sl
II	60	Sm
II	61	Sm
II	62	Sm
II	63	Ssm/Sm/gunk
II	64	Ssm/Sm
II	65	Ssm/Sm
II	66	Ssm/Sm
II	67	Ssm/Sm
II	68	Ssm/Sm
III	1	Gmr
III	2	Gmr
III	3	Gmr/Gcm
III	4	Gmr
III	5	Sl
III	6	Gmr
III	7	Gmr
III	8	Sl
III	9	Gmr
III	10	Sma
III	11	Sma
III	12	Ssm
III	13	Sma
III	14	SSm
III	15	Sl
III	16	Ssm
III	17	Sm
III	18	Ssm
III	19	Sm
III	20	Ssm
III	21	Ssm
III	22	Sma
III	23	Ssm
III	24	Srx
III	25	Ssm
III	26	Sm
III	27	Sm
III	28	Sm
III	29	Ssm
III	30	Ssm/Sm
III	31	Ssm/Sm
IV	Individual beds not described due to number and complex geometry. Mostly interbeds of Gcm, Ssm, Sl, and Sm	

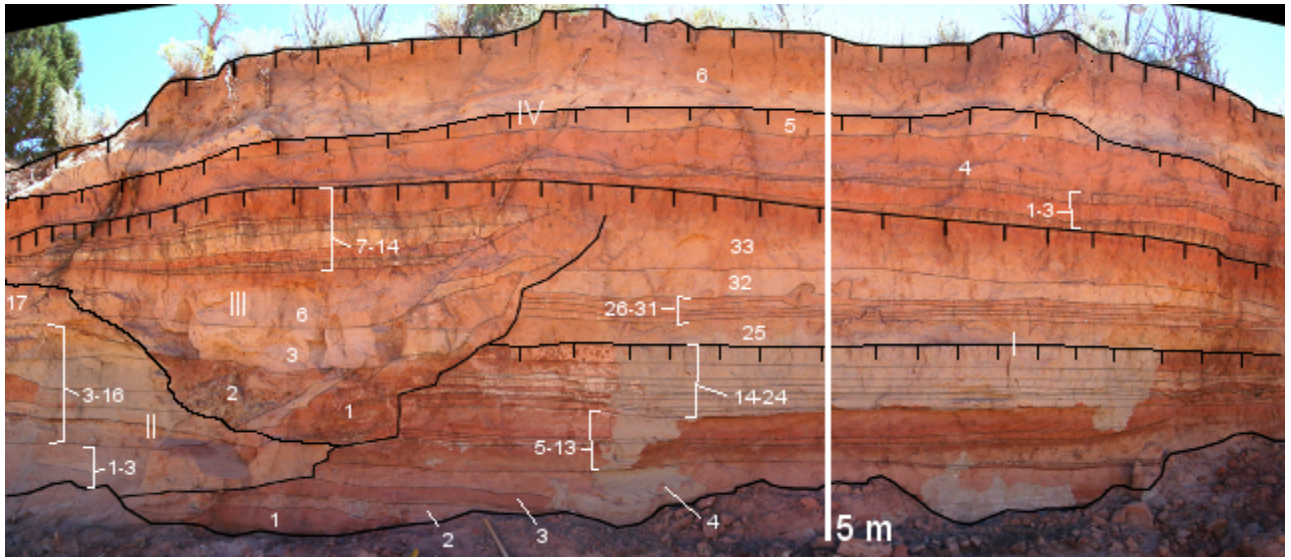

Figure B-2 – Key to units at study site KCW-B.

Table B-3 – Facies designations for study site KCW-B.

Package	Unit	Facies Code
I	1	Sm
I	2	Spx
I	3	Sl
I	4	Sl
I	5	Sl
I	6	Ssm
I	7	Sm
I	8	Ssm
I	9	Sm
I	10	Sl
I	11	Ssm
I	12	Mcg
I	13	Srx
I	14	Ssm
I	15	Mcg
I	16	Ssm
I	17	Mcg
I	18	Ssm
I	19	Mcg
I	20	Ssm
I	21	Mcg
I	22	Ssm
I	23	Mcg
I	24	Sm
I	25	Sma
I	26	Sm
I	27	Ssm
I	28	Ssm
I	29	Sm
I	30	Mcg
I	31	Ssm/Sm
I	32	Ssm/Sm
I	33	Ssm/Sm
II	1	Spx
II	2	Spx
II	3	Sl
II	4	Spx
II	5	Sl
II	6	Sl
II	7	Spx
II	8	Sl
II	9	Sl
II	10	Sl
II	11	Sl
II	12	Srx

II	13	Sma
II	14	Sm
II	15	Sl
II	16	Ssm
II	17	Sm
III	1	Gcm
III	2	Gcm
III	3	Spx
III	4	Sl
III	5	Sl
III	6	Sm
III	7	Mcg
III	8	Ssm
III	9	Mcg
III	10	Ssm
III	11	Mcg
III	12	Ssm
III	13	Mcg
III	14	Sm
IV	1	Mcg
IV	2	Sm
IV	3	Mcg
IV	4	Sm
IV	5	Sm
IV	6	Sm

Figure 3-3 – Key to units at study site COY-A.

Table B-4 – Facies designations for study site COY-A.

Package	Unit	Facies Code
I	1	Sma
I	2	Mcg
I	3	Mcg
I	4	Sma
I	5	Mcg
I	6	Sma
I	7	Mcg
I	8	Sma
I	9	Mcg
I	10	Mcg
I	11	Mcg
I	12	Mcg
I	13	Mcg
I	14	Mcg
I	15	Mcg
I	16	Mcg
I	17	Mcg
I	18	Mcg
I	19	Mcg
I	20	Sma
I	21	Mcg
I	22	Mcg
I	23	Mcg
I	24	Mcg
I	25	Mcg
I	26	Mcg
I	27	Ssm
I	28	Ssm
I	29	Ssm
I	30	Ssm
I	31	Sm
I	32	Sm
I	33	Sm
II		Individual beds not counted due to heavy bioturbation and complexity of outcrop. Lower portion contains several lenses of Gci and Gcm within a mass of Sm. There are 5 siltier horizons within the package that probably represent exposure surfaces and eolian silt input.
III		lower units (not pictured) across the wash include a dominant lens of Gci, overlain by ~10 beds of Ssm, Sm, and Sl.
III	1	Sm
III	2	Sma
III	3	Spx
III	4	Spx
III	5	Sm

III	6	Sl
III	7	Ssm
III	8	Sm
III	9	Sm

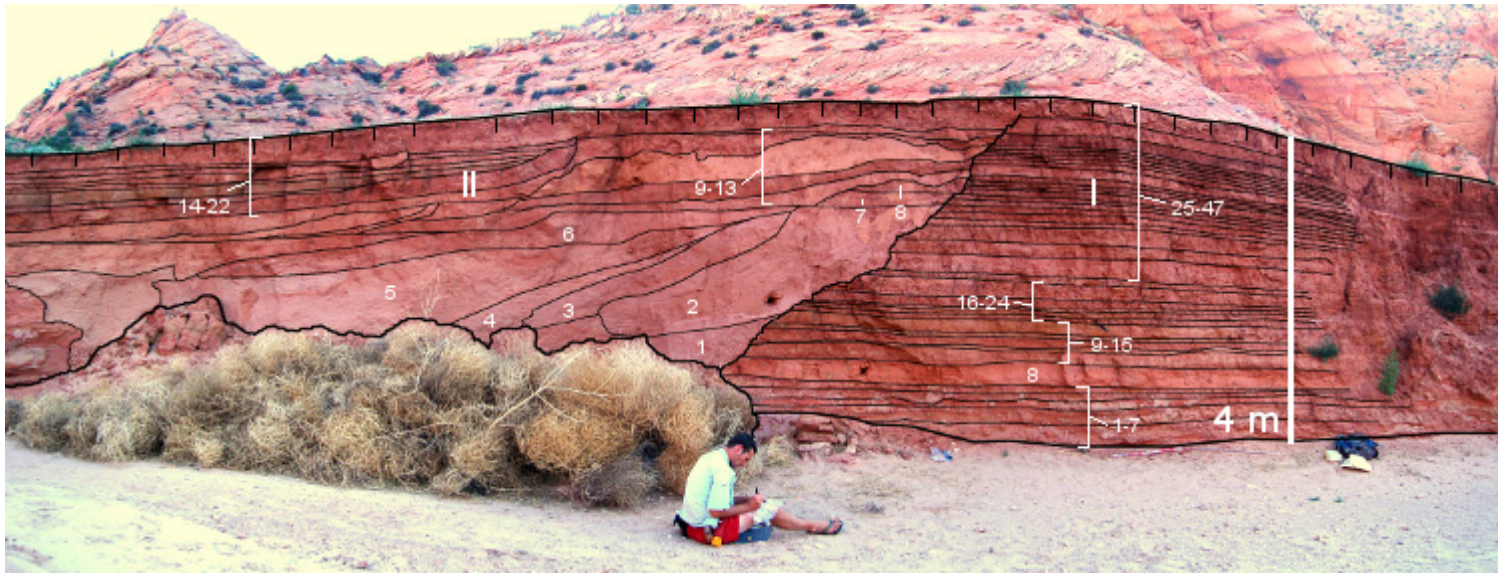

Figure B-4 – Key to units at study site BG-A.

Table B-5 – Facies designations for study site BG-A.

Package	Unit	Facies Code
I	1	Sl
I	2	Sl
I	3	Sma
I	4	Sl
I	5	Sl
I	6	Sm
I	7	Sm
I	8	Sl
I	9	Sma
I	10	Ssm
I	11	Sl
I	12	Ssm
I	13	Sl
I	14	Mcg
I	15	Sl
I	16	Ssm
I	17	Ssm
I	18	Ssm
I	19	Mcg
I	20	Ssm
I	21	Ssm
I	22	Sl
I	23	Ssm
I	24	Sl
I	25	Ssm
I	26	Ssm
I	27	Ssm
I	28	Sl
I	29	Ssm
I	30	Ssm
I	31	Ssm
I	32	Sl
I	33	Ssm
I	34	Sl
I	35	Sl
I	36	Ssm
I	37	Sl
I	38	Ssm
I	39	Sm
I	40	Ssm
I	41	Sm
I	42	Ssm
I	43	Ssm
I	44	Ssm
I	45	Ssm
I	46	Sm

I	47	Sm
II	1	Spx
II	2	Sl
II	3	Sl
II	4	Sl
II	5	Sl
II	6	Sl
II	7	Sl
II	8	Sl
II	9	Sma
II	10	Sl
II	11	Ssm
II	12	Ssm
II	13	Sl
II	14	Ssm
II	15	Sm
II	16	Ssm
II	17	Sm
II	18	Mcg
II	19	Sma
II	20	Ssm
II	21	Ssm
II	22	Sm

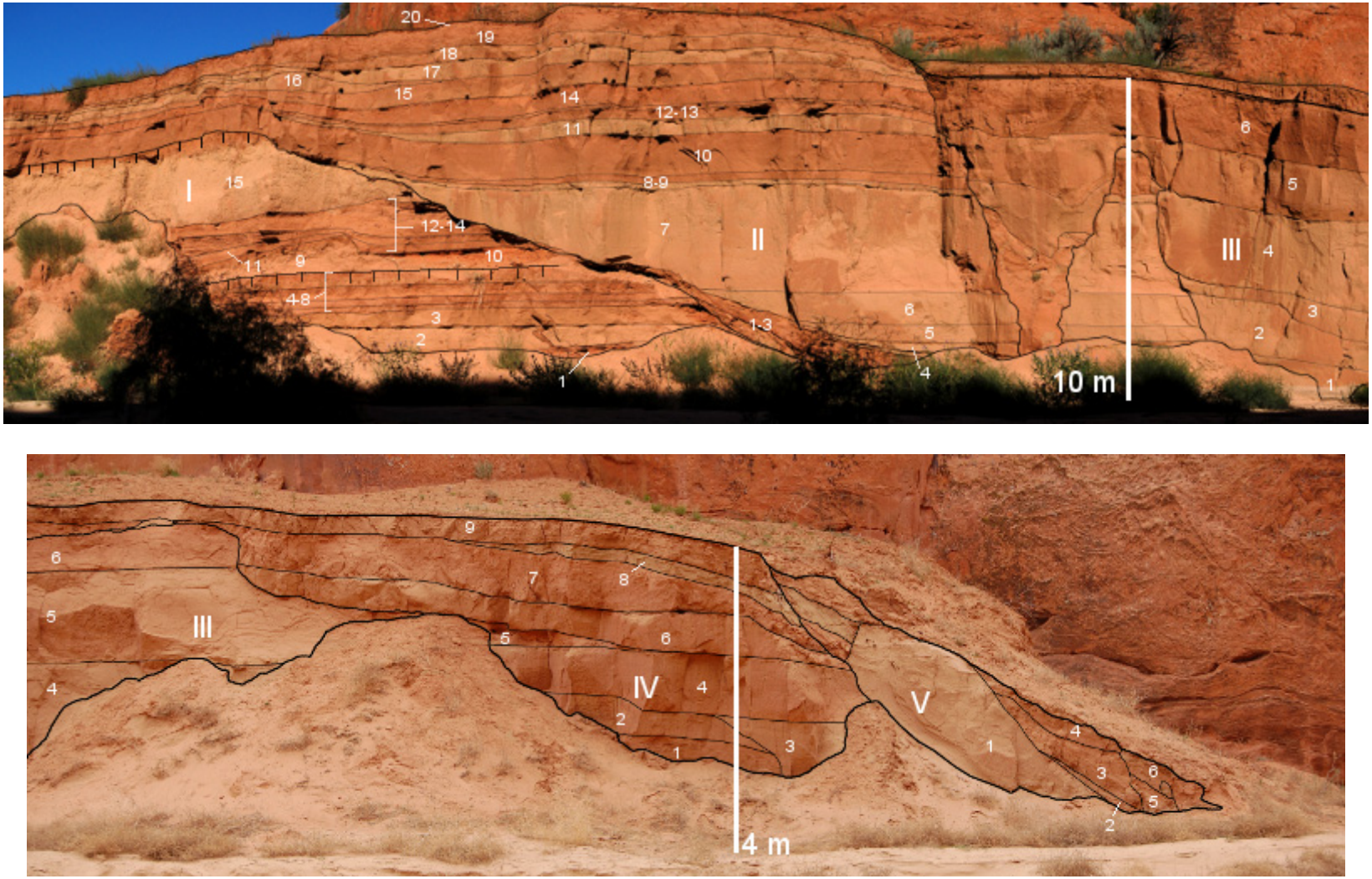

Figure B-5 – Keys to units at study site BG-B.

Table B-6 – Facies designations for study site BG-B.

Package	Unit	Facies Code
I	1	Sl
I	2	Sl
I	3	Sl/Srx
I	4	Sl
I	5	Sm
I	6	Sm
I	7	Sm
I	8	Sl
I	9	Srx/Sm
I	10	Gcm
I	11	Srx
I	12	Srx
I	13	Sl
I	14	Ssm
I	15	Srx/Sm
II	1	Gcm
II	2	Sl
II	3	Sl
II	4	Sl/Srx
II	5	Sl/Srx
II	6	Srx
II	7	Srx
II	8	Ssm
II	9	Srx
II	10	Srx
II	11	Sma
II	12	Srx
II	13	Ssm
II	14	Srx
II	15	Sl
II	16	Sl
II	17	Sl/Srx
II	18	Sl/Srx
II	19	Sl
II	20	Sl
III	1	Sma
III	2	Sl
III	3	Sma
III	4	Sl
III	5	Srx
III	6	Sl/Srx
IV	1	Sl/Srx
IV	2	Sl

IV	3	Sl
IV	4	Sma
IV	5	Sl
IV	6	Sl
IV	7	Sl
IV	8	Sl
IV	9	Sl
V	1	Sl
V	2	Sl
V	3	Sl
V	4	Ssm
V	5	Sl
V	6	Sl

Figure B-6 – Key to units at study site BG-C.

Table B-7 – Facies designations for study site BG-C.

Package	Unit	Facies Code
I	1	Sl/Srx
I	2	Sl
I	3	Sl
I	4	Sl
I	5	Sma
I	6	Sma
I	7	Sma
I	8	Sma
I	9	Sl/Sm
I	10	Sma
I	11	Sma
I	12	Sl/Sma
I	13	Srx
I	14	Srx
I	15	Sm
I	16	Sma
I	17	Sl
I	18	Srx
I	19	Srx
I	20	Sma
I	21	Srx
I	22	Srx
I	23	Srx
I	24	Srx
I	25	Sl
I	26	Srx
I	27	Srx
I	28	Sl
I	29	Ssm
I	30	Sl
I	31	Sl

Appendix C. Permission Letter

September 04, 2009

Jon Harvey
1 Park Place
Port Alsworth, AK, 99653
(907) 781-2107 (phone)
jon_harvey@partner.nps.gov

Dear Ms. Harden:

I am in the process of preparing my Master's thesis in the Geology Department at Utah State University. I hope to complete in the Fall of 2009.

I am requesting your permission to include the attached material as shown. I will include appropriate citations to your work as shown and copyright and reprint rights information in a special appendix. The bibliographical citation will appear at the end of the chapter in which the figure is used. Please advise me of any changes you require.

Please indicate your approval of this request by signing in the space provided, attaching any other form or instruction necessary to confirm permission. If you charge a reprint fee for use of your material, please indicate that as well. If you have any questions, please call me at the number above.

I hope you will be able to reply immediately. If you are not the copyright holder, please forward my request to the appropriate person or institution.

Thank you for your cooperation,

Jon Harvey

x

I hereby give permission to Jon Harvey to reprint the following material in his Masters Thesis:

Figure 4 on p. 25

from

Harden, T. M., 2007, A 12,000-Year Probability-Based Flood Record in the Southwestern United States [M.S. Thesis]: Tuscon, University of Arizona, 34 p.